Genomic profiling in rare kidney disease

Inaugural-Dissertation

zur

Erlangung des Doktorgrades

der Mathematisch-Naturwissenschaftlichen Fakultät

der Universität zu Köln

vorgelegt von

Nikolai Tschernoster

aus Köln

Köln, Mai 2023

Berichterstatter (Gutachter):

Prof. Dr. Peter Nürnberg

Prof. Dr. Paul Brinkkötter

Tag der mündlichen Prüfung:

14.08.2023

Table of Contents

List of Abbreviations I
Abstract III
Zusammenfassung IV
Introduction 1
Interesting titbits to tantalize your mind 1
Rare kidney disease 1
Nephrotic Syndrome 3
Anatomy of the renal system and the slit diaphragm 4
Glomerular disease 5
FAT1 6
Hippo Signaling 6
Disease spectrum 7
The complement system 8
Atypical haemolytic uremic syndrome 9
The renal tubular system 11
Evolution of DNA Sequencing 13
Non-sequence-based analysis: Molecular combing 15
Published Studies 16
Expanding the Spectrum of FAT1 Nephropathies by Novel Mutations That Affect Hippo Signaling 16
Unraveling Structural Rearrangements of the CFH Gene Cluster in Atypical Hemolytic Uremic Syndrome Patients Using Molecular Combing and Long-Fragment Targeted Sequencing 28
Long-read sequencing identifies a common transposition haplotype predisposing for *CLCNKB* deletions 42
Abstract 43
Background 43
Methods 43
Results 43
Conclusions 43
Keywords: 44
Abbreviations 44
Introduction 45
Methods 48

Patients 48
High molecular weight DNA isolation 48
Whole Exome Sequencing (WES) 48
10x Genomics linked-read analysis 48
Samplix Xdrop indirect sequence capture and ONT long-read sequencing 49
Long-range polymerase chain reaction (PCR) and amplicon-based SMRT sequencing 49
PacBio whole genome long-read sequencing (Single-molecule real-time SMRT-Seq) 50
ClC-Kb/ClC-Ka hybrid protein structure predictions 50
Results 51
Genetic workup of Family P1 51
Results of the genomic workup of the cohort 54
CLCNKA/CLCNKB hybrid gene 60
Predicted ClC-Ka/ClC-Kb hybrid proteins 61
Discussion 64
Conclusions 66
Declarations 67
Ethics approval and consent to participate 67
Consent for publication 67
Availability of data and materials 67
Competing interests 67
Funding 67
Acknowledgement 67
Publication bibliography 68
General Discussion 72
Expanding the Spectrum of FAT1 Nephropathies by Novel Mutations That Affect Hippo Signaling 72
Unraveling Structural Rearrangements of the CFH Gene Cluster in Atypical Hemolytic Uremic Syndrome Patients Using Molecular Combing and Long-Fragment Targeted Sequencing 74
Long-read sequencing identifies a common transposition haplotype predisposing for *CLCNKB* deletions 77
Conclusion 79
Publication bibliography 80
Further publications 101

Acknowledgements 102
Supplemental Material 103
Supplementary Material Manuscript 1 103
Supplementary Material Manuscript 2 106
Supplementary Material Manuscript 3 112
Curriculum vitae 120
Eidestattliche Erklärung 124

List of Abbreviations

NS:	Nephrotic syndrome
SRNS:	Steroid-resistant nephrotic syndrome
SSNS:	Steroid-sensitive nephrotic syndrome
FSGS:	Focal segmental glomerulosclerosis
ESRD:	End-stage renal disease
NGS:	Next-generation sequencing
GPS:	Gene-panel sequencing
WES:	Whole exome sequencing
WGS:	Whole genome sequencing
LRS:	Long-read sequencing
SV:	Structural variant
RCA:	Regulators of complement activation
CO:	Cardiac output
HUS:	Haemolytic uremic syndrome
aHUS:	atypical haemolytic syndrome
rTMA:	renal thrombotic microangiopathy
CKD:	Chronic kidney disease
GBM:	Glomerular basement membrane
kDa:	Kilo Dalton
eGFR:	estimated glomerular filtration rate
NDR:	Nuclear dbf2-related

C3G:	C3 glomerulopathy
GN:	Glomerulonephritis
SLE:	Systemic lupus erythematosus
AMD:	Age-related macular degeneration
TTP:	Thrombocytopenic purpura
CFH:	Complement factor H
CFI:	Complement factor I
CFB:	Complement factor B
NAHR:	non-allelic homologous recombination
BS:	Bartter syndrome
GS:	Gitelman syndrome
SLTs:	Salt-losing tubulopathies
ENaC:	Expressed sodium channel
Bp:	Base pair
Kb:	Kilo-bases
Mbp:	Mega-base pair
dNTPs:	Deoxynucleotide Triphosphates
CNV:	Copy number variation
CGH:	Comparative genomic hybridization
FISH:	Fluorescent *in-situ* hybridization
MLPA:	Multiplex ligation-dependent probe amplification
PCR:	Polymerase chain reaction

Abstract

Rare diseases (RD), generally defined by an incidence of less than 1:2000, affect about 3-6% of the population. To date, over 600 different genetic kidney diseases have been identified. Most of them with the exception of autosomal dominant polycystic kidney disease (ADPKD) are rare to ultrarare disorders. Due to their rarity and often genetic heterogeneity, analysis is difficult and diagnosis is frequently delayed. Clinically, (rare) kidney diseases (RKD) are mainly divided into the following categories: Congenital or developmental kidney and urogenital tract malformations, electrolytes or metabolic disorder, glomerular disease, secondary renal, hereditary renal cancer syndromes, or tubulointerstitial kidney disease. Steroid-resistant nephrotic syndrome (SRNS) and focal segmental glomerulosclerosis (FSGS), are leading causes of end-stage renal disease (ESRD) in children, adolescents, and adults. Although several SRNS genes could be identified mostly in younger children, the genetic basis of SRNS/FSGS in adolescents and adults is far from being completely understood. Reliable discrimination of genetic versus non-genetic forms is an imperative as the identification of monogenic rare kidney disease has numerous implications in a precision medicine setting. Currently, the predominant application of short-read based sequencing techniques results in preferential detection of point mutations and small-sized deletions/insertions while larger structural aberrations (large deletions/insertions), gene rearrangements, and mutations in homologous or repetitive regions frequently escape detection. This project combines short-read based high throughput next-generation sequencing (GPS/WES/WGS) with unparalleled structural variant analyses to overcome previous limitations in genetic analyses. Clinically relevant examples, that such structural variants (SV) are important in rare kidney diseases, are complement activation gene cluster (RCA; chromosome1q32) in atypical haemolytic uremic syndrome (aHUS) as well as the deletion of the chloride channel ClC-Kb associated with Bartter syndrome type 3. The major goal of this project is to unravel the genetic basis of genetic forms of RKD like SRNS/FSGS, aHUS, and tubulopathies and to define a pipeline for the molecular genetic analyses of rare kidney diseases as a best-practice clinical routine at the University Hospital of Cologne. Specifically, my aim was to perform profound genome analyses using biosamples from a cohort of paediatric and adult SRNS/FSGS patients, that have been collected over the last years and integrate this with already existing genetic data. By a comprehensive genomic approach, we aim to improve the diagnostics of chronic kidney disease, enhance our

understanding of the underlying pathomechanisms, and contribute to practice-changing discoveries by precision diagnostics, that allow individualized therapies.

Zusammenfassung

Seltene Erkrankungen, definiert durch eine Inzidenz von weniger als 1:2000, betreffen etwa 3-6 % der Bevölkerung. Bis heute wurden bereits über 600 verschiedene genetische Nierenerkrankungen identifiziert. Die meisten von ihnen, mit Ausnahme der autosomal dominanten polyzystischen Nierenerkrankung (ADPKD), sind seltene bis sehr seltene Erkrankungen. Aufgrund ihrer Seltenheit und oft genetischen Heterogenität ist die Analyse schwierig und die Diagnose wird häufig verzögert. Klinisch werden (seltene) Nierenkrankheiten hauptsächlich in die folgenden Krankheitskategorien eingeteilt: Angeborene oder entwicklungsbedingte Fehlbildungen der Nieren und des Urogenitaltrakts, Elektrolyt- oder Stoffwechselstörungen, glomeruläre Erkrankungen, sekundäre Nierenerkrankungen, erbliche Nierenkrebssyndrome oder tubulointerstitielle Nierenerkrankungen. Das steroidresistente nephrotische Syndrom (SRNS) und sein histomorphologisches Hauptkorrelat die fokal-segmentale Glomerulosklerose (FSGS) stellen eine bedeutende Ursache für die terminale Niereninsuffzienz im Kindesalter, als auch bei erwachsenen Patienten dar. Trotz Identifikation vieler monogenetischer Veränderungen, ist die genetische Grundlage des SRSN/FSGS-Komplex für die Mehrheit der älteren Kinder, Jugendlichen und Erwachsenen bisher nicht gut verstanden. Die eindeutige Abgrenzung genetischer Ursachen für seltene Nierenerkrankungen ist unerlässlich, da sich bereits heute hieraus eine Vielzahl an klinischen Implikationen ergeben. Die Identifikation unbekannter Erkrankungsallele oder Erkrankungsgene kann Erkenntnisse bringen, die ein gänzlich neues Verständnis der Pathomechanismen ermöglichen. Durch systematische repetitive Analyse einer ausreichend großen Patientenkohorte ist eine hypothesenfreie genetische Testung möglich, die auch die methodischen Schwächen der bislang von „short-reads“ dominierten Sequenziertechnologien kompensieren kann. Wir haben in unserer Studie Whole-Exome/Genome Sequenzierungs-Verfahren (WES/WGS) mit Methoden kombiniert, die eine Erfassung von Strukturvarianten (SV) (große heterozygote Deletionen/Insertionen, balancierte Translokationen, Gen-Rearrangements, etc.) erlauben. Eindrückliche Beispiele, dass solche SV auch bei seltenen Nierenerkrankungen von Bedeutung sind, zeigen Befunde zum Komplement-Aktivierungs Gencluster (RCA; Chromosom1q32) bei atypischem

Hämolytisch Urämischem Syndrom (aHUS) sowie die vollständige Deletion des Chloridkanals ClC-Kb ursächlich für Bartter Syndrom Typ 3. Konkret ist es mein Ziel, tiefgreifende Genomanalysen anhand von Bioproben aus einer Kohorte pädiatrischer und erwachsener Patienten mit genetisch bedingten Formen der seltenen Nierenerkrankungen wie SRNS/FSGS, aHUS und Tubulopathien durchführen, die in den letzten Jahren gesammelt wurden und diese in bereits vorhandene genetische Daten integrieren. Durch eine umfassende genomischen Analyse wollen wir die Diagnostik von chronischen Nierenerkrankungen verbessern, unser Verständnis der zugrunde liegenden Pathomechanismen erweitern und zu praxisverändernden Entdeckungen durch Präzisionsdiagnostik beitragen, die letztendlich individuelle und gezielte Therapiemöglichkeiten ermöglichen soll.

Introduction

Interesting titbits to tantalize your mind

In the average healthy human body, approximately 1.2 litre blood are pumped through the kidneys every minute. This equals 20-25 % of the whole human body's cardiac output (CO). The CO is defined by the volume of blood pumped through the heart over a time-span of one minute and is calculated by the heart rate and the stroke volume. At rest, the CO of a healthy individual is about 5 L/min (Field et al. 2010). About 10 % of the blood that flows through both kidneys, namely 180 litres are filtered in the kidneys every day (~125 ml per minute). That is the equivalent of the water that fits into a normal-sized bathtub. Every day! Considering a normal urine excretion volume of between 1-2 litre per day, 99 % of the filtrate is reabsorbed by the kidney and resupplied into the blood (Wallace 1998). In relation, the proportion of the hearts' cardiac output to the brain has been reported to be between 15-20 % (Williams and Leggett 1989; Xing et al. 2017), emphasising, that the kidneys are very important and fascinating organs that should be of more interest in the society.

Rare kidney disease

The term "rare disease" (interchangeably used "orphan disease") does not succumb to standardized regulations and is subjectively defined differently from country to country. In the US a disease is considered rare if there are less than 200.000 individuals affected (Thomas and Caplan 2019). In Europe its fewer than 1:2000 (Nguengang Wakap et al. 2020), and in Japan fewer than 1.2500 (Hayashi and Umeda 2008). Globally, between 3.5-5.9 % of the population (estimated prevalence of rare diseases between ~3482–5910 per 100.000 individuals) is affected by a rare disease at any time of which approximately 72 % are of genetic origin (Nguengang Wakap et al. 2020).

Many of the rare kidney diseases show variable expressivity even intrafamilial. Subtle metabolic and biochemical clues can be obscured by the broad metabolic changes seen in progressive kidney disease. Non-standardized molecular genetic diagnostic protocols, extremely small numbers of patients, and scarcity of clinical consensus guidelines make comprehensive clinical care still difficult for many entities (Watson et al. 2008). However, genomic research into RKD has already been demonstrated to be one of the main drivers of

knowledge into renal development and physiology and the underlying molecular basis of kidney disease (Soliman 2012).

In 1990, the genetic basis of X-linked Alport syndrome (AS), the most common type of AS was unravelled by identification of causative mutations in the *COL4A5* gene (Barker et al. 1990). During the next 10 years, for growing number kidney diseases the genetic basis was discovered, including many classic rare kidney disorders like nephrogenic diabetes insipidus (Rosenthal et al. 1992), autosomal dominant polycystic kidney disease type 1 (Harris et al. 1995 Oct), pseudoaldosteronism (Liddle's syndrome) (Shimkets et al. 1994), nephrolithiasis associated to Dent's disease (Lloyd et al. 1996), salt-wasting in Bartter and Gitelman syndrome (Simon et al. 1996a; Simon et al. 1996c), nephropathic cystinosis (Town et al. 1998), and steroid-resistant nephrotic syndrome (Olsen et al. 1996; Boute et al. 2000). In terms of kidney diseases, over 600 mendelian kidney diseases have been reported until know, most of which have been considered rare in Europe and the USA, with a combined prevalence of 60-80 cases per 100.000 citizens (Rasouly et al. 2019). These more than 600 genetic diseases can be assigned to the following main types: Congenital or developmental kidney and urogenital tract malformations (341), electrolytes or metabolic disorders (150), glomerular disease (83), secondary renal (28), renal cancer syndromes (17), and tubulointerstitial disease (6) (Rasouly et al. 2019).

The use of NGS technologies dramatically improved genetic testing and expanded the spectrum of nephrotic diseases especially when clinical phenotyping remained inconclusive (Stokman et al. 2016). The presentation of phenotypic variations may be due to genetic heterogeneity. A precise genetic diagnosis may already have direct therapeutic implications. For example, the effectiveness of plasmapheresis and outcome of kidney transplantation in haemolytic uremic disorder is strongly associated to the affected disease-causing gene. Patients with mutations in genes encoding fluid phase circulating proteins like CFH and CFI accompany a more severe clinical outcome compared to those carrying mutations in MCP (CD46) that encodes a cell-associated protein (Caprioli et al. 2006). However, the underlying monogenetic cause can only be identified in ~ 20-30 % (and one study with 73 %) of cases with SRNS (Trautmann et al. 2018; Cheong 2020; Najafi et al. 2022), congenital tubulopathy (30-50 %) (Devuyst et al. 2014; Hureaux et al. 2019), or aHUS (50-60 %) (Noris and Remuzzi 2009; Nester et al. 2015).

While we performed molecular diagnostics of the more than 300 RKD patients, individual groups of patients emerged. I focused my work on three entities: *FAT1*-associated nephropathy, *CFH*-associated aHUS, and *CLCNKB* deletion-associated BS 3. Detailed investigations were carried out using up-to-date molecular genetic methods, which could be introduced as standard in the analysis of the respective diseases in the future. The work-up of these rare diseases produced clinically relevant insights, represented in the three publications of this thesis.

Nephrotic Syndrome

Nephrotic syndrome (NS), with an estimated incidence of 1-2:100.000, is the most common glomerular disease in paediatrics, accounting for ~10 % of all early-onset chronic kidney diseases (CKD) (Wong 2007; Filler et al. 2003; Smith et al. 2007). Approximately 80-90 % of these patients clinically respond to treatment with glucocorticoids and are classified as steroid-sensitive NS (SSNS), whereas the remaining 10-20 % are steroid-resistant (Koskimies et al. 1982; Tarshish et al. 1997; Carter et al. 2020; Wong 2007).

In contrast to steroid-sensitive nephrotic syndrome (SSNS) which usually presents as a benign disease, steroid-resistant nephrotic syndrome SRNS/FSGS has long been recognized as a major cause of paediatric and adolescent end-stage renal disease (ESRD) (Trautmann et al. 2017; Harambat et al. 2013). 15 % of all ESRD cases with an onset of disease before the age of 25 are caused by NS (Smith et al. 2007). Much of our understanding of podocyte biology and how the podocyte function impacts the function and integrity of the glomerular filter is derived from genetic studies on familial/genetic forms of FSGS. Histologically, SRNS is mainly characterized by focal segmental glomerular sclerosis (FSGS) the segmental solidification (scarring) of scattered areas of the glomerular tufts (focal). The glomerular scarring (sclerosis) is characterized by the collapse of the capillaries and an increase of the extracellular matrix but only affects portions of the glomerular (segmental) (Ichikawa and Fogo 1996). Other frequent manifestations are membranous nephropathy characterized by the thickening of the glomerular capillary walls due to immune complex accumulation (Couser 2017), and minimal change disease characterized by increased renal membrane permeability and proteinuria due to glomerular filtration barrier damage (Vivarelli et al. 2017; Go et al. 2021).

Anatomy of the renal system and the slit diaphragm

Macroscopically, the kidney consists of four major sections: (1) the cortex, which contains the renal corpuscles, consisting of the glomeruli and Bowman capsules. (2) The medulla, which can be further divided into a narrower outer medulla and a thicker inner medulla, organized as cones containing the medullary pyramids. The tips of the kidney pyramids form papillae (3) through which the urine coming from the collecting ducts is collected and passed into cup-shaped calyces (renal pelvis (4)) before flowing through the ureters into the bladder and through the urethra out of the body (Figure 1A) (Radi 2019; Akilesh 2014).

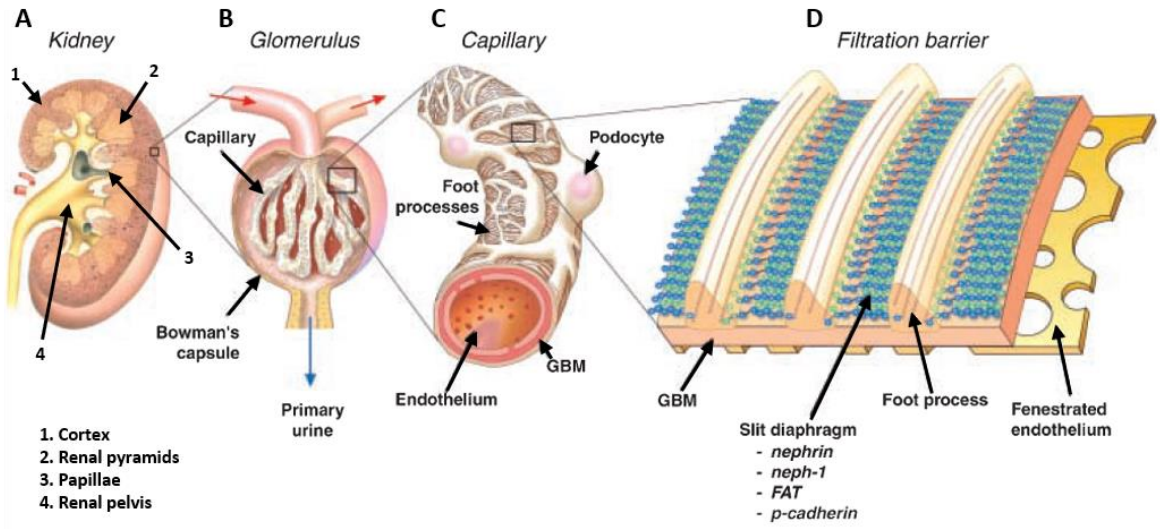

Figure 1: Anatomy of the Kidney, Glomerulus, Capillary, and Filtration barrier. Adapted from Tryggvason et al. 2003 and modified by Nikolai Tschernoster.

Urine production is the interplay of three major processes: glomerular filtration, tubular reabsorption, and secretion (Chen et al. 2017). Functionally, the urine-producing unit is called the Nephron with parts being located in both the cortex and the medulla. In total, each of the kidneys contains approximately 1-1.3 million nephron units (Wallace 1998; Murray and Paolini 2022). The nephron consists of multiple specialized compartments, each with its own important function.

The glomerulus contains a capillary tuft of afferent arterioles through which blood is transported into the glomeruli and efferent arterioles through which exit the glomeruli (Figure 1B). The specialized large porous surface of the capillaries is optimized for filtration (Murray and Paolini 2022). The actual filtration unit (glomerular filtration barrier) encases the capillaries and is composed of three layers. The fenestrated endothelium as the inner layer, the 300-350 nm thick glomerular basement membrane (GBM), and the podocytes as the outer

endothelial layer (Figure 1C, D) (Tryggvason and Pettersson 2003). As the final layer, podocytes are functional of utmost importance in the prevention of proteins larger than 90 kDa, like albumin and immunoglobulins, from leaking into the primary urine, while allowing smaller molecules such as water, ions, creatine and glucose, and small proteins to pass through (Murray and Paolini 2022). Functionally, branching foot processes of adjacent podocytes form a sieve-like complex, separated by an ultrathin gab, called slit diaphragm surrounding the glomerular capillaries within the Bowman capsules (Tryggvason and Pettersson 2003; Rice et al. 2013). The slit diaphragm is a very specialized junction containing proteins belonging to the adherents junction such as P-cadherin, ß-catenin (Reiser et al. 2000), and FAT (Inoue et al. 2001), as well as proteins belonging to the tight junction family such as ZO-1, JAM-A occludin and cingulin (Fukasawa et al. 2009). Together with FAT and P-cadherin, the transmembrane proteins Nephrin, (Ruotsalainen et al. 1999; Tryggvason 1999) Podocin, (Schwarz et al. 2001; Roselli et al. 2002) NEPH1, (Donoviel et al. 2001) Neurexin-1 (Saito et al. 2011) and Ephrin-B1 (Hashimoto et al. 2007) form the molecular sieve of the slit diaphragm (Figure 1D). Over the progressive stages of kidney disease, the glomerular filter starts to fail, altering podocyte and slit diaphragm morphology and permeability, thus larger and more proteins, ions, and minerals are excreted through the urine (Butt et al. 2020). Clinically, kidney damage can be identified by measuring serum creatinine levels, the of loss of protein in the urine by analysing the urinary albumin-creatinine ratio or the estimated glomerular filtration rate (eGFR) by taking blood creatinine levels, the age, body size, and gender into the equation (Wang et al. 2019; Devarajan et al. 2022). GFR measurements of less than 60 ml/min/1.73m², albuminuria of >300 mg within 24 hours, or an urine albumin-to-creatinine ratio of >30 mg/g persisting over a period of three months is classified as clinically relevant CKD (Stevens and Levin 2013).

Glomerular disease

The first SRNS/FSGS genes discovered encoded proteins localized to the slit diaphragm (Somlo and Mundel 2000; Tryggvason et al. 2006). Today the spectrum of genes, and mutations that affect podocyte's homeostasis and survival and cause FSGS is far more diverse and complex including genes encoding for additional slit diaphragm components (*NPHS1* (nephrin), *NPHS2* (podocin), *CD2AP*, *CRB2*), actin-binding proteins (*ACNT4*, *INF2*, *MYH9*, *MYO1E*), actin regulators (*ARHGDIA*, *KANK1*,*2*,*4*), focal adhesion proteins (*ITGA3*, *LAMB2*), and proteins controlling transcriptional processes (*WT1*, *LMX1B*, *WDR73*, *SMARCAL1*, *NUP93*, *NUP107*,

NUP205). 84.4 % of all SRNS cases, with congenital onset of disease within the first 3 months of life, are caused by mutations in one of only four genes: *NPHS1, NPHS2, LAMB2,* and *WT1*. If the onset of the disease lies within the first year of life, those four genes still account for 66.3 % of cases (Hinkes et al. 2007). Considering their functional relevance as the glomerular filtration layer, it is not surprising that dysfunctional proteins cause a broad variety of glomerular diseases.

FAT1

The FAT atypical cadherin (FAT) ortholog Ft was first discovered in Drosophila (Evang 1925). Four human FAT orthologs are identified today with conserved structure and function (Down et al. 2005; Tanoue and Takeichi 2005). Of all four FAT proteins, FAT1 is characterized the most due to its involvement in multiple different disease entities (Valletta et al. 2014; Mariot et al. 2015; Lahrouchi et al. 2019) and is linked to the Wnt/β-catenin (Morris et al. 2013), the Hippo (Ahmed et al. 2015) and the MAPK/ERK signaling pathways (Hu et al. 2017). In the kidney, FAT1 is located in the podocytes and part of the slit diaphragm, and FAT1 deficiency is associated with decreased cell adhesion and podocyte malformations (Yaoita et al. 2005; Lahrouchi et al. 2019).

Hippo Signaling

The Hippo pathway and its first pathway core components NDR family protein kinase Warts (*Wts*) (Xu et al. 1995), WW domain-containing protein Salvador (*Sav*) (Tapon et al. 2002), Ste20-like protein kinase Hippo (*Hpo*) (Wu et al. 2003), and the tumour suppressor Mob (*Mats*) (Lai et al. 2005) were first discovered in *Drosophila melanogaster*. When active, the mammalian Hpo core kinases MST1/2 form heterodimers with the Sav ortholog SAV1 to phosphorylate SAV1 (Park and Lee 2011), the Mats ortholog MOB1 (Praskova et al. 2008), and the Wts ortholog kinases LATS1/2 (Chan et al. 2005). LATS1/2 phosphorylate yes-associated protein (YAP) and WW domain-containing transcription regulator protein 1 (TAZ) preventing their translocation into the nucleus (Zhao et al. 2007). When inactive, dephosphorylated YAP and TAZ translocate into the nucleus and act as co-regulators together with TEAD transcription factors to induce cell proliferation, cell-cell survival, and migration (Zhao et al. 2008; Zhang et al. 2009). Dysregulation of the Hippo pathway components has been frequently reported in multiple cancer types, including glioma (Masliantsev et al. 2021), colorectal cancer (Cheung et al. 2020; Sun et al. 2020), pancreatic cancer (Ansari et al. 2019), breast cancer (Yousefi et al.

2022), and endometrial cancer (Moon et al. 2022). Furthermore, the Hippo Pathway plays essential roles in immunity (Wang et al. 2017; Du et al. 2018), embryogenesis (Wu and Guan 2021), angiogenesis (Boopathy and Hong 2019), cardiovascular diseases (Leach et al. 2017), fibrotic diseases (Mia and Singh 2022), and kidney diseases (Müller and Schermer 2020; Sun et al. 2022; Zhang et al. 2022). Focusing on kidney disease, it has been shown, that the Hippo pathway is involved in kidney cancer (Rybarczyk et al. 2017; White et al. 2019), ADPKD-associated cystic kidney disease (Cai et al. 2018; Kunnen et al. 2018), CKD (Patel et al. 2019), and FAT1-associated kidney disease (Gee et al. 2016; Sethi et al. 2022). Recessive FAT1 mutations have been reported in patients with SRNS, nephropathy, syndactyly, and neurological and ocular features (Gee et al. 2016; Lahrouchi et al. 2019).

Disease spectrum

Unfortunately, the SRNS/FSGS spectrum becomes genetically much more heterogeneous with age (Hinkes et al. 2007; Büscher et al. 2016; Sadowski et al. 2015). To date over 40 monogenic forms of SRNS/FSGS have been identified making this group one of the most genetically heterogeneous rare kidney diseases. In general, monogenetic causes of kidney disease are present in ~10 % of adult cases and 20 % of children (Vivante and Skorecki 2019; Groopman et al. 2019). Recent studies report that genetic testing with WES or gene panel sequencing result in a diagnostic rate of 30 % in paediatric and 5-30 % in adult patients with CKD (Connaughton and Hildebrandt 2020). In specialized disease groups, diagnostic yields can reach up to ~80 % (Morinière et al. 2014).

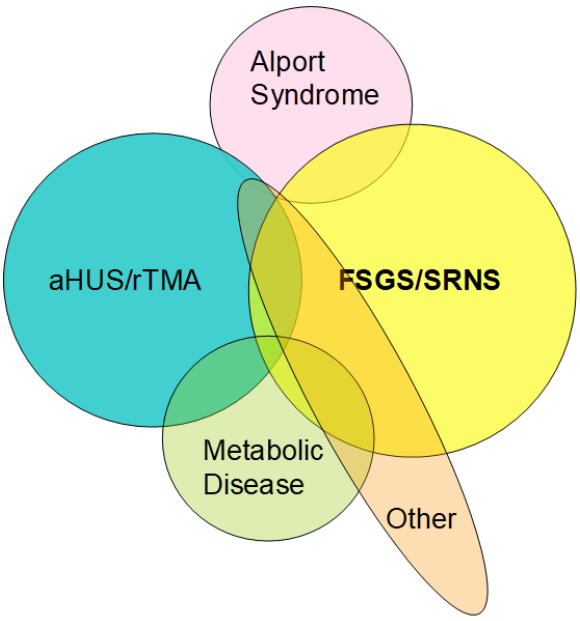

Figure 2: Overlapping phenotype correlation between FSGS/SRNS, aHUS, Alport syndrome and other diseases.

Additionally, the FSGS spectrum shows substantial clinical and histological overlap with other clinically significant disease entities like Alport syndrome (Gast et al. 2016), the spectrum of renal thrombotic microangiopathies/atypical haemolytic uremic syndrome (rTMA/aHUS), which may result in nephrotic range proteinuria (Costero et al. 2010; Manenti et al. 2013), specific metabolic disease e.g. DGKE associated aHUS/SRNS (Lemaire et al. 2013), or *MMACHC* associated cobalamin C deficiency (Beck et al. 2017), and other rare kidney diseases like Bartter Syndrome (Figure 2) (Su et al. 2000; Lee et al. 2011). Mutations in complement regulators (e.g. CFH, CFI) have also been reported as the cause of SRNS/FSGS (Sethi et al. 2012; Manenti et al. 2013).

The complement system

The name “complement”, derives from the heat-sensitive lytic components exhibiting non-specific antimicrobial properties, complementing heat-stable serum proteins like antibodies, found in blood by Jules Bordet and therefore was termed “complement” by Paul Ehrlich in the year 1899 (Ling and Murali 2019; Chaplin, JR 2005). Today the complement system is known for its essential role in our innate immune system in the defence against microbial pathogens including bacteria, fungi and viruses, for removing apoptotic cells and debris from circulation and damaged tissue and in the inflammatory response (Mevorach et al. 1998; Schifferli et al. 1986).

The complement system consists of a broad range of over 50 circulating fluid phase- and cell-surface-associated proteins that are mostly produced in the liver (Gadjeva 2014). Activation of the classical and the lectin pathways are initiated by binding to immune complexes or pathogens (Merle et al. 2015a). The alternative pathway however, does not require initial activation and remains constitutively active at a low level, ready to be enhanced to “tick over”

to full activity if a certain level of stimulus is reached (Merle et al. 2015b). Each of the three pathways leads to the cleavage and activation of the central complement component C3 which activates C5 convertase that initiates the agglomeration of multiple complement components (C5b-C9n) that form the lytic membrane attack complex that punctures the target cell and destroys it (Müller-Eberhard 1986; Schröder-Braunstein and Kirschfink 2019). To regulate the alternative pathway and differentiate between "self" and "non-self" cells there exist multiple regulating proteins that act both circulating in fluid phase like complement factor H (CFH) and complement factor I (CFI) as well as on cell surfaces like membrane cofactor protein (CD46) (Merle et al. 2015a). Dysfunction of any of the many complement cascade components or regulating proteins may cause complement deficiency and subsequently follow-up diseases like thrombotic microangiopathy (TMA), C3 glomerulopathy (C3G) (Smith et al. 2019), glomerulonephritis (GN) (Kaartinen et al. 2019), systemic lupus erythematosus (SLE) (Weinstein et al. 2021), and age-related macular degeneration (AMD) (Armento et al. 2021). TMAs can be further divided into primary TMAs like *ADAMTS13*-associated thrombotic thrombocytopenic purpura (TTP) (Zheng et al. 2002), and HUS/aHUS (Jokiranta 2017), or secondary HUS, caused by complement activation through other disease processes like infection (Kavanagh et al. 2013), autoimmune disease (Babar and Cohen 2018), drugs (Hunt et al. 2017), pregnancy-associated TMA (Cody et al. 2022), and malignant hypertension-associated TMA (Cavero et al. 2022).

Atypical haemolytic uremic syndrome

rTMAs/HUS/aHUS are commonly characterized by thrombocytopenia, mechanical haemolytic anaemia, intravascular haemolysis, and acute renal injury (Loirat and Frémeaux-Bacchi 2011). While HUS usually manifests after clinical gastroenteritis caused by the Shiga toxin-producing Escherichia coli (STEC; STEC-HUS) (Riley et al. 1983), aHUS constitutes a genetic, or acquired disease caused by mutations in the complement components CFH (Warwicker et al. 1998), C3 (Frémeaux-Bacchi et al. 2008), CD46 (Richards et al. 2003), CFI (Kavanagh et al. 2005), and complement factor B (CFB) (Goicoechea de Jorge et al. 2007). Additionally, some patients with aHUS have been reported to carry mutations in genes that are not directly associated with the complement system (Lemaire et al. 2013; Bu et al. 2014; Delvaeye et al. 2009). Here, we focused on CFH-associated aHUS. CFH is one of the key components of the alternative pathway of the complement system, regulating the complement pathway activation by

competing against CFB in the binding of C3b (Conrad et al. 1978). Factor H (formally known as beta 1 H globulin) acts as a cofactor for plasma serine protease CFI-mediated C3b degradation and C3b inactivator accelerator, both in the fluid phase and on cell surfaces (Whaley and Ruddy 1976; Pangburn et al. 1977). The N-terminal area is responsible for the decay-acceleration and the co-factor activity, while the C-terminal end of CFH is correlated with cell surface recognition (Gordon et al. 1995; Józsi et al. 2007). The CFH protein family includes the complement regulator CFH and the five CFH-related proteins CFHR1-CFHR5. Because of successive large genomic duplication events, CFH and its five related proteins show high sequence and structural homology which predispose to structural recombination (Zipfel et al. 1999). Until today, multiple different SVs have been found in the large *CFH*/*CFHR* gene cluster, mainly caused by non-allelic homologous recombination (NAHR) (Heinen et al. 2006; Venables et al. 2006; Moore et al. 2010; Maga et al. 2011; Francis et al. 2012; Eyler et al. 2013).

The renal tubular system

The glomerulus opens into the renal tubules consisting of the proximal convoluted tubule (A), the loop of Henle (B), the distal convoluted tubule (C), and the collecting duct (D).

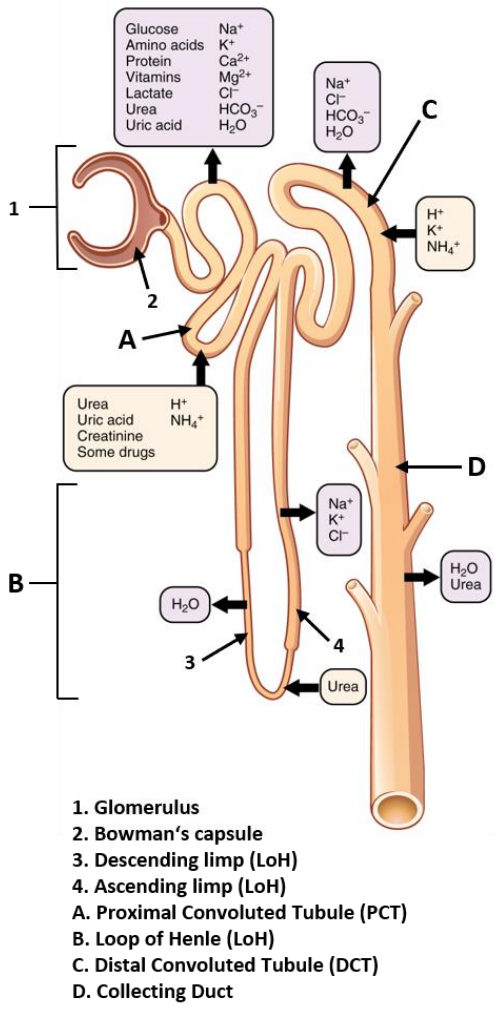

Figure 3: Anatomy of the nephron. Adapted from "Anatomy and Physiology by J. Gordon Betts (2013)" and modified by Nikolai Tschernoster.

The Bowman's capsule gives rise to the first portion of the renal tubular system, the proximal convoluted tubule. Plastered with microvilli to enlarge their luminal surface area, the proximal convoluted tubule epithelial cells are capable to reabsorb between 60-80 % of the glomerular filtrate, nearly all of the glucose, 90 % of calcium 50 % of the urea, most of the bicarbonate, phosphate, citrate and amino acids, vitamins, sulphate, much of the chloride and 65 % sodium and potassium (Figure 3A) (Brown, JR 1966; Radi 2019).

The proximal convoluted tubule turns into the descending limb of the loop of Henle. Here, up to 15 % of water is passively reabsorbed through permanent aquaporin channels and sodium chloride is actively absorbed by ATPase pumps. Urea passively diffuses into the lumen (Kokko 1970; J. Gordon Betts et al. 2013 // 2013-). In the following ascending limb of the loop of Henle however, aquaporin channels are completely absent and no water is reabsorbed. Here, approximately 30 % sodium, chloride, and potassium are actively reabsorbed from the lumen through the epithelial cells into the blood by co-transporting channels (ATPase pumps) (Figure 3B). Mutations in these channels cause different types of "salt-losing tubulopathies" that have been merged under the general term of Bartter Syndrome (BS type 1-5) (Ares et al. 2011; Simon et al. 1996b; Simon et al. 1996a; Simon et al. 1997; BARTTER et al. 1962; Schlingmann et al. 2004; Laghmani et al. 2016; Seyberth et al. 1985). In BS, mutations in *SLC12A1* or *KCNJ1* are linked to a severe neonatal onset, while mutations in *CLCNKB* usually cause a milder course and later onset of symptoms.

BS 3 results from mutations in, or the whole deletion of, the *CLCNKB* gene encoding the ClC-Kb chloride channel (Simon et al. 1997). Whole gene deletion of *CLCNKB* is considered the most frequent mutation among BS 3 (Simon et al. 1997; Konrad et al. 2000; Han et al. 2017; Han et al. 2020; Seys et al. 2017; Najafi et al. 2019). BS 3 is classified as classical BS with variable onset of the disease ranging from the antenatal to the adult stage (Seys et al. 2017). Overlapping phenotypes to antenatal/neonatal BS and Gitelman Syndrome have also been described (Brochard et al. 2009b; Jeck et al. 2000; Konrad et al. 2000; Matsunoshita et al. 2016; Seys et al. 2017). Patients with mutations in *CLCNKB* are prone to develop CKD (25 %) which can progress to end-stage renal disease in ~8 % of cases (Seys et al. 2017; Matsunoshita et al. 2016). Central clinical feature of BS 3 is severe hypochloraemia and the most frequent symptoms are hypokalaemia, polyuria, polydipsia, vomiting, constipation, dehydration, hypotonia, and failure to thrive (Brochard et al. 2009b; Han et al. 2017; García Castaño et al. 2017). CKD has frequently been reported in several BS subtypes (exception BS 5) (Kiran et al. 2014; Brochard et al. 2009b; Palazzo et al. 2022; Yamazaki et al. 2009), characterized by proteinuria, low GFR, and FSGS (Bettinelli et al. 2007; Akil et al. 2010).

In the distal convoluted tubule, another 10-15 % of water and 7-10 % of calcium are reabsorbed. Contrary, hydrogen ions, and creatinine are actively secreted (J. Gordon Betts et al. 2013 // 2013-; Radi 2019). An additional 10 % of magnesium is reabsorbed by the $Mg2^{+}$ Influx channel, encoded by the *TRPM6* gene (Hierholzer and Wiederholt 1976; Voets et al. 2004), and 5-10 % of sodium is transported out of the lumen by the NaCl cotransporter (NCC) (Figure 3C) (Subramanya and Ellison 2014). The disease resulting from mutations in the *SLC12A3* gene, encoding the NCC channel is named Gitelman syndrome (GS). GS is also included in the various types of “salt-losing tubulopathies” and clinically closely related to the classical BS 3 symptoms, with overlapping clinical manifestations like polydipsia, polyuria, hypokalaemia, and less frequent a short statue (Gitelman et al. 1966; Fujimura et al. 2019). In patients, lacking distinctive GS features like hypercalciuria or hypomagnesemia, a definitive diagnosis can only be made by genetic testing (Simon et al. 1996c; Matsunoshita et al. 2016; Seys et al. 2017). Since BS 3 and GS are often difficult to distinguish and only genetic testing can reliably discriminate these two pathologies, proposals have been made to combine BS 3 and GS into the single disease entity of “hereditary salt-losing tubulopathies” (SLTs) (Seyberth 2008; Seyberth and Schlingmann 2011). In the collecting ducts, two distinct cell types regulate

the water and electrolyte homeostasis (Roy et al. 2015). Principal cell, expressed sodium channels (ENaC) and Aquaporin2 water channels regulate the final sodium and water reabsorption, respectively, whereas intercalated cell expressed vacuolar-type ATPases (V-ATPase) and carbonic anhydrase II regulate the secretion of protons and reabsorption of bicarbonates, respectively (Figure 3D) (Roy et al. 2015). After final manipulation, the "tubular fluid" exits the collecting ducts through the papillae into the renal pelvis, and accumulates in the bladder before excretion (Chen et al. 2017).

Evolution of DNA Sequencing

Since the discovery of the DNA structure in 1953 (WATSON and CRICK 1953), the race has begun to unravel the "human blueprint". The first method of DNA sequencing was published 24 years later by Sanger et al. (Sanger et al. 1977). Known as Sanger sequencing, the technique involves the use of a DNA polymerase enzyme and the chain-termination method to synthesize a single-stranded copy of a DNA molecule, followed by the use of a labelled nucleotide to terminate the strand at specific nucleotide positions. The labelled strands are then separated by size on a polyacrylamide gel and visualized using autoradiography (after 1986 fluorescence labelling (Smith et al. 1986)). Sanger sequencing evolved with the use of capillary electrophoresis and was the gold standard of sequencing for decades and is still broadly available today. This "first" generation of sequencing was time and cost-effective but was highly limited in throughput. In the 1990s the "International Human Genome Sequencing Consortium" containing research groups from 6 countries, the first human genome was sequenced using the Sanger sequencing method. This effort took 13 years and ~ 3 billion dollars to complete and in 2001 the first human genome was published in Nature and Science (Lander et al. 2001; Venter et al. 2001). Between 2004 and 2006, new technologies known as "next-generation sequencing (NGS)" were developed to expand our sequencing abilities. These advancements in nanotechnology principles and innovations allowed for the massive parallel sequencing of single DNA molecules, resulting in a dramatic increase in sequencing data output and a massive reduction of sequencing costs. Since 2005 new technologies were released capable of generating more and more reads per run (Margulies et al. 2005; Shendure et al. 2005). NGS technologies use massive parallel sequencing to sequence large amounts of DNA rapidly and cost-effectively. The sequencing process involves the fragmentation of the DNA into small fragments followed by sequencing each fragment in parallel in a high-

throughput manner. During sequencing, the DNA is denatured and then read in a sequencing-by-synthesis process. Here, a fluorescently labelled nucleotide is added to the DNA template and the fluorescence is detected and recorded, allowing the sequence to be determined. The fragments are then either aligned to a reference or assembled into a continuous sequence without reference (Mardis 2013). These NGS technologies however are based on relatively short read lengths of up to 300 bp, which do not allow the coverage of >70 % of human genome structural variations of over 50 bp in size as well as the analysis of larger repetitive regions and the 5 % of our genome containing large segmental duplications (Bailey et al. 2001; Chaisson et al. 2019). This analytical gap has led to the emergence of new technologies, called third-generation long-read Sequencing (LRS) that can generate longer continuous fragments of several kilobases to up to mega-base pairs (Mbp) (Oxford Nanopore Technology) instead of base pairs, which can be used to reliably detect larger repetitive regions of the genome or complex SVs (Clarke et al. 2009; Rhoads and Au 2015). For example, PacBio's HiFi library preparation system is based on circular DNA molecules, which contain a double-stranded DNA insert with single-stranded hairpin adapters at either end. This insert has a length ranging from 1 kb to over 100 kb, allowing for the production of long sequencing reads. During the process, a polymerase moves along the template, incorporating fluorescently labelled dNTPs into the growing strand. Each time a nucleotide is added, a laser is used to activate the fluorophore, and the emission is recorded by a camera. Following this, the fluorophore is cut away from the nucleotide, and the cycle is repeated to uncover the identity and sequence of each base of the long DNA fragment (Eid et al. 2009).

For the analysis of the different genomic loci in FAT1 nephropathy, Bartter syndrome, and aHUS we utilized the combination of Sanger sequencing, NGS, and LRS, together with non-sequence-based molecular genetic methods to elucidate the genomic background in our patients.

Non-sequence-based analysis: Molecular combing

The challenge of NGS short-read sequencing to capture large copy number variations (CNVs), repetitive areas, and structural variants results in a significant gap in obtaining comprehensive genetic data. Traditional cytogenetic analysis, which examines the condensed DNA of metaphase chromosomes, provides partial resolution to this issue. However, this method is confined to a resolution of ~5 Mbp, so individual genes cannot be examined (Levy-Sakin and Ebenstein 2013). Furthermore, comparative genomic hybridization (CGH) array analysis enables the recognition of chromosomal CNVs on a wide scale with high resolution, yet it is merely able to detect quantitative CNVs and does not provide specific locus details (Pinkel and Albertson 2005; Kallioniemi et al. 1992). In an effort to bridge the gap between classic cytogenetics and NGS, Fiber fluorescent in-situ hybridisation (FISH) was created in the 1990s. This family of techniques involves stretching chromosomal DNA in its linear form onto hydrophobic surfaces for FISH examination. By utilizing FISH probes, specific patterns including CNVs, SVs, and repetitive regions can be observed along the DNA molecules, allowing access to individual genes and genomic DNA ranging from 1 kb to more than 1 Mb. Molecular combing takes advantage of the effects of a moving liquid edge to stretch and order DNA molecules onto a salinized glass slide. This technique has two major benefits. To start with, all molecules are uniformly extended across the surface with a constant stretching factor, enabling direct and reliable measurements to be taken on the desired genetic region. Additionally, a large number of molecules equivalent to hundreds of genomes can be combed on a single surface, ensuring a statistically representative set of measurements (Bensimon et al. 1994).

Published Studies

Expanding the Spectrum of FAT1 Nephropathies by Novel Mutations That Affect Hippo Signaling

Francesca Fabretti[1], Nikolai Tschernoster[1], Florian Erger, Andrea Hedergott, Anja K. Buescher, Claudia Dafinger, Bjoern Reusch, Vincent K. Köntges, Stefan Kohl, Malte P. Bartram, Lutz Thorsten Weber, Holger Thiele, Janine Altmüller, Bernhard Schermer, Bodo B. Beck and Sandra Habbig

[1]FF and NT are co-first authors.

Published in Kidney International Reports 6 (2021) 1368-1378.

Reprint with permission from Fabretti, Tschernoster et al. 2021 published by Elsevier Inc.

KEYWORDS: children; genetic kidney disease; Hippo signaling; podocyte; TAZ; YAP

Author contributions:

FF: data analysis and generation, manuscript writing; **NT: data analysis and generation, manuscript writing;** FE: sample collection, data generation, and manuscript writing; AH: clinical care, ophthalmologic investigation, and manuscript writing; AKB: clinical care and sample collection; CD: sample collection; BR: data generation; VKK: sample collection; SK: clinical care; MPB: sample collection, data interpretation, and manuscript writing; LTW: clinical care; HT: data generation; JA: data generation and interpretation and manuscript writing; BS: study conception, data generation, and interpretation, and manuscript writing; BBB: study conception, sample collection, data generation and interpretation, and manuscript editing; SH: study conception, sample collection, data generation and interpretation, manuscript writing, and final approval.

Supplementary Material is listed in Supplementary Material Manuscript 1.

KI REPORTS
KIReports.org
TRANSLATIONAL RESEARCH

Expanding the Spectrum of FAT1 Nephropathies by Novel Mutations That Affect Hippo Signaling

Check for updates

Francesca Fabretti[1,2,3,9], Nikolai Tschernoster[4,5,9], Florian Erger[4], Andrea Hedergott[6], Anja K. Buescher[7], Claudia Dafinger[1,8], Bjoern Reusch[4], Vincent K. Köntges[1,2,3], Stefan Kohl[8], Malte P. Bartram[1,2], Lutz Thorsten Weber[8], Holger Thiele[5], Janine Altmueller[5], Bernhard Schermer[1,2,3], Bodo B. Beck[4] and Sandra Habbig[8]

[1]Department II of Internal Medicine, University of Cologne, Faculty of Medicine and University Hospital Cologne, Cologne, Germany; [2]Center for Molecular Medicine Cologne (CMMC), University of Cologne, Faculty of Medicine and University Hospital Cologne, Cologne, Germany; [3]Cologne Excellence Cluster on Cellular Stress Responses in Aging-Associated Diseases (CECAD), University of Cologne, Cologne, Germany; [4]Institute of Human Genetics, University of Cologne, Faculty of Medicine and University Hospital Cologne, Cologne, Germany; [5]Cologne Center for Genomics, University of Cologne, Cologne, Germany; [6]Department of Ophthalmology, University of Cologne, Faculty of Medicine and University Hospital Cologne, Cologne, Germany; [7]Children's Hospital, Pediatrics II, University of Duisburg-Essen, Essen, Germany; and [8]Department of Pediatrics, University of Cologne, Faculty of Medicine and University Hospital Cologne, Cologne, Germany

Introduction: Disease-causing mutations in the protocadherin *FAT1* have been recently described both in patients with a glomerulotubular nephropathy and in patients with a syndromic nephropathy.

Methods: We identified 4 patients with *FAT1*-associated disease, performed clinical and genetic characterization, and compared our findings to the previously published patients. Patient-derived primary urinary epithelial cells were analyzed by quantitative polymerase chain reaction (qPCR) and immunoblotting to identify possible alterations in Hippo signaling.

Results: Here we expand the spectrum of *FAT1*-associated disease with the identification of novel *FAT1* mutations in 4 patients from 3 families (homozygous truncating variants in 3, compound heterozygous missense variants in 1 patient). All patients show an ophthalmologic phenotype together with heterogeneous renal phenotypes ranging from normal renal function to early-onset end-stage kidney failure. Molecular analysis of primary urine-derived urinary renal epithelial cells revealed alterations in the Hippo signaling cascade with a decreased phosphorylation of both the core kinase MST and the downstream effector YAP. Consistently, we found a transcriptional upregulation of *bona fide* YAP target genes.

Conclusion: A comprehensive review of the here identified patients and those previously published indicates a highly diverse phenotype in patients with missense mutations but a more uniform and better recognizable phenotype in the patients with truncating mutations. Altered Hippo signaling and derepressed YAP activity might be novel contributing factors to the pathomechanism in *FAT1*-associated renal disease.

Kidney Int Rep (2021) **6,** 1368–1378; https://doi.org/10.1016/j.ekir.2021.01.023
KEYWORDS: children; genetic kidney disease; Hippo signaling; podocyte; TAZ; YAP
© 2021 International Society of Nephrology. Published by Elsevier Inc. This is an open access article under the CC BY-NC-ND license (http://creativecommons.org/licenses/by-nc-nd/4.0/).

The rapid development of novel sequencing technologies has substantially improved molecular diagnosis of genetic kidney diseases in children and adults. The continuous identification of novel disease-causing genes and new genotypes in established monogenic disorders is a powerful and effective approach to gain deeper insights in underlying pathogenic mechanisms of renal disease. This is the prerequisite to ultimately develop specific therapeutic strategies to improve the treatment of these genetic diseases. Affected proteins in genetic kidney diseases show a huge variety of different expression patterns and molecular functions. Subsequently, phenotypes can range from an isolated kidney pathology with only 1 specific cell type affected (e.g., podocytes in *NPHS1*-associated congenital nephrotic syndrome[1]) to a syndromic

Correspondence: Sandra Habbig, Department of Pediatrics, University of Cologne, Faculty of Medicine and University Hospital Cologne, Kerpener Str. 62, 50935 Cologne, Germany. E-mail: sandra.habbig@uk-koeln.de

[9]FF and NT are co-first authors.

Received 19 October 2020; revised 15 January 2021; accepted 18 January 2021; published online 29 January 2021

phenotype with 2 or more organ systems involved (e.g., autosomal dominant or recessive polycystic kidney disease (ADPKD, ARPKD), or nephronophthisis (NPH) and nephronophthisis-related ciliopathies).[2] As to the kidney, the disease-causing phenotype is often restricted to 1 distinct population of epithelial cells and leads to pathologies, for example, in either podocytes or tubular epithelial cells in specific segments of the nephron. Interestingly, mutations in the gene encoding for the giant protocadherin FAT1 have been identified in a subset of patients, with very heterogeneous phenotypes displaying isolated kidney disease in some and multisystemic disorders in other cases.[3–7] This kidney disease has been characterized as a glomerulotubular nephropathy because both podocytes and tubular cells are affected.[5] Consistently, podocyte-specific loss of *FAT1* in mice leads to severe glomerular disease,[5] whereas loss of *FAT1* in zebrafish causes cyst formation in the pronephros which is ameliorated by depletion of the Hippo effector Yap1.[8] Interestingly, somatic mutations in *FAT1* have been identified in numerous tumor diseases and, consistent with the observation in zebrafish,[8] *FAT1* has been shown to be a potent regulator of Hippo signaling,[9–12] a well-established tumor-suppressor pathway. The Hippo pathway has also been shown to be associated to several kidney diseases,[8,13–22] with evidence for both overactivation and inactivation of Hippo signaling as possible pathomechanisms.

We here report 4 patients from 3 families with *FAT1*-associated syndromic nephropathy caused by novel mutations that have been identified within the framework of our clinical research unit (CRU329) during the last 12 months. In addition, we present first evidence that loss of *FAT1* leads to dysregulation of the Hippo pathway.

PATIENTS AND METHODS

Patients

All patients were analyzed within an interdisciplinary approach of our clinical research unit (CRU329). The study was approved by the ethics committee of the University Hospital Cologne, Germany (15-215). DNA samples were obtained with written informed consent from their guardians, and clinical and biochemical data were collected retrospectively from medical charts.

Genetic Analysis

A custom gene panel consisting of 122 genes that are associated with monogenic forms of proteinuria, as well as other nephropathies with possible concomitant proteinuria, was used (CRU329 Nephropathy Plus Proteinuria Gene Panel; see Supplementary Table S1).

Whole exome sequencing was performed using the Agilent SureSelect Human All Exom V7 enrichment (Agilent Technologies Inc., Santa Clara, CA) followed by next-generation sequencing on an Illumina HiSeq 4000 sequencing platform (Illumina, San Diego, CA). TruSight One gene panel sequencing was performed on an Illumina HiSeq 2500 sequencing platform. WES and gene panel data analysis and filtering of variants were carried out using the exome and genome analysis pipeline "Varbank2, varpipe v.3.3" of the Cologne Center for Genomics (University of Cologne). Variants were classified in accordance with the ACMG standards and guidelines for the interpretation of sequence variants.[23]

Ophthalmologic Examination

Ophthalmologic examination comprised refraction, best-corrected visual acuity (BCVA), anterior segment examination, funduscopy with dilated pupil and fundus photography, cycloplegic refraction, and an orthoptic examination. The orthoptic examination included measurement of binocular functions with Bagolini striated glasses test, Lang test, and evaluation of oculomotor findings such as smooth pursuit and saccades. Strabismus was examined by prism-cover test and by alternating cover test with prism at near and far fixation.

Isolation and Culture of Patient-Derived Primary Urine-Derived Renal Epithelial Cells

The protocol for the generation of primary urinary epithelial cells was performed as previously described.[24] Urine-derived epithelial cells were cultured from patients 2 and 3 and from 6 healthy controls. Briefly, the urine collected was transferred in 1 or more 50-ml tubes and centrifuged at 400 × *g* for 10 minutes at room temperature. The pellets were washed in wash buffer (1X phosphate-buffered saline + 100 U/ml penicillin + 100 μg/ml streptomycin + 500 ng/ml amphotericin B) and centrifuged at 200 × *g* for 10 minutes at room temperature. After that, the pellets were resuspended in 2 ml of Dulbecco's modified Eagle's medium (DMEM)–nutrient mixture F-12 ham (Sigma D6421; Sigma-Aldrich, St. Louis, MO) containing 10% fetal bovine serum, 1% GlutaMAX, 100 U/ml penicillin, 100 μg/ml streptomycin, 500 ng/ml amphotericin B, REGM renal epithelial cell growth medium SingleQuots Kit supplements (Lonza CC-4127; Lonza, Basel, Switzerland) and transferred in a 12-well plate, previously coated with 0.1% sterile gelatin for 30 minutes at 37 °C. The plates were then incubated at 37 °C in the presence of 5% CO_2, and the first colonies were visible after 4 to 5 days. Once colonies were visible, the cells were switched to proliferation medium (1:1

mixture from renal epithelial and mesenchymal cells medium). The renal epithelial medium was purchased (CC-3190 + Supplements; Lonza). The mesenchymal cell medium was prepared with DMEM with high glucose (Gibco, Waltham, MA) containing 10% fetal bovine serum, 100 U/ml penicillin, 100 μg/ml streptomycin, 1% nonessential amino acid solution (Gibco), 5 ng/ml fibroblast growth factor–basic (PeproTech, Rocky Hill, NJ), 5 ng/ml platelet-derived growth factor–AB (PeproTech) and 5 ng/ml epidermal growth factor (PeproTech). When the cells reached a confluency of 70% to 80%, they were passaged using TrypsinLE (Gibco).

Quantitative Real-Time PCR

The primary urine-derived renal epithelial cells were harvested and frozen at −80 °C in TRI Reagent (Sigma). RNA was extracted with Direct-zol RNA Miniprep kit (Zymo Research, Irvine, CA) following manufacturer instructions and cDNA was reverse transcribed using a high-capacity cDNA reverse transcription kit (Thermo Fisher Scientific, Waltham, MA) according to manufacturer instructions. Quantitative real-time PCR was performed on a QuantStudio 12K Flex systemcycler (Thermo Fisher Scientific) using 2 ng of reverse-transcribed RNA per well and TaqMan Gene Expression Master Mix (Thermo Fisher Scientific) according to manufacturer instructions. The probe-based assays used are listed in Supplementary Table S2.

The relative quantity was calculated using the ΔΔCt method. Briefly, the expression of each gene was normalized vs the amplification of either HPRT, GAPDH, or POLR2A, calculating the ΔCt. The relative quantity was calculated using as reference the average ΔCt of all 5 healthy controls. Relative quantities were then transformed in $\log_2$ and analyzed for significance using *t* test (GraphPad Prism 8; GraphPad Software Inc., San Diego, CA).

Immunoblotting

Whole protein lysates were prepared from primary urine-derived renal epithelial cells resuspending cell pellets in 1× sodium dodecyl sulfate (SDS) sample buffer and boiling at 95 °C for 5 minutes. Proteins were separated by SDS polyacrylamide gel electrophoresis. After transfer onto a polyvinylidene fluoride membrane, and blocking in 5% bovine serum albumin, the membranes were stained with anti phospho-Mst1 (Thr183) / Mst2 (Thr180), anti-MST1, anti-GAPDH, anti-phospho-YAP (Ser127), anti-YAP, and anti-CDC42 (Cell Signaling Technology, Inc., Danvers, MA, catalog nos. 3681, 3682, 5174, 13008, 14074; and BD Biosciences, Franklin Lakes, NJ, catalog no. 610928). The signal was visualized using enhanced chemiluminescence after incubation of the membranes with secondary antibodies conjugated to horseradish peroxidase. Images were acquired with a Fusion Solo S (Vilber Lourmat Germany GmbH, Eberhardzell, Germany). Densitometric analysis was performed using the software Image Studio, version 5.2 (LI-COR Biosciences GmbH, Hamburg, Germany).

Systematic Literature Review

A systematic literature review on patients with mutations in the *FAT1* gene was performed. The genotypes and phenotypes identified in this study were discussed in relation to the previously described patients.

RESULTS

Genetic Data

Patient 1 (*2006) is the offspring of consanguineous parents (Figure 1a). By gene panel analysis, a novel homozygous nonsense variant (c.5648T>A) in exon 10 of the *FAT1* gene was identified. This variant results in a premature stop codon at position 1883 (p.Leu1883*) (Figure 1b). Segregation analysis confirmed the variant in a heterozygous state in both healthy parents. The homozygous stop mutation was also identified in his younger sister (patient 2, *2015). The variant was absent from the genome aggregation database (gnomAD, last accessed in December 2020; Table 1).

In patient 3, gene panel analysis identified the homozygous frameshift variant c.8446_8447dupGC in exon 10 of the *FAT1* gene (p.Phe2817Hisfs*13). This variant has not been described before and was not found in the gnomAD database. Segregation analysis confirmed the variant in a heterozygous state in both consanguineous parents. In patients 1 to 3, no other causative mutation was identified in the gene panel analysis.

Patient 4 is the son of nonconsanguineous partners and had previously received comprehensive genetic testing with karyotyping, array comparative genomic hybridization, targeted Sanger sequencing of the genes *LAMB2*, *LAMC1*, *PLCE1*, *WT1*, and *SMARCAL1* and TruSight One gene panel sequencing, which all yielded unremarkable results. The most recent gene panel analysis identified 2 missense variants in the *FAT1* gene, later confirmed to be in a compound-heterozygous state: c.2563G>A (p.Gly855Arg) in exon 2 and c.5539G>A (p.Val1847Ile) in exon 10. Because both variants were classified as variants of unknown significance, a trio exome (both parents and the patient) analysis was performed. This analysis confirmed the compound-heterozygosity for the aforementioned *FAT1* variants, but identified no *de novo* variants in the patient. Biallelic variants in only 4 other OMIM annotated genes (*RLF*, *ASAP3*, *DNAH14*, and

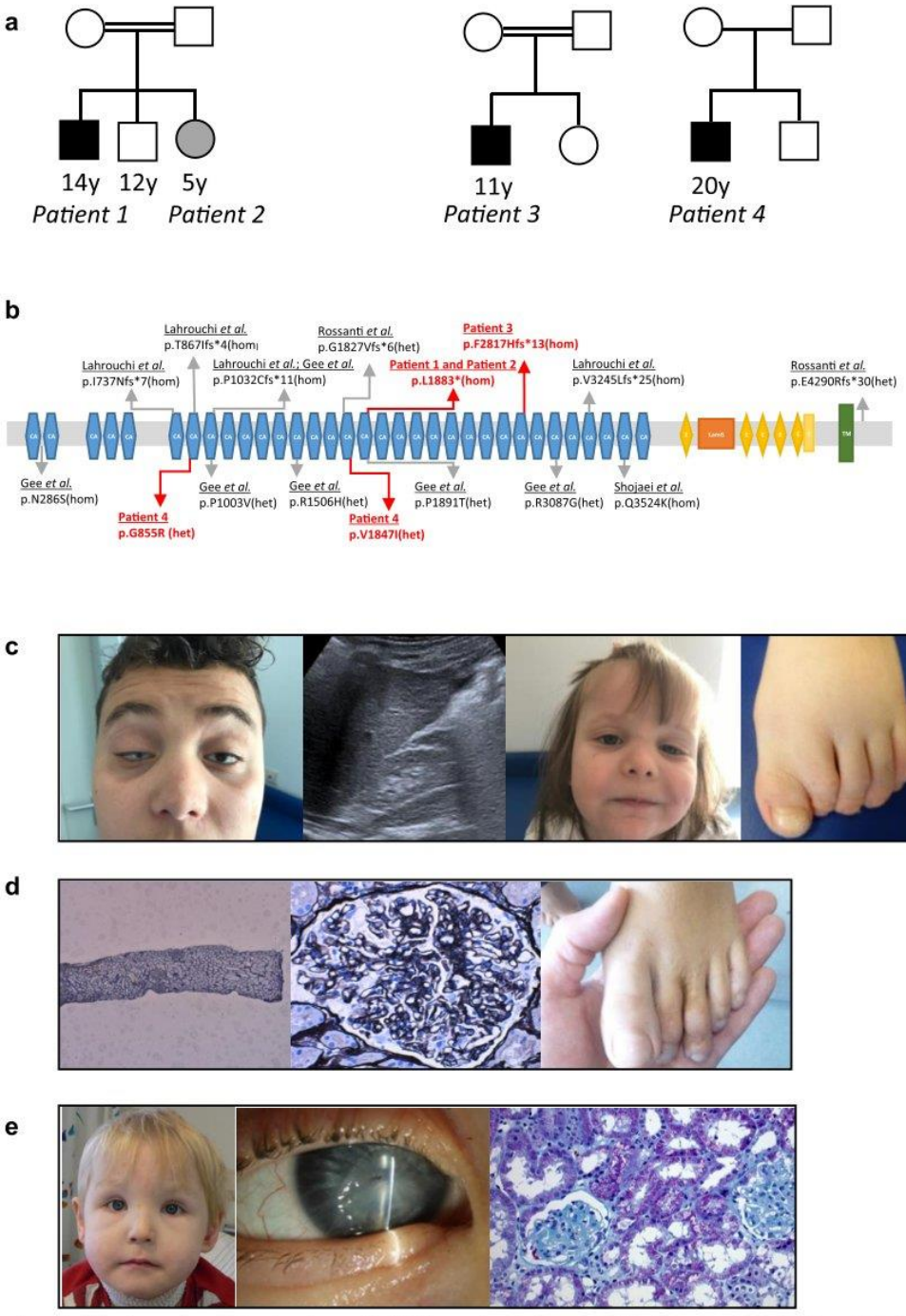

Figure 1. Genetic and clinical overview of the 4 patients with *FAT1*-associated disease. (a) Pedigrees of the 3 families. (b) Schematic view of the FAT1 protein domains. The FAT1 protein consists of 33 cadherin domains (CA), 1 laminin G domain (LamG), 5 epidermal growth factor–like domains (E), a calcium-binding domain (C) and the transmembrane domain (TM). Mutations previously described are labeled in black, novel mutations identified in this study are labeled in red. Truncating mutations are indicated above the protein scheme, missense mutations below the protein scheme. (c) Bilateral ptosis, highly arched eyebrows, and ultrasonography of the hypodysplastic right kidney of patient 1 and typical eye phenotype and feet syndactyly of patient 2. (d) Kidney biopsy in patient 3 showed low glomerular density and glomerular hypertrophy (300 µm). Syndactyly was surgically resolved in patient 3. (e) Highly arched eyebrows in patient 4 (left), anterior segment changes: micropupil, shallow anterior chamber, and trophic corneal ulcer (middle) OD; kidney biopsy in patient 4 showed diffuse mesangial sclerosis (DMS). hom, homozygous; het, heterozygous.

Table 1. Detected *FAT1* variants in 4 patients from 3 families

Patient, sex, age at investigation	Ethnic origin	Consanguinity	Nucleotide change	Exon (zygosity)	Amino acid change	Cadherin domain	Mutation taster	Frequency in gnomAD database
Patient 1, male, 14 yr	Syrian	Yes	c.5648T>A (novel)	10 (homozygous)	p.Leu1883*; truncating			
Patient 2, female, 5 yr, sister of patient 1	Syrian	Yes	c.5648T>A (novel)	10 (homozygous)	p.Leu1883*; truncating	17	Disease causing	None
Patient 3, male, 5 yr	Turkish	Yes	c.8446_8447dupGC (novel)	10 (homozygous)	p.Phe2817Hisfs*13; truncating	26	Disease causing	None
Patient 4, male, 20 yr	German	No	c.2563G>A (novel) c.5539G>A (novel)	2 10 (compound heterozygous)	p.Gly855Arg p.Val1847Ile 2 missense mutations	7 16	Disease causing Disease causing	0.21% 0.002%

FBN3) were identified. Variants in *RLF*, *ASAP3*, and *DNAH14* have not been associated with a human disease phenotype so far. Two other compound-heterozygous variants in *FBN3*—different from the variants identified in patient 4—were previously reported to segregate in a Chinese family in 2 siblings affected with a Bardet-Biedl syndrome–associated disease without renal manifestation.[25]

The homozygous truncating mutations identified in patients 1 to 3 and the compound heterozygous missense mutations identified in patient 4 are located to the cadherin repeats as outlined in the schematic of the FAT1 protein (Figure 1b).

Clinical Presentation

The diagnosis of bilateral kidney hypodysplasia in patient 1 was made at the age of 2 years. He was then lost to follow-up and presented to the hospital with acute appendicitis at the age of 9 years. Laboratory evaluation revealed end-stage kidney disease, and peritoneal dialysis was initiated immediately. The family then moved to Germany, and the patient received a living donor kidney transplant from his mother at the age of 11 years. At first clinical evaluation in Germany, his protein-creatinine ratio was elevated (3000 mg/g creatinine) with normal serum albumin. Kidney graft function is optimal at current investigation at the age of 14 years. Extrarenal symptoms are summarized in Table 2. His sister (patient 2) was born in 2015 and presented with bilateral ptosis (Figure 1c). Webbed toes (1 and 2) on the left foot were revised surgically (Figure 1c). At current investigation at the age of 5 years, there is no sign of proteinuria, arterial hypertension, or decreased kidney function in patient 2, and kidney ultrasonography shows no abnormality.

Patient 3 presented at the age of 6 months with recurrent urinary tract infections. A voiding cystourethrography identified a bilateral vesicoureteral reflux grade 3 that spontaneously resolved. At the age of 2 years, he was diagnosed with gross albuminuria (albumin-creatinine ratio 1000 mg/g creatinine) and arterial

Table 2. Synopsis of clinical findings in the patients with *FAT1* mutations

	Renal phenotype (age of onset)		Ocular manifestation	Further (extrarenal/extraocular) manifestations
	Glomerular	Other		
Patient 1	Proteinuria (protein-creatinine: 3000 mg/g at ESKD)	Kidney hypodysplasia ESKD/peritoneal dialysis (9 yr) Living-donor KTx (11 yr)	Congenital ptosis OD>OS Highly arched eyebrows Microphthalmos OD>OS with corneal opacity OD>OS, shallow anterior chamber, corectopia Lower eyelid entropion (OS) Visual impairment OD>OS	Syndactyly toes 2 and 3 (bilateral) Brachytelephalangy digitus 3, left hand Small pineal cyst Elevation of transaminases and LDH (with normal liver synthesis)
Patient 2	None	None	Congenital ptosis OS>OD	Syndactyly toes 1 and 2, left foot Mild psychomotor delay
Patient 3	Proteinuria (2 yr) Glomerular hypertrophy, low glomerular density (biopsy, 5 yr) CKD 3 (10 yr)	Vesicoureteral reflux (6 mo), spontaneous resolution at 2 yr of age	Myopia OD/OS Astigmatism OS Mild ptosis OS>OD Highly arched eyebrows	Recurrent pulmonary infections (first years of life) Bronchial asthma Syndactyly toes 1 and 2, right foot and Syndactyly toes 2 and 3, left foot
Patient 4	Nephrotic range proteinuria (6 yr) Diffuse mesangial sclerosis (biopsy, 6 yr) ESKD/hemodialysis (7 yr) KTx (9 yr)	Tubular ectasia and atrophy (biopsy, 6 yr)	Anterior segment dysgenesis Bilateral microcoria Shallow anterior chamber Bilateral neurotrophic keratopathy with trophic corneal ulcer OD and mild ptosis OD High hyperopia OD/OS Astigmatism OS Reduced visual acuity	Severe psychomotor developmental delay Epileptic seizures Deafness Congenital hypothyroidism Hypophyseal adenoma Post-transplant diabetes

CKD 3, chronic kidney disease stage 3; ESKD, end-stage kidney disease; KTx, kidney transplant; LDH, lactate dehydrogenase; OD, oculus dexter; OS, oculus sinister.

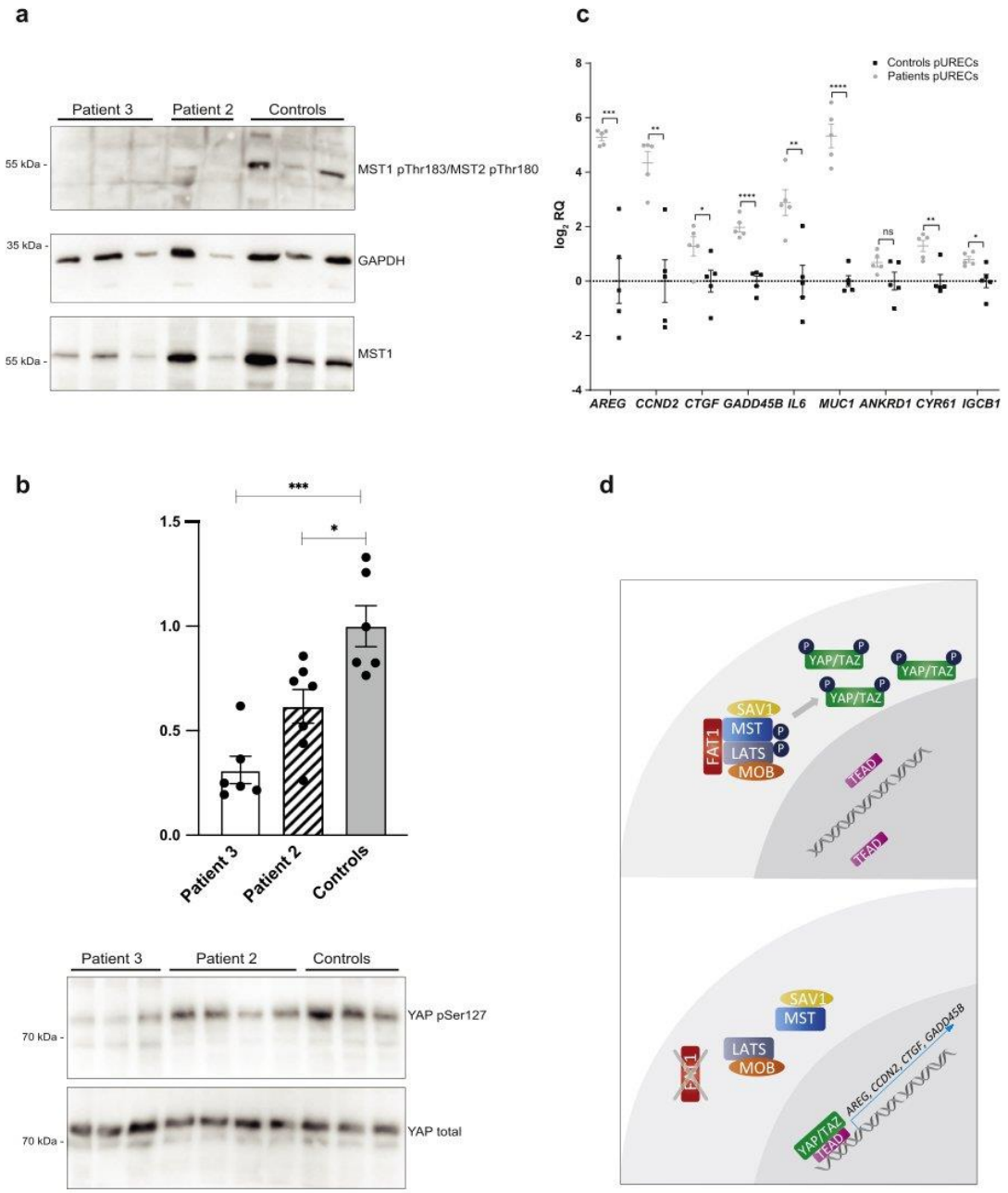

Figure 2. Dysregulation of Hippo signaling in patient-derived cells. Protein extracts from primary urine-derived renal epithelial cells (pURECs) derived from patients 3 and 2 showed a decreased phosphorylation of the central Hippo kinase MST (MST1 pThr183/MST2 pThr180) in Western blot, compared with cells derived from healthy individuals. (a) Western blot for MST1 and GAPDH was performed as loading control. (b) Protein extracts from pURECs derived from patients 3 and 2 showed a significantly decreased phosphorylation on YAP Ser127 relative to the total amount of YAP ($P < 0.05$) as shown in the Western and in the densitometric analysis. Bars show the SEM, and asterisks indicate statistical significance: $^{*}P < 0.05$ and $^{***}P < 0.005$. (c) qPCR performed on RNA derived from those cells confirmed the upregulation of the Hippo target genes. Bars show the SEM, and statistical significance is indicated by asterisks as follows: $^{*}P < 0.05$, $^{**}P < 0.01$, $^{***}P < 0.005$, $^{****}P < 0.001$. (d) Schematic representation of a possible pathomechanism in *FAT1* nephropathy. In healthy individuals (upper panel), Hippo signaling is active: the core kinase MST is phosphorylated, resulting in phosphorylation (and inactivation) of the effector proteins YAP and TAZ that are retained in the cytoplasm. Loss of FAT1 results in inactivation of MST1/2 (decreased phosphorylation) and subsequent nuclear translocation of the active (dephosphorylated) effector proteins YAP and TAZ, which act as transcriptional coactivators (lower panel). ns, not significant; SEM, standard error of the mean.

hypertension. Kidney function was normal. Therapy with renin-angiotensin-aldosterone system inhibition and β-blockers resulted in normalized blood pressure and temporarily decreased proteinuria. Renal biopsy was performed at the age of 5 years because of increased albuminuria and showed severe glomerular hypertrophy and low glomerular density without any signs of focal segmental glomerulosclerosis (Figure 1d). Since the age of 10 years, patient 3 presents with nephrotic range proteinuria and constantly decreasing kidney function (current glomerular filtration rate [full age spectrum equation] 50–60 ml/min). Syndactyly on both feet (syndactyly toes 1+2 right, 2+3 left) was surgically managed in early childhood. His eye phenotype includes the typical bilateral ptosis and highly arched eyebrows.

Patient 4 presented at the age of 6 years to our unit with nephrotic range proteinuria. Kidney biopsy showed diffuse mesangial sclerosis and partial tubular ectasia (Figure 1e). Renal function rapidly declined and hemodialysis was initiated at the age of 7 years. The patient received a cadaveric-donor kidney transplant at the age of 9 years with good transplant function during the last 12 years. Furthermore, the patient presents with a severe psychomotor delay, deafness, and recurrent epileptic seizures. His eye phenotype comprises anterior segment dysgenesis, bilateral microcoria, shallow anterior chamber, bilateral neurotrophic keratopathy with trophic corneal ulcer and mild ptosis (oculus dexter), bilateral high hyperopia, astigmatism, and severely reduced visual acuity (Figure 1e). These findings were consistent with microphthalmos, but determination of the axial length was not possible because of a lack in cooperation.

Analysis of Primary Urine-Derived Renal Epithelial Cells From Patients

As FAT1 is known to regulate the Hippo signaling pathway in the fly[12] and in certain types of cancer cells,[9] we aimed to analyze possible alterations in Hippo signaling activity in our patients and therefore isolated primary urine-derived renal epithelial cells from the 2 patients with naïve kidneys (patients 2 and 3) and from healthy controls. Protein lysates from those cells were analyzed for expression and phosphorylation of components of the Hippo pathway. This revealed decreased phosphorylation of MST1/2, the ortholog of the Hippo kinase in drosophila, in cells from the patients as compared with those from healthy individuals (Figure 2a). In addition, the phosphorylation of YAP as the main downstream effector protein of Hippo signaling was significantly decreased in patient cells as compared with controls (Figure 2b). Consistent with these data, target genes of the Hippo effector proteins YAP and TAZ were significantly upregulated in the patient cells (Figure 2c). Quantitative PCR analysis also revealed a significant upregulation of the Hippo pathway core kinases on the mRNA level, whereas expression of the Hippo effector protein YAP was not altered (Supplementary Figure S1A). Interestingly, the level of CDC42 mRNA did not significantly differ between patient and control cells, whereas immunoblot analysis revealed a significant reduction of CDC42 protein levels in patient cells compared with healthy individuals (Supplementary Figures S1B and S1C).

Literature Review

To date, 15 patients with *FAT1* mutations have been described, among these 11 with a truncating mutation and 4 with homozygous or compound heterozygous missense mutations.[3–7] The mutations identified in these patients are inserted in the gene scheme in Figure 1b. Table 3 gives an overview on the clinical characteristics of the patients published recently and of the patients of this study.

DISCUSSION

We here expand the clinical spectrum of *FAT1*-associated disease by reporting 4 further patients from 3 families. A comprehensive review of the clinical phenotypes of these patients indicates a highly diverse phenotype in patients with missense mutations but a more uniform and therefore better recognizable phenotype in the patients with truncating mutations (Table 3):

Including the present study, the cohort of patients with homozygous truncating mutations comprises 14 individuals from 8 families.[3,6] The majority of these patients presented with a specific ocular phenotype: uni- or bilateral ptosis in nearly all patients (12/14), uni- or bilateral coloboma in 9 patients (iris n=3 and retinal coloboma n=6) and microphthalmia in 4 of the 14 patients. In addition, 11 of the 14 patients presented with feet syndactyly. Intriguingly, the kidney phenotype, however, is quite variable, with absence of renal manifestations in 6 of 14 patients, asymptomatic proteinuria in 4 of 14 patients, nephrotic syndrome/proteinuria plus chronic kidney disease in 3 of 14 and bilateral renal hypodysplasia and end-stage kidney disease in 1 of 14 patients. In summary, the co-occurrence of ptosis (with or without coloboma) and webbed toes seems to be highly suggestive of a *FAT1*-truncating mutation, irrespective of the presence and the kind of associated kidney disease.

The cohort of patients with *FAT1* missense mutations comprises only 5 patients: 3 patients described by Gee *et al.*,[5] 1 described by Shojaei *et al.*,[4] and patient 4 from this study. These patients do not display the above-mentioned hallmark combination of an ocular phenotype combined with feet syndactyly. However,

all patients presented with steroid-resistant nephrotic syndrome. Kidney biopsy performed in 3 of the patients yielded minimal-change nephrotic syndrome (n=1) and diffuse mesangial sclerosis (n=2). The type of extrarenal involvement in patients with missense mutations seems to be highly variable: Gee *et al.* (2016) reported 2 patients presenting with tumors (Ewing sarcoma at the age of 13 years and Hodgkin lymphoma at the age of 10 years) and 1 girl with hydrocephalus.[5] There was no comment on extrarenal disease in the Iranian case. The patient reported in this study (patient 4) suffers from a severe multisystemic disorder with psychomotor delay, deafness, a severe eye phenotype, and endocrinologic disease features (Table 2), which prompted us to perform a trio exome analysis to look for further variants to explain this severe phenotype.

After a careful analysis of the data, we are confident that the mutation in the gene *FAT1* is the most likely explanation for the disease in patient 4 because of the following reasons: The type of kidney disease with evidence of diffuse mesangial sclerosis is in line with the previously published patients. The mutation affects one of the cadherin domains, which has been described for other disease-causing missense mutations as well. Comprehensive trio exome analysis did not identify any alternative monogenic disorder or additional pathogenic sequence variants that could contribute to the complex phenotype. Still, we note that one of the identified variants in this patient (c.2563G>A) has an allele frequency of 0.21%, which is higher than expected in the healthy reference population, with 2 homozygous individuals listed in the gnomAD database. A possible explanation for the hypothesized disease-causing effect of this variant in our patient may be a negative epistatic effect in conjunction with the second variant *in trans* (c.5539G>A). Such epistatic effects of common variants have been shown in other monogenic nephropathies including *NPHS2*-associated steroid-resistant nephrotic syndrome.[26]

A thorough phenotype review of the patients identified so far suggests a genotype-phenotype correlation, with missense mutations being commonly associated with nephrotic syndrome with variable extrarenal disease. In contrast, truncating variants result in the hallmark combination of ptosis and feet syndactyly with variable kidney disease.

Interestingly, the kidney phenotype previously described was a primarily glomerular phenotype with proteinuria ranging from early-onset proteinuria with ESKD in early childhood (e.g., patient 4) to proteinuria with a slowly progressive chronic kidney disease (e.g., patient 3 or F3IV1 with focal segmental glomerulosclerosis at the age of 20 years[3]) to asymptomatic proteinuria. Tubular ectasia was found in biopsies (without clinical evidence of a tubular disease) resulting in the classification as a glomerulotubular nephropathy.[5] Remarkably, 2 patients of our study also presented with CAKUT features: patient 1 with bilateral kidney hypodysplasia and patient 3 with bilateral vesicoureteral reflux, which was also reported in 1 patient by Gee *et al.*[5]

Further genotype-phenotype studies will be definitely needed to understand the broad and heterogenic spectrum of *FAT1*-associated disease, related to the type of kidney disease but also to the variety of extrarenal manifestations.

This study adds dysregulation of Hippo signaling to the possible pathomechanisms underlying *FAT1*-associated disease**.** The giant protocadherin FAT1 was described as a component of the glomerular slit diaphragm in rats as early as 2001[27] (at the time referred to as FAT) and, shortly after, FAT1 was localized to the intercellular junctions of podocytes.[28] A conventional knockout mouse of *Fat1* showed perinatal lethality with defect forebrain development, failure of eye development, and foot process effacement.[29] Podocyte-specific deletion of *Fat1* resulted in proteinuria and focal segmental glomerulosclerosis at the age of 4 months with abnormal foot process and slit-diaphragm development already shortly after birth.[5] The same study suggested decreased cell adhesion and migration in podocytes due to reduced Rho-like small GTPase activity as one potential mechanism involved in the pathogenesis of the FAT1 nephropathy.[5] We here confirmed these data and show a reduced level of CDC42 in urinary cells derived from our patients (Supplementary Figure S1C). Interestingly, the Rho-GTPase Cdc42 has been linked to Hippo signaling since kidney-specific knock-out of *Cdc42* results in developmental defects that phenocopy loss of *Yap*.[17,30] The authors therefore already speculated about a possible role of Hippo signaling in *FAT1*-associated disease.[5] Shortly after that study, Martin *et al.* reported that FAT1 assembles a Hippo signaling complex, which results in the activation (phosphorylation) of the Hippo core kinases (MST, MOB, LATS) with subsequent repression of YAP/TAZ transcriptional activity.[9]

We therefore decided to analyze Hippo signaling in our patients harboring *FAT1* mutations and used patient-derived renal epithelial cells from the 2 patients with naïve kidneys, one of them (patient 2) without any sign of kidney disease and one (patient 3) with nephrotic range proteinuria and chronic kidney disease stage 3. Intriguingly, Hippo signaling was dysregulated on several levels: First, loss of *FAT1* resulted in decreased phosphorylation (inactivation) of MST as one of the Hippo core kinases. Second, the main effector protein YAP was activated as shown by reduced phosphorylation in patient cells. Third, as a result of the inactivated Hippo signaling cascade and

Table 3. Synopsis of phenotypes associated with truncating and phenotypes associated with missense mutations in *FAT1*

Truncating Mutations					
Study	***n***	**Ocular features**	**Feet syn-dactyly**	**Kidney disease**	**Intellectual disability**
Lahrouchi et al. (2019)	10	9/10	8/10	5/10	3/10
pat. #1 (F1,IV:1)		ptosis, coloboma,	-	proteinuria	no
pat. #2 (F1,IV:3)		ptosis	bilateral	-	no
pat. #3 (F1,IV:5)		ptosis, coloboma, microphthalmia	bilateral	proteinuria	no
pat. #4 (F2,III:2)		ptosis, coloboma	unilateral	none	no
pat. #5 (F2,IV:1)		ptosis, coloboma, microphtalmia	unilateral	none	no
pat. #6 (F2,IV:3)		ptosis, coloboma, microphtalmia	bilateral	none	no
pat. #7 (F3,IV:1)		-	unilateral	FSGS, proteinuria, CKD	no
pat. #8 (F3,IV:3)		ptosis, coloboma, microphtalmia	unilateral	proteinuria	yes
pat. #9 (F4,II:2)		ptosis	bilateral	none	yes
pat. #10 (F4,II:2)/A4623, Gee et al (2016)		ptosis	-	proteinuria; SRNS	yes
Rossanti (2020)	1	0/1	0/1	1/1	0/1
one patient		-	-	proteinuria	no
Our study	3	3/3	3/3	2/3	0/3
patient #1		ptosis	bilateral	proteinuria, hypodysplasia, ESKD	no
patient #2		ptosis	unilateral	none	no
patient #3		ptosis	bilateral	proteinuria, VUR, CKD	no
all	**14**	**12/14 (ptosis 12/14; coloboma 6/14)**	**11/14**	**8/14 (proteinuria 8/14, CAKUT/VUR 2/14)**	**3/14**
Missense Mutations					
Gee (2016)	3	0/3	0/3	3/3	0/3
A3027		-	-	nephrotic syndrome, VUR, ESKD	no
A789		-	-	nephrotic syndrome, MCNS	no
A3507		-	-	nephrotic syndrome, DMS	no
Serajpour (2019)	1	0/1	0/1	1/1	0/1
one patient		-	-	nephrotic syndrome, SRNS	-
Our study	1	1/1	0/1	1/1	1/1
patient#4		ptosis	-	nephrotic syndrome, DMS, ESKD	Yes
all	**5**	**1/5 (ptosis 1/5)**	**0/5**	**5/5 (nephrotic syndrome 5/5, VUR 1/5)**	**1/5**

CAKUT, congenital anomalies of the kidney and urinary tract; CKD, chronic kidney disease; DMS, diffuse mesangial sclerosis; ESKD, end-stage kidney disease; FSGS, focal segmental glomerulosclerosis; MCNS, minimal change nephrotic syndrome; SRNS, steroid resistant nephrotic syndrome; VUR, vesicourethral reflux.

de-repressed YAP signaling, numerous YAP target genes were significantly upregulated in the cells derived from patients with *FAT1*-associated disease compared with those from healthy controls. The potential pathomechanism based on our findings is illustrated in Figure 2d.

Our observations are completely in line with the above-mentioned data derived from cancer cells and confirm the central role of Hippo signaling in kidney development and disease. Besides the role of the Hippo pathway in cystic kidney disease, recent studies also demonstrated the importance of the pathway in podocytes.[8,16,31–35] Interestingly, both Hippo inactivation and subsequent YAP activation as well as YAP inactivation or depletion resulted in glomerular disease and a very well-regulated balance seems to be indispensable for normal podocyte function. It is therefore tempting to speculate that dysregulation of Hippo signaling with variable compensatory mechanisms in several kidney cell types could explain the broad phenotypic spectrum of kidney disease in *FAT1*-associated disease. Of note, the dysregulation of Hippo signaling could be used as a diagnostic measure in *FAT1*-associated disease by applying the Hippo qPCR panel used in this study to urinary cells from patients suspected to harbor mutations in *FAT1*. Intriguingly, the Hippo pathway dysregulation was observed in both patients, in the one without any kidney disease phenotype (patient 2) and in the one with nephrotic range proteinuria and chronic kidney disease (patient 3).

Although the Hippo signaling pathway might represent a potential target of future therapeutic strategies, our findings have 1 additional implication. Notably, none of the patients with truncating mutations and complete loss of FAT1 presented with any type of cancer. Whether the described tumors in 2 patients with missense mutations (Ewing sarcoma and Hodgkin lymphoma) are associated with the loss of the established tumor suppressor *FAT1* and the consecutive dysregulation of Hippo signaling remains unclear. The role of the compensatory upregulation of other Hippo components such as LATS, MST, MOB, and Salvador (on mRNA level) as tumor suppressors and

possible protective factors remains as speculative as the question whether any type of tumor might have a more aggressive course or a higher incidence in FAT1 patients. Thorough clinical follow-up of patients with mutations in *FAT1* is therefore indispensable and might allow assessing the risk of tumors in the future.

In summary, this study extends the spectrum of mutations in *FAT1* and provides a detailed genotype-phenotype correlation. In addition, our data provide evidence that genetic alterations of a Hippo regulator are in a prime position to cause defects in multiple renal cell types, which could explain the broad spectrum of renal phenotypes observed in patients carrying a *FAT1* mutation.

DISCLOSURE

All the authors declared no competing interests.

ACKNOWLEDGMENTS

We thank the study's participants for their willingness to contribute to this project. We additionally thank M. Brütting and S. Keller for excellent technical support.

This work was supported by the Deutsche Forschungsgemeinschaft (DFG [German Research Foundation]), Clinical research unit (CRU 329). JA (AL901/2-1 and AL901/3-1), BBB (BE6072/2-1 and BE6072/3-1), BS (SCHE 1562/7-1 and 1562/8-1), and SH (HA8479/1-1) received funding from the DFG.

AUTHOR CONTRIBUTIONS

FF: data analysis and generation, manuscript writing; NT: data analysis and generation, manuscript writing; FE: sample collection, data generation, and manuscript writing; AH: clinical care, ophthalmologic investigation and manuscript writing; AKB: clinical care and sample collection; CD: sample collection; BR: data generation; VKK: sample collection; SK: clinical care; MPB: sample collection, data interpretation, and manuscript writing; LTW: clinical care; HT: data generation; JA: data generation and interpretation and manuscript writing; BS: study conception, data generation and interpretation, and manuscript writing; BBB: study conception, sample collection, data generation and interpretation, and manuscript editing; SH: study conception, sample collection, data generation and interpretation, manuscript writing, and final approval. SH confirms to have full access to all data.

All authors read and approved the final manuscript.

SUPPLEMENTARY MATERIAL

Supplementary File (PDF)

Table S1. Screening panel of 122 genes that are associated with monogenic forms of proteinuria, as well as other nephropathies with possible concomitant proteinuria.

Table S2. List of probe-based assays.

Figure S1. qPCR analysis of RNA extracted from pURECs derived from patients 2 and 3.

REFERENCES

1. Kestilä M, Lenkkeri U, Männikkö M, et al. Positionally cloned gene for a novel glomerular protein–nephrin–is mutated in congenital nephrotic syndrome. *Mol Cell*. 1998;1:575–582.
2. Hildebrandt F, Benzing T, Katsanis N. Ciliopathies. *N Engl J Med*. 2011;364:1533–1543.
3. Lahrouchi N, George A, Ratbi I, et al. Homozygous frameshift mutations in FAT1 cause a syndrome characterized by colobomatous-microphthalmia, ptosis, nephropathy and syndactyly. *Nat Commun*. 2019;10:1180.
4. Shojaei A, Serajpour N, Karimi B, et al. Molecular genetic analysis of steroid resistant nephrotic syndrome, detection of a novel mutation. *Iran J Kidney Dis*. 2019;13:165–172.
5. Gee HY, Sadowski CE, Aggarwal PK, et al. FAT1 mutations cause a glomerulotubular nephropathy. *Nat Commun*. 2016;7:10822.
6. Rossanti R, Watanabe T, Nagano C, et al. FAT1 biallelic truncating mutation causes a non-syndromic proteinuria in a child. *CEN Case Rep*. 2021;10:100–105.
7. Nagano C, Yamamura T, Horinouchi T, et al. Comprehensive genetic diagnosis of Japanese patients with severe proteinuria. *Sci Rep*. 2020;10:270.
8. Skouloudaki K, Puetz M, Simons M, et al. Scribble participates in Hippo signaling and is required for normal zebrafish pronephros development. *Proc Natl Acad Sci U S A*. 2009;106:8579–8584.
9. Martin D, Degese MS, Vitale-Cross L, et al. Assembly and activation of the Hippo signalome by FAT1 tumor suppressor. *Nat Commun*. 2018;9:2372.
10. Ahmed AF, de Bock CE, Lincz LF, et al. FAT1 cadherin acts upstream of Hippo signalling through TAZ to regulate neuronal differentiation. *Cell Mol Life Sci CMLS*. 2015;72:4653–4669.
11. Katoh M. Function and cancer genomics of FAT family genes. *Int J Oncol*. 2012;41:1913–1918.
12. Willecke M, Hamaratoglu F, Kango-Singh M, et al. The fat cadherin acts through the hippo tumor-suppressor pathway to regulate tissue size. *Curr Biol*. 2006;16:2090–2100.
13. Habbig S, Bartram MP, Müller RU, et al. NPHP4, a cilia-associated protein, negatively regulates the Hippo pathway. *J Cell Biol*. 2011;193:633–642.
14. Frank V, Habbig S, Bartram MP, et al. Mutations in NEK8 link multiple organ dysplasia with altered Hippo signalling and increased c-MYC expression. *Hum Mol Genet*. 2013;22:2177–2185.
15. Habbig S, Bartram MP, Sägmüller JG, et al. The ciliopathy disease protein NPHP9 promotes nuclear delivery and activation of the oncogenic transcriptional regulator TAZ. *Hum Mol Genet*. 2012;21:5528–5538.
16. Rinschen MM, Grahammer F, Hoppe AK, et al. YAP-mediated mechanotransduction determines the podocyte's response to damage. *Sci Signal*. 2017;10, eaaf8165.
17. Reginensi A, Scott RP, Gregorieff A, et al. Yap- and Cdc42-dependent nephrogenesis and morphogenesis during mouse kidney development. *PLoS Genet*. 2013;9, e1003380.

18. Happé H, van der Wal AM, Leonhard WN, et al. Altered Hippo signalling in polycystic kidney disease. *J Pathol*. 2011;224:133–142.
19. Müller RU, Schermer B. Hippo signaling—a central player in cystic kidney disease? *Pediatr Nephrol Berl Ger*. 2020;35:1143–1152.
20. Ma S, Guan KL. Polycystic kidney disease: a Hippo connection. *Genes Dev*. 2018;32:737–739.
21. Wong JS, Meliambro K, Ray J, Campbell KN. Hippo signaling in the kidney: the good and the bad. *Am J Physiol Renal Physiol*. 2016;311:F241–F248.
22. Xu D, Lv J, He L, et al. Scribble influences cyst formation in autosomal-dominant polycystic kidney disease by regulating Hippo signaling pathway. *FASEB J*. 2018;32:4394–4407.
23. Richards S, Aziz N, Bale S, et al. Standards and guidelines for the interpretation of sequence variants: a joint consensus recommendation of the American College of Medical Genetics and Genomics and the Association for Molecular Pathology. *Genet Med*. 2015;17:405–424.
24. Bartram MP, Habbig S, Pahmeyer C, et al. Three-layered proteomic characterization of a novel ACTN4 mutation unravels its pathogenic potential in FSGS. *Hum Mol Genet*. 2016;25:1152–1164.
25. Wang Y, Garraoui A, Zeng L, et al. FBN3 gene involved in pathogenesis of a Chinese family with Bardet-Biedl syndrome. *Oncotarget*. 2017;8:86718–86725.
26. Tory K, Menyhárd DK, Woerner S, et al. Mutation-dependent recessive inheritance of NPHS2-associated steroid-resistant nephrotic syndrome. *Nat Genet*. 2014;46:299–304.
27. Inoue T, Yaoita E, Kurihara H, et al. FAT is a component of glomerular slit diaphragms. *Kidney Int*. 2001;59:1003–1012.
28. Yaoita E, Kurihara H, Yoshida Y, et al. Role of Fat1 in cell-cell contact formation of podocytes in puromycin aminonucleoside nephrosis and neonatal kidney. *Kidney Int*. 2005;68:542–551.
29. Ciani L, Patel A, Allen ND, ffrench-Constant C. Mice lacking the giant protocadherin mFAT1 exhibit renal slit junction abnormalities and a partially penetrant cyclopia and anophthalmia phenotype. *Mol Cell Biol*. 2003;23:3575–3582.
30. Huang Z, Zhang L, Chen Y, et al. Cdc42 deficiency induces podocyte apoptosis by inhibiting the Nwasp/stress fibers/YAP pathway. *Cell Death Dis*. 2016;7:e2142.
31. Keyvani Chahi A, Martin CE, Jones N. Nephrin suppresses Hippo signaling through the adaptor proteins Nck and WTIP. *J Biol Chem*. 2016;291:12799–12808.
32. Kann M, Ettou S, Jung YL, et al. Genome-wide analysis of Wilms' tumor 1-controlled gene expression in podocytes reveals key regulatory mechanisms. *J Am Soc Nephrol*. 2015;26:2097–2104.
33. Bonse J, Wennmann DO, Kremerskothen J, et al. Nuclear YAP localization as a key regulator of podocyte function. *Cell Death Dis*. 2018;9:850.
34. Wennmann DO, Vollenbröker B, Eckart AK, et al. The Hippo pathway is controlled by Angiotensin II signaling and its reactivation induces apoptosis in podocytes. *Cell Death Dis*. 2014;5:e1519.
35. Chung JJ, Goldstein L, Chen YJJ, et al. Single-cell transcriptome profiling of the kidney glomerulus identifies key cell types and reactions to injury. *J Am Soc Nephrol JASN*. 2020;31:2341–2354.

Unraveling Structural Rearrangements of the CFH Gene Cluster in Atypical Hemolytic Uremic Syndrome Patients Using Molecular Combing and Long-Fragment Targeted Sequencing

Nikolai Tschernoster, Florian Erger, Patrick R. Walsh, Bairbre McNicholas, Margareta Fistrek, Sandra Habbig, Anna-Lena Schumacher, Kat Folz-Donahue, Christian Kukat, Mohammad R. Toliat, Christian Becker, Holger Thiele, David Kavanagh, Peter Nürnberg, Bodo B. Beck, and Janine Altmüller

Published in the Journal of Molecular Diagnostics 24 (2022) 619-631.

Reprint with permission from Tschernoster et al. 2022 published by Elsevier Inc.

Author contributions:

NT: data analysis and generation, figure design, and manuscript writing; FE: bioinformatic; PRW: clinical care and sample collection; BM: clinical care and sample collection; MF: clinical care and sample collection; SH: clinical care and sample collection; ALS: data generation; KF: data generation; CK: data generation; MRT: data generation; CB: data generation; HT: bioinformatic; DK: sample collection; PN: supervision; BBB: study conception, sample collection, data interpretation, manuscript writing, and final approval; JA: study conception, data interpretation, manuscript writing, and final approval.

Supplementary Material is listed in Supplementary Material Manuscript 2.

The Journal of Molecular Diagnostics, Vol. 24, No. 6, June 2022

ELSEVIER

the Journal of Molecular Diagnostics

jmdjournal.org

Unraveling Structural Rearrangements of the *CFH* Gene Cluster in Atypical Hemolytic Uremic Syndrome Patients Using Molecular Combing and Long-Fragment Targeted Sequencing

Nikolai Tschernoster,*†‡ Florian Erger,†‡ Patrick R. Walsh,§ Bairbre McNicholas,¶ Margareta Fistrek,‖ Sandra Habbig,** Anna-Lena Schumacher,†† Kat Folz-Donahue,†† Christian Kukat,†† Mohammad R. Toliat,* Christian Becker,* Holger Thiele,* David Kavanagh,§ Peter Nürnberg,*† Bodo B. Beck,†‡ and Janine Altmüller*†‡‡§§

From the Cologne Center for Genomics, the Center for Molecular Medicine Cologne,† the Institute of Human Genetics,† and the Department of Pediatrics,** University of Cologne, Faculty of Medicine and University Hospital Cologne, Cologne, Germany; the National Renal Complement Therapeutics Centre,§ Royal Victoria Infirmary and Translational and Clinical Research Institute, Newcastle University, Newcastle upon Tyne, United Kingdom; the School of Medicine,¶ National University of Ireland Galway, Galway, Ireland; the Division of Nephrology, Arterial Hypertension Dialysis and Transplantation,‖ Department of Internal Medicine, University Hospital Center Zagreb, School of Medicine, University of Zagreb, Zagreb, Croatia; the FACS & Imaging Core Facility,†† Max Planck Institute for Biology of Ageing, Cologne, Germany; the Berlin Institute of Health at Charité—Universitätsmedizin Berlin,‡‡ Core Facility Genomics, Berlin, Germany; and the Max Delbrück Center for Molecular Medicine in the Helmholtz Association,§§ Berlin, Germany*

Accepted for publication February 25, 2022.

Address correspondence to Janine Altmüller, M.D., Max Delbrück Center for Molecular Medicine in the Helmholtz Association, Hannoversche Strasse 28, 10115 Berlin, Germany; or Nikolai Tschernoster, M.Sc., Cologne Center for Genomics, University of Cologne, Faculty of Medicine and University Hospital Cologne, Weyertal 115b, 50931 Cologne, Germany.
E-mail: janine.altmueller@bih-charite.de or nikolai.tschernoster@uk-koeln.de.

Complement factor H (CFH) and its related proteins have an essential role in regulating the alternative pathway of the complement system. Mutations and structural variants (SVs) of the *CFH* gene cluster, consisting of *CFH* and its five related genes (*CFHR1-5*), have been reported in renal pathologies as well as in complex immune diseases like age-related macular degeneration and systemic lupus erythematosus. SV analysis of this cluster is challenging because of its high degree of sequence homology. Following first-line next-generation sequencing gene panel sequencing, we applied Genomic Vision's Molecular Combing Technology to detect and visualize SVs within the *CFH* gene cluster and resolve its structural haplotypes completely. This approach was tested in three patients with atypical hemolytic uremic syndrome and known SVs and 18 patients with atypical hemolytic uremic syndrome or complement factor 3 glomerulopathy with unknown *CFH* gene cluster haplotypes. Three SVs, a *CFH/CFHR1* hybrid gene in two patients and a rare heterozygous *CFHR4/CFHR1* deletion in *trans* with the common *CFHR3/CFHR1* deletion in a third patient, were newly identified. For the latter, the breakpoints were determined using a targeted enrichment approach for long DNA fragments (Samplix Xdrop) in combination with Oxford Nanopore sequencing. Molecular combing in addition to next-generation sequencing was able to improve the molecular genetic yield in this pilot study. This (cost-)effective approach warrants validation in larger cohorts with CFH/CFHR-associated disease. *(J Mol Diagn 2022, 24: 619—631; https://doi.org/10.1016/j.jmoldx.2022.02.006)*

Complement factor H (CFH) is long known for its essential role in regulation of the alternative pathway of the complement system. The CFH protein family includes the complement regulator CFH and CFH-like protein 1, a shorter alternative splicing product of CFH, as well as the five CFH-related proteins, CFHR1, CFHR2, CFHR3, CFHR4, and CFHR5.[1,2] Together, they form the *CFH* gene

Supported by the Deutsche Forschungsgemeinschaft (DFG; German Research Foundation) clinical research unit (KFO 329) AL901/2-1 and AL901/3-1 (J.A.) and clinical research unit (KFO 329) BE6072/2-1 and BE6072/3-1 (B.B.B.). This work received additional support by the DFG Research Infrastructure as part of the Next Generation Sequencing Competence Network (project 423957469).

B.B.B. and J.A. contributed equally to this work.

Disclosures: None declared.

Copyright © 2022 Association for Molecular Pathology and American Society for Investigative Pathology. Published by Elsevier Inc.
This is an open access article under the CC BY-NC-ND license (*http://creativecommons.org/licenses/by-nc-nd/4.0*).
https://doi.org/10.1016/j.jmoldx.2022.02.006

cluster spanning over approximately 360 kb.[3] Because of successive large genomic duplication events during human evolution, *CFH* and its five related genes (*CFHR1* to *CFHR5*) show high sequence and structural homologies and lie in a head-to-tail arrangement within the regulators of the complement activation gene cluster on chromosome 1q32.[4–6] These genomic structural variants are most probably caused by nonallelic homologous recombination[7,8] and interlocus gene conversion[2] or a mechanism called microhomology-mediated end joining, reported by Challis et al[9] and Francis et al,[10] respectively. The circulating plasma protein CFH is primarily produced in the liver and is composed of individual folding domains called short consensus repeats. CFH's C-terminal region has a surface recognition function, whereas the N-terminal region mediates cofactor and decay-acceleration activity.[11] Zipfel et al[12] reviewed the composition and functionality of CFH and its related proteins in more detail. Mutations and structural variants (SVs) have been reported for atypical hemolytic uremic syndrome (aHUS), glomerulonephritis, immune complex membranoproliferative glomerulonephritis and complement factor 3 glomerulopathy (C3G),[13,14] dense-deposit disease,[15] and systemic lupus erythematosus (SLE).[16] A missense variant in *CFH* (Y402H) has been proposed to be a major risk variant in age-related macular degeneration pathology.[17] In contrast, the common *CFHR3/CFHR1* deletion has been confirmed to protect against age-related macular degeneration as *CFHR3/CFHR1* deletion is less frequent in individuals with age-related macular degeneration pathology than in controls.[18–20] In aHUS, the *CFHR3/CFHR1* deletion is associated as risk factor for the development of anti-CFH autoantibodies, resulting in a disease called deficiency of CFHR plasma proteins and autoantibody-positive form of hemolytic uremic syndrome (DEAP-HUS).[21,22] In addition, the *CFHR3/CFHR1* deletion is proposed to lower the risk of IgA nephropathy.[23] There were also conflicting results published regarding CFH (eg, the possible role of variant Y402H for susceptibility and severity of schizophrenia).[24,25] Noteworthy, just recently, Tang et al[26] showed that there is evidence of increased CFH protein levels in patients with anhedonia in drug-naïve major depression disorder, expanding the spectrum of CFH involvement in a great variety of pathologies.

Atypical Hemolytic Uremic Syndrome

Hemolytic uremic syndrome (HUS; Online Mendelian Inheritance in Man number 235400) is a rare but severe and genetically heterogeneous disease that belongs to the group of thrombotic microangiopathies and arises from an initial endothelial cell injury.[27] aHUS is mainly caused by deregulation of the alternative pathway of the complement system and follows an acute episodic clinical course.[28] The immunohistologic finding of glomerular C3 deposition is termed C3 glomerulopathy (C3G) and represents a separate disease entity. Thrombotic microangiopathy is not observed, and the disease course is often chronic-progressive. However, the pathomechanistic cause of C3G also lies in an inadequately increased activity of the alternative pathway of the complement system.[29] Research into the genetic basis of both aHUS and C3G has identified pathogenic variants, including structural variants in several different complement-associated genes. Genomic aberrations or structural variants affecting the complement factor H (*CFH*) gene cluster were reported in approximately 4.5% of patients, in a cohort of 154 individuals with aHUS analyzed by multiplex ligation-dependent probe amplification (MLPA),[7] and are often caused by nonallelic homologous recombination events.[7,9,10] Incomplete penetrance is frequently observed in families with autosomal dominant aHUS, where unaffected family members carry the causative aberration as well.[30,31] These variants either decrease the activity of the complement-regulating proteins or increase the activity of complement activator proteins, leading to a decreased threshold for inappropriate pathologic complement activation.

The current routine molecular diagnostics for aHUS patients consist of next-generation sequencing (NGS) or Sanger sequencing, augmented by deletion and duplication testing using MLPA.[7,9,32]

CFH/CFHR hybrid gene identification can be performed using either chromosomal microarray[7,33] or PCR-based approaches, the latter of which may also allow for breakpoint detection.[7,9,33] CFH autoantibodies are associated with the frequent homozygous *CFHR3/CFHR1* deletions and are often tested with enzyme-linked immunosorbent assay.[33,34] In a research setting, Cantsilieris et al[4] performed high-quality sequencing, including six primate lineages and multiple human haplotypes, to analyze the evolutionary development of the highly homologous *CFH* gene cluster using bacterial artificial chromosomes, fosmids, and long-read sequencing approaches. The synthesis of hybrid transcripts and secretion of hybrid proteins can be analyzed by Western blot analysis.[7,9]

This study aimed to increase the molecular genetic diagnostic yield of patients presenting with unresolved aHUS and C3G disease by combining NGS with molecular combing and breakpoint identification in the *CFH* gene cluster.

Materials and Methods

Patient Cohort

A total of 21 patients with a clinical diagnosis of aHUS ($n = 15$) or C3G ($n = 6$) were included in this study (Supplemental Table S1). Infection- and medication-associated causes of hemolytic uremic syndrome were excluded in all patients. Three patients with a known structural aberration (F15, F19, and F20) in the *CFH* gene cluster were used as positive controls. DNA of the remaining 18 unresolved patients (the discovery cohort), including two sisters from family 10 with homozygous *CFH*

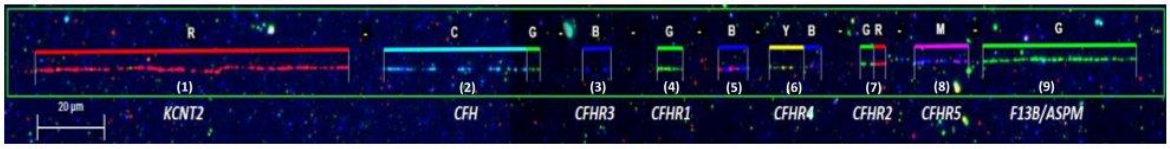

Figure 1 Reference complement factor H (*CFH*) gene cluster on chromosome 1q32. *CFH/CFHR1-5* gene-cluster identification on a hybridized Combicoverslip of a patient with no structural aberrations detected using the FiberStudio software version 2.0.2. All molecular combing images were taken at FiberStudio's zoom level (−7) with a ×40 magnification. Validated signal with labeled genes from left ro right: red, *KCNT2* (1); cyan/green, *CFH* (2); blue, *CFHR3* (3); green, *CFHR1* (4); blue, intronic region (5); yellow/blue, *CFHR4* (6); green/red, *CFHR2* (7); magenta, *CFHR5* (8); green, *F13B* + *ASPM* (9). *CFH* is labeled in cyan with a short region at the C-terminus labeled in green. *CFHR3* labeled in blue, followed by *CFHR1* labeled in green. An intronic region between *CFHR1* and *CFHR4* is labeled in alternating red and blue with a remarkable cyan end. *CFHR4* is labeled in yellow with a short C-terminal region labeled in blue. *CFHR2* is equally labeled in green (N-terminus) and red (C-terminus). *CFHR5* is labeled in magenta. Flanking the *CFH/CFHR* gene cluster, the control gene *KCNT2* (5′) is labeled in red and control gene *F13B* + *ASPM* (3′) is labeled in green. In 10 of the 21 patients, the wild-type *CFH/CFHR* gene cluster appears in its head-to-tail arrangement, as previously described by Heinen et al.[2] Scale bar = 20 μm.

mutations and discordant clinical course,[35] were analyzed at the Institute of Human Genetics of the University Hospital of Cologne for complement-associated nephropathies. Inclusion criteria were a clinical diagnosis of aHUS/renal thrombotic microangiopathy/C3G, no causative variant in the genes associated with aHUS using NGS panel analysis (except F10, this family was screened for the presence of genetic disease modifiers), and availability of a high-molecular-weight DNA sample.

This study was approved by the ethics committee of the Medical Faculty of the University of Cologne (identifier 15-215). All patients gave written informed consent for their participation in this study.

Molecular Combing

Venous blood samples were obtained from each patient for high-molecular-weight DNA isolation and extraction. High-molecular-weight DNA was extracted using the Genomic Vision DNA extraction kit (EXTR-001; Genomic Vision, Bagneux, France), according to the manufacturer's specifications. In short, leukocytes were isolated and embedded into agarose gel plugs. The agarose plugs were treated with proteinase K overnight at 50°C, melted at 68°C, and digested with β agarase at 42°C overnight. High-molecular-weight DNA was released into DNA reservoirs (RES-001) containing 1.2 μL Combing buffer (included in DNA extraction kit; Genomic Vision). Engraved vinyl-silane coated coverslips (COV-002-RUO; Genomic Vision) were embedded into the high-molecular-weight DNA solution. DNA was stretched onto coverslips by pulling the coverslip out of the DNA solution with a constant speed of 300 μm/second using the Fibercomb system (MCS-001; Genomic Vision) and permanently immobilized at 60°C for at least 2 hours. FiberProbes (FB-OD) DNA fluorescent *in situ* hybridization probes were custom designed in cooperation with Genomic Vision. Combed DNA fibers were hybridized with the FiberProbes CFH using a hybridizer (Dako/Agilent, Santa Clara, CA) and corresponding antibodies. Hybridized coverslips were scanned using the FiberVision automated scanner, and the image analysis and signal measurement were done using the FiberStudio software version 2.0.2 (Genomic Vision). Each *CFH* gene cluster signal was manually marked, and fragment lengths were measured by the FiberStudio software. Genomic Vision molecular combing technology allowed hybridization of the full approximately 360-kb complement factor H gene cluster and its flanking control genes *KCNT2* and *F13B/ASPM* (total approximately 600 kb). Of the 21 samples, 19 gave satisfactory results, enabling a good overview of both alleles (except F7 and F16). Molecular combing results were determined satisfactory if the full *CFH/CFHR* gene cluster plus flanking genes were clearly visible and the gene lengths were measurable using the FiberStudio software. Hybridization signals of all patients were summarized in Supplemental Figure S1. *CFH* and each of the *CFH*-related genes of the *CFH* gene cluster were specifically labeled in a distinctive color and pattern to unequivocally differentiate between each gene (Figure 1).

Samplix Xdrop Target Enrichment and Oxford Nanopore Long-Read Sequencing

To identify the breakpoints of the *CFHR3/CFHR1* and *CFHR4/CFHR1* deletion, Xdrop indirect sequence capture (Samplix, Birkerød, Denmark) was performed in Patient F18. In short, high-molecular-weight DNA is encapsulated with a PCR mix. A short fluorescence-labeled amplicon located in close proximity to the estimated breakpoints is used to mark our region of interest. The primer pairs used to generate two different amplicons were designed to specifically bind to a region in *CFHR3* to capture the DNA fragments containing the *CFHR4/CFHR1* deletion and a region in *CFHR4* to capture the DNA fragments containing the *CFHR3/CFHR1* deletion (Figure 2). With this approach, two libraries were generated (one for each allele) per patient. Droplets containing our genomic region of interest were enriched using a FACS Aria IIIu (BD Biosciences, Franklin Lakes, NJ) by using the 100-μm nozzle at 20 psi pressure, gating based on forward scatter pulse height, side scatter pulse height, and droplet fluorescence pulse height. Droplets were sorted using the Yield precision mode for best possible recovery of

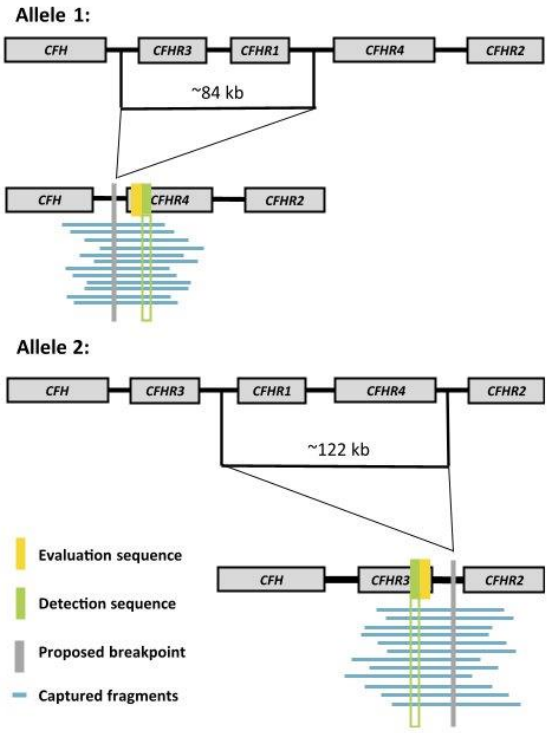

Figure 2 Schematic view of the Samplix Xdrop custom sequence capture design. (Allele 1) Detection and evaluation sequence design in *CFHR4* to identify the common *CFHR3/CFHR1* deletion. Proposed breakpoint in the intronic region between *CFH* and *CFHR3*. (Allele 2) Detection and evaluation sequence design in *CFHR3* to identify the *CFHR4/CFHR1* deletion. Proposed breakpoint in the intronic region between *CFHR3* and *CFHR2*. Primers used for the detection and evaluation sequence are listed in Table 2.

droplets of interest. The sorting of droplets is described in more detail by Madsen et al.[36] DNA is released from the isolated droplets and encapsulated again containing a multiple displacement amplification mix for target enrichment followed by long-read sequencing using a GridIon sequencing device from Oxford Nanopore (Oxford Nanopore Technologies, Oxford, UK). Sequencing reads were then aligned using the minimap2 software[37] version 2.17 (*https://github.com/lh3/minimap2*) with the prespecified *map-ont* parameter. The resulting alignment files were then sorted and indexed using samtools[38] version 1.7 (*https://github.com/samtools*) and finally visualized in the Integrative Genomics Viewer software[39] version 2.10.2 (*https://software.broadinstitute.org/software/igv*).

NGS Sequencing

For 18 patients with aHUS or C3G, custom-designed Agilent SureSelect gene panel enrichment, followed by NGS on an Illumina NextSeq500 or Illumina HiSeq 4000 platform (Illumina, San Diego, CA) of the aHUS- and C3G-associated genes *ADAMTS13*, *C3*, *CD46*, *CFB*, *CFH*, *CFHR1*, *CFHR2*, *CFHR3*, *CFHR4*, *CFHR5*, *CFI*, *DGKE*, and *MMACHC* was performed. Data were analyzed and NGS-based copy number variation (CNV) detected using the Cologne Center for Genomics Varbank2 application version 3.3 (Cologne Center for Genomics, Cologne, Germany) and the QIAGEN CLC Biomedical Genomics Workbench version 5.0.1 (Qiagen, Hilden, Germany), respectively. In particular, the approach filtered for high-quality (coverage >15-fold; phred-scaled quality >25), rare (minor allele frequency ≤0.01), and enabled CNV analysis. To exclude pipeline-related artifacts (minor allele frequency ≤0.01), the approach filtered against variants from in-house whole exome sequencing data sets. Using a comparative CNV analysis of NGS data, deviation from average coverage suggested underlying SVs in the Patients F15, F20, F18, and F3 (Figures 3A, 4A, 5A, and 6A). The annotation of *CFH* exons 1 to 23 is based on the most commonly used nomenclature to ensure compatibility.[40,41]

PCR and Sanger Sequencing

To define the breakpoints of the *CFH/CFHR1* hybrid gene, specific primers were designed that exclusively amplify a 749-bp region covering the breakpoints, as reported by Venables et al.[40] Additional primers were designed to amplify an alternative breakpoint (1017 bp) for the *CFH/CFHR1* hybrid gene found in family F15 (Table 1). Breakpoint PCR was performed for all patients, showing the *CFHR3/CFHR1* deletion in the molecular combing fluorescent *in situ* hybridization analysis because the common *CFHR3/CFHR1* deletion and the rare *CFH/CFHR1* hybrid gene could not be differentiated based on the molecular combing approach alone (data not shown). To further map the breakpoints, additional Sanger sequencing was performed for the Patients F3 and F15 (Figures 3C and 6C). Breakpoint mapping using sequencing was also performed addressing the *CFH/CFHR3* hybrid gene, the *CFHR4/CFHR1* deletion, and the common *CFHR3/CFHR1* deletion.

PCR was performed with 6 ng genomic DNA and 0.2 μmol/L of primers (Table 1) using the DNA-Taq polymerase and 10× PCR-Buffer, including 1.5 mmol/L Mg^{2+} (Analytic Jena, Jena, Germany). PCR products were visualized by gel electrophoresis using a 2% agarose gel (232-731-8; Roth, Karlsruhe, Germany) and ethidium bromide (214-984-6; Sigma-Aldrich, St. Louis, MO). PCR products were purified using the ExoSap purification kit (78200.200.UL; Thermo Fisher Scientific, Waltham, MA), according to the manufacturer's specifications. The sequence reaction was performed using the BigDye 1.1 Terminator mix (4337451; Thermo Fisher Scientific) and sequenced on the ABI Prism 3730 DNA-Analyzer platform (Applied Biosystems/Thermo Fisher Scientific).

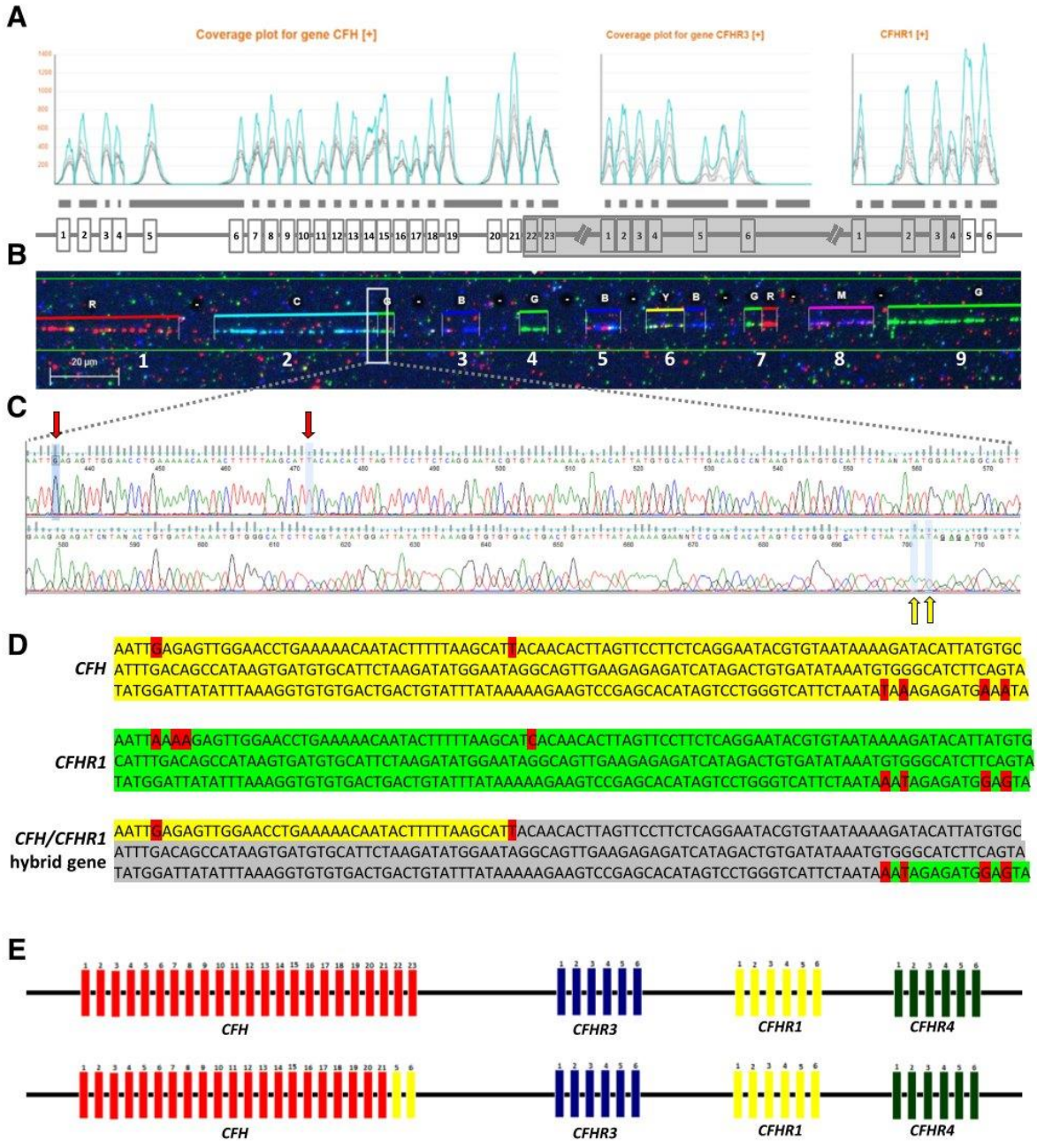

Figure 3 Patient F15. **A:** Copy number variation (CNV) visualization in Varbank2 based on CNV calling from XHMM and CONIFER. Gene coverage of single exons is shown. Patient is indicated in blue, and five controls are indicated in gray. Reduced gene coverage for exons 22 and 23 of *CFH*, normal gene coverage for *CFHR3*, and elevated gene coverage for exons 5 and 6 of *CFHR1*. **B:** Molecular combing showing the mutated allele. Wild-type allele is not shown. Fluorescent images were taken at ×40 magnification level. Validated signal with labeled genes from left ro right: red, *KCNT2* (1); cyan/green, *CFH* (2); blue, *CFHR3* (3); green, *CFHR1* (4); blue, intronic region (5); yellow/blue, *CFHR4* (6); green/red, *CFHR2* (7); magenta, *CFHR5* (8); green, *F13B* + *ASPM* (9). **C:** Breakpoint identification using PCR and Sanger sequencing (Table 1). **Red arrows** and light blue highlighted nucleotides, last nucleotides that identify the *CFH* sequence; **yellow arrows** and light blue highlighted nucleotides, first nucleotides that identify the *CFHR1* sequence. **D:** Schematic view of the breakpoint region. *CFH* sequence of the breakpoint region (yellow). *CFHR1* sequence of the breakpoint region (green). (Red) nucleotides that differ between the *CFH* and *CFHR1* sequence. Breakpoints occur within the homologous region (gray). **E:** Schematic visualization of the heterozygous *CFH/CFHR1* hybrid gene. Exons are numbered and indicated by vertical bars. *CFH* (red), *CFHR3* (blue), *CFHR1* (yellow), and *CFHR4* (green). Scale bar = 20 µm (**B**).

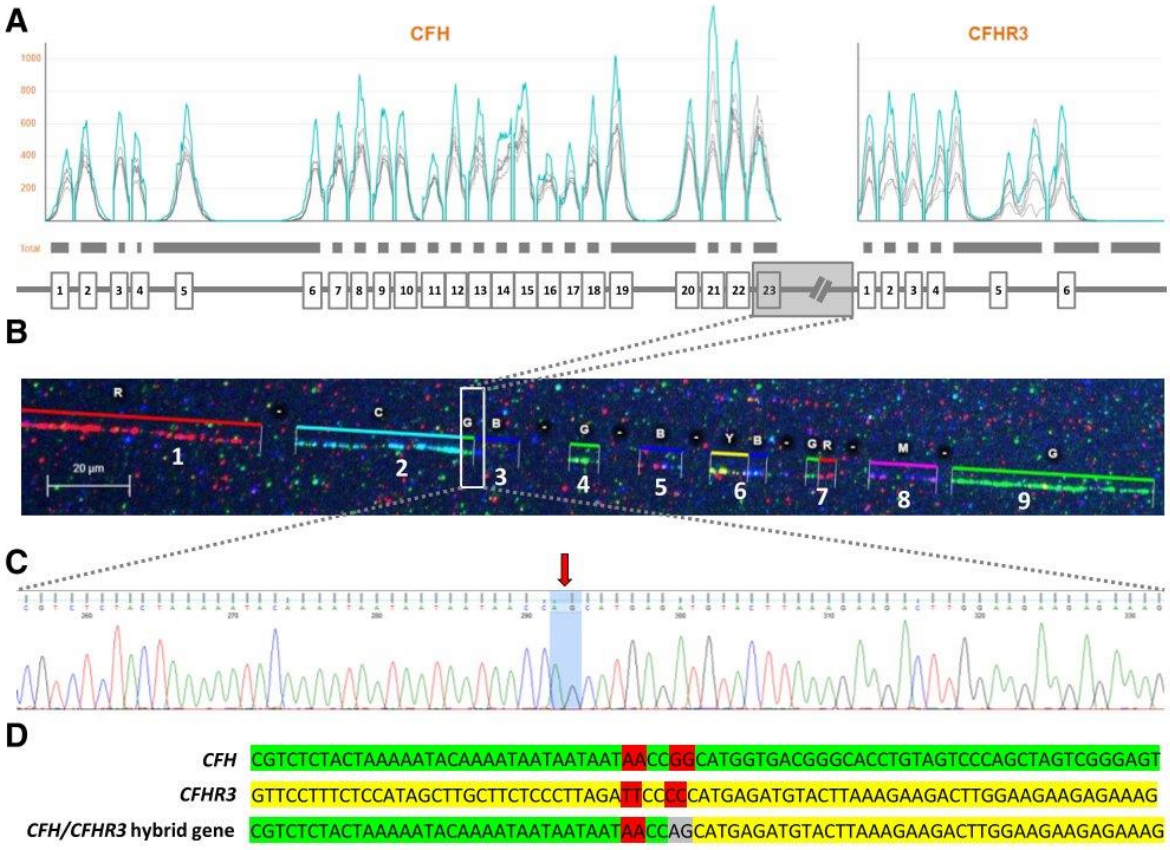

Figure 4 Patient F20. **A:** Copy number variation (CNV) visualization in Varbank2 based on CNV calling from XHMM and CONIFER. Gene coverage of single exons is shown. Patient is indicated in blue, and five controls are indicated in gray. Reduced coverage for exon 23 of *CFH*, and normal gene coverage of *CFHR3*. **B:** Molecular combing showing the *CFH/CFHR3* hybrid gene. Wild-type allele is not shown. Fluorescent images were taken at ×40 magnification level. Validated signal with labeled genes from left to right: red, *KCNT2* (1); cyan/green, *CFH* (2); blue, *CFHR3* (3); green, *CFHR1* (4); blue, intronic region (5); yellow/blue, *CFHR4* (6); green/red, *CFHR2* (7); magenta, *CFHR5* (8); green, *F13B* + *ASPM* (9). **C:** Breakpoint identification using PCR and Sanger sequencing (Table 1). **Red arrow** and light blue highlighted nucleotides, nucleotides that are different in the *CFH/CFHR3* hybrid gene sequence. **D:** Schematic view of the breakpoint region. *CFH* sequence of the breakpoint region (yellow). *CFHR3* sequence of the breakpoint region (green). (Red) nucleotides that differ between the *CFH* and *CFHR3* sequence. Sequence of the hybrid gene AG (gray) as previously described by Francis et al.[10] Scale bar = 20 μm (**B**).

Results

CFH Gene Cluster Analysis in the Screening Cohort

In total, 21 patients from 20 families were analyzed by molecular combing and sequencing (Supplemental Figure S1 and Supplemental Table S1).

The SVs previously identified in three patients (F15 and F20,[10] detailed workup shown below) with aHUS were recovered by our combined analysis approach.

In Patient F15, a *CFH/CFHR1* hybrid gene was re-identified using Sanger sequencing (Figure 3C). Primers are listed in Table 1. Patient F19 showed a *CFH/CFHR1* hybrid gene as well (data not shown), in *trans* with the common *CFHR3/CFHR1* deletion. The *CFHR3/CFHR1* deletion could be re-identified using molecular combing.

In Patient F20, molecular combing was able to visualize the previously described *CFH/CFHR3* hybrid gene that was later confirmed by Sanger sequencing (Figure 4C).

After having identified the SVs in the screening cohort, 18 additional patients with aHUS and C3G pathology were analyzed. In Patient F18, a rare *CFHR4/CFHR1* deletion was identified in *trans* with the common *CFHR3/CFHR1* deletion (Figure 5). In addition, a second rare high-penetrance *CFH/CFHR1* hybrid gene was identified in Patient F3 (Figure 6) in addition to F15. The common approximately 84-kb *CHFR3/CFHR1* deletion was found in eight patients (38.1%). Two patients were homozygous for the *CFHR3/CFHR1* deletion (F11 and F13). These two patients also showed CFH autoantibodies (DEAP-HUS). Of the 21 patients, 10 (47.6%) analyzed patients showed no structural aberrations in the *CFH* gene cluster.

Detailed Workup of Patients with Remarkable SV Findings

Patient F15: *CFH/CFHR1* Hybrid Gene

This patient presented at age 1 year and was initially treated with plasma exchange as eculizumab was not in clinical practice at that time. At age 6 years, he presented again with aHUS and was treated with eculizumab. The patient remains off dialysis 9 years later and on eculizumab treatment. Molecular combing showed no abnormalities in the structural arrangement of the *CFH* gene cluster because the C-terminal region of *CFH* and *CFHR1* both are labeled in green and *CFHR3* is still present in this variant of a *CFH/CFHR1* hybrid gene (Figure 3B). However, NGS-based CNV detection indicated the heterozygous loss of exons 22 and 23 of *CFH* and an additional copy of exons 4 and 5 of *CFHR1* (Figure 3, A and C). Presence of the *CFH/CFHR1* hybrid gene was confirmed by PCR and Sanger sequencing (Figure 3, C and D). Breakpoint PCR primers, which were used to identify the hybrid gene in Patient F3 (Table 1), failed to identify the hybrid gene variant in Patient F15, suggesting a different breakpoint in this patient. Identification of the *CFH/CFHR1* hybrid gene in Patient F15 required the design of additional primers (Table 1). The resulting heterozygous *CFH/CFHR1* hybrid gene is visualized in Figure 3E.

Patient F20: *CFH/CFHR3* Hybrid Gene

This male patient, aged 65 years, is an unaffected carrier of the mutation. He has a history of prostate cancer treated with brachytherapy in 2013, and otherwise had no other medical condition. The patient was previously described by Francis et al[10] using MLPA and Sanger sequencing approaches. The patient was included in this study to reidentify the *CFH/CFHR3* hybrid gene using the molecular combing method. NGS-based CNV detection showed the heterozygous deletion of exon 23 of *CFH* (Figure 4A). Molecular combing identified the presence of the rare heterozygous *CFH/CFHR3* hybrid gene (Figure 4B) that was confirmed by PCR and Sanger sequencing, as reported by Francis et al[10] (Figure 4, C and D).

Patient F18: Compound-Heterozygous *CFHR4/CFHR1* and *CFHR3/CFHR1* Deletion

This female patient initially developed nephrotic syndrome during pregnancy in 2013 at the age of 34 years (initial proteinuria, 8 g/day; later up to 28 g/day). The pregnancy was terminated after 22 weeks because of nephrotic syndrome and high blood pressure. A kidney biopsy was performed, which showed cellular variant focal-segmental glomerulosclerosis with a moderate degree of acute tubular lesion. The patient showed no response to immunosuppressive treatment with corticosteroids, cyclosporine, rituximab, and plasmapheresis and developed end-stage kidney disease 3 years after initial presentation; hemodialysis was started in 2016. In March 2017, the patient presented with severe neurologic symptoms (headache, nausea, and grand-mal seizures), hypertensive episode, and nephritic syndrome (vomiting, hematuria, and proteinuria). Because of an initial progression of neurologic symptoms, the patient required mechanical ventilation. Brain magnetic resonance imaging at this time showed encephalopathy with a suspicion of posterior reversible encephalopathy syndrome or acute disseminated encephalomyelitis. Cerebrospinal fluid cytology showed 88 lymphocytes/μL. Cerebrospinal fluid protein levels were elevated at 0.62 g/L (normal, <0.45 g/L), and glucose was normal. Serum creatinine was elevated at 1146 μmol/L (normal, 49 to 90 μmol/L), but serum electrolytes were within the normal range. The serologic testing for viral and bacterial causes was negative. Under a combinatorial therapy with pulsed glucocorticoids, plasmapheresis, and fresh frozen plasma infusions, the patient's neurologic symptoms improved and she could be extubated. At this time, her C3 and C4 levels were both decreased at 0.56 g/L (normal, 0.9 to 1.8 g/L) and 0.07 g/L (normal, 0.1 to 0.4 g/L), respectively. Her antinuclear antibody and antineutrophil cytoplasmic antibody titers were normal. DNA of Patient F18 was submitted for genetic testing with the clinical suspicion of a monogenic form of aHUS with central nervous system manifestations. The NGS-based CNV analysis of the *CFH* gene cluster showed evidence of a heterozygous deletion of *CFHR3* and *CFHR4* as well as the complete loss of *CFHR1* (Figure 5A). This structural aberration was confirmed by molecular combing, resolving a compound heterozygous deletion of *CFHR3/CFHR1* in *trans* with a heterozygous *CFHR4/CFHR1* deletion (Figure 5B). Breakpoint mapping was done using Oxford Nanopore long-read sequencing after long-fragment target enrichment covering the breakpoint region of the *CFHR4/1* and *CFHR3/1* deletion, respectively (Figure 5, C and D). *CFHR3/CFHR1* deletion breakpoints were refined to a 40-bp region of chromosome 1:196,733,321-196,733,362; chromosome 1:196,817,998-196,818,039 (GRCh37/hg19). *CFHR4/CFHR1* deletion breakpoints were located in a region of 385 bp between chromosome 1:196,783,258-196,783,644; chromosome 1:196,905,155-196,905,541 (GRCh37/hg19).

Patient F3: *CFH/CFHR1* Hybrid Gene

Patient F3 presented at age 16 years with diarrhea-negative hemolytic anemia and thrombocytopenia in chronic kidney disease stage 4 with focal seizures and quickly progressed to end-stage renal failure. For suspected thrombotic microangiopathy, plasma exchange was performed, but could not prevent manifestation of end-stage renal failure. Genetic testing and eculizumab were not clinical practice at that time. The patient remained on chronic hemodialysis treatment for 9 years and received a first cadaveric renal transplant at the age of 23 years. He quickly lost the renal graft 6 months later and returned to chronic hemodialysis treatment. He received a second renal graft in August 2019 under eculizumab and retained a stable graft function with creatinine levels of 120 to 130 μmol/L. A standard gene panel analysis for aHUS yielded unremarkable results, but exome-based reanalysis with bioinformatic CNV analysis

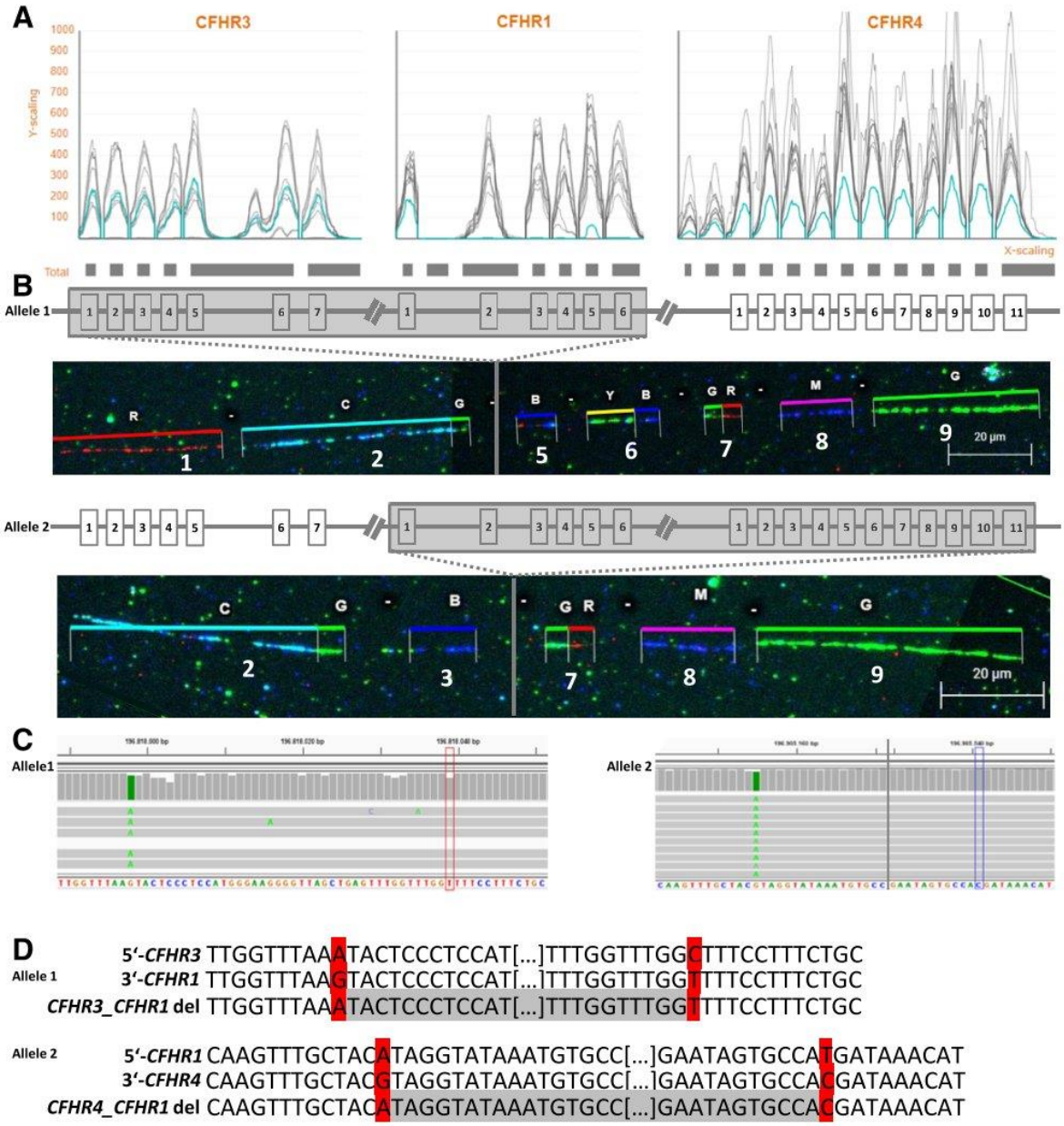

Figure 5 Patient F18. **A:** Copy number variation (CNV) visualization in Varbank2 based on CNV calling from XHMM and CONIFER. Gene coverage of single exons is shown. Patient is indicated in blue, and 10 controls are indicated in gray. (Heterozygous *CFHR3/CFHR1* deletion polymorphism in controls.) Reduced gene coverage for *CFHR3* and *CFHR4*, full loss of *CFHR1*. **B:** Molecular combing showing both alleles. Fluorescent images were taken at ×40 magnification level. Validated signal with labeled genes from left to right: red, *KCNT2* (1); cyan/green, *CFH* (2); blue, *CFHR3* (3); blue, intronic region (5); yellow/blue, *CFHR4* (6); green/red, *CFHR2* (7); magenta, *CFHR5* (8); green, *F13B* + *ASPM* (9). (Allele 1) *CFHR3/CFHR1* deletion. (Allele 2) *CFHR4/CFHR1* deletion. **C:** Breakpoint identification using Oxford Nanopore long-read sequencing after Xdrop sample preparation. (Allele 1) Nucleotide A (green) resembles the last nucleotide that identifies the 5′-*CFHR3* sequence before the breakpoint. Nucleotide T (red) resembles the first nucleotide that identifies the 3′-*CFHR1* sequence after the breakpoint. The breakpoint lies within the homologous region between the nucleotides A and T. (Allele 2) Nucleotide A (green) resembles the last nucleotide that identifies the 5′-*CFHR1* sequence before the breakpoint. Nucleotide C (blue) resembles the first nucleotide that identifies the 3′-*CFHR4* sequence after the breakpoint. The breakpoint lies within the homologous region between the nucleotides A and C. Long-read sequence of allele 2 showing the *CFHR4/CFHR1* deletion was cut to accommodate for the 385-bp homologous gap between the distinguishable nucleotide's A and C (gray vertical bar). **D:** Schematic view of the breakpoints. Single nucleotides (red) distinguish between the *CFHR4/CFHR1* and *CFHR3/CFHR1* sequences. Breakpoints occur within the homologous region of 40 bp (allele 1, *CFHR3/CFHR1* deletion) and 385 bp (allele 2, *CFHR4/CFHR1* deletion), indicated in gray. Homologous breakpoint region (gray) was shortened for visualization purposes. Scale bar = 20 µm (**B**).

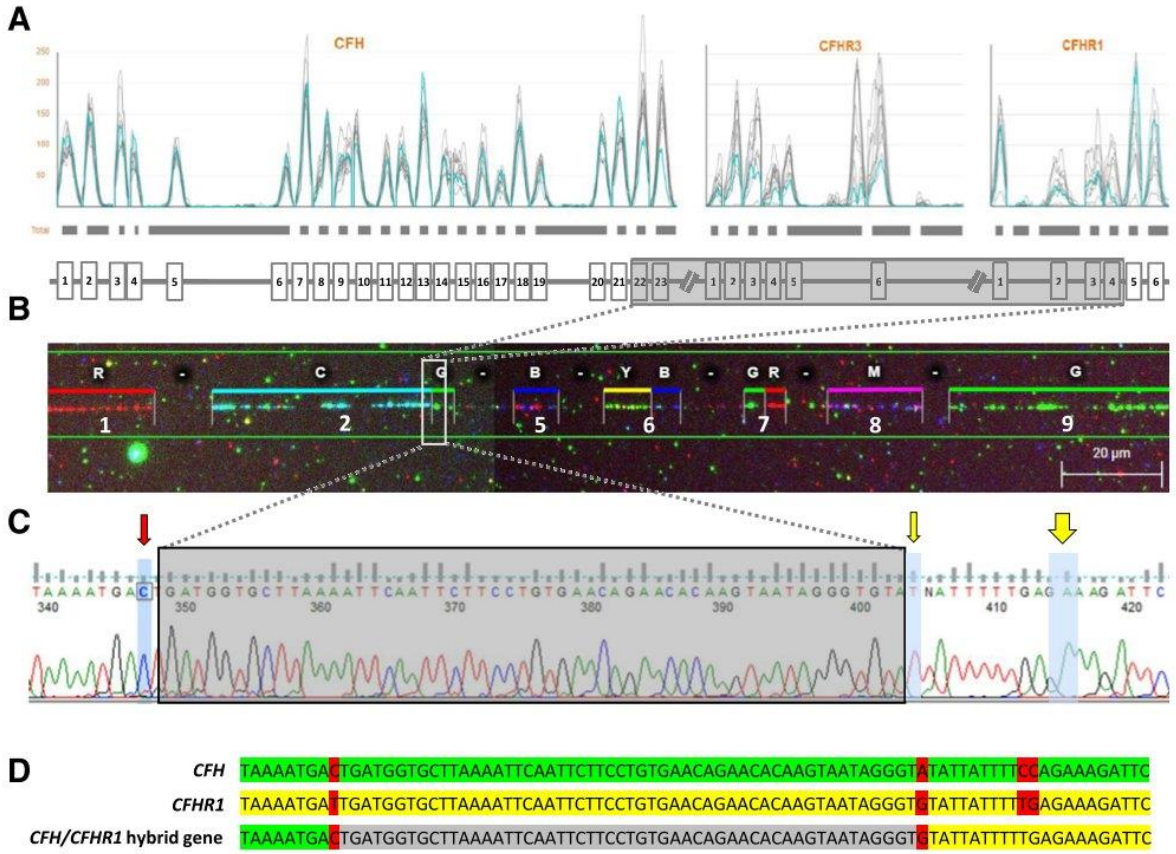

Figure 6 Patient F3. **A:** Copy number variation (CNV) visualization in Varbank2 based on CNV calling from XHMM and CONIFER. Gene coverage of single exons is shown. Patient is indicated in blue, and 10 controls are indicated in gray. Reduced gene coverage for exons 22 and 23 of *CFH*, the whole gene *CFHR3*, and exons 1 to 4 of *CFHR1*. Gene coverage of the first exon of *CFHR1* is most likely an artifact due to the high sequence homology between *CFH* and *CFHR1*. **B:** Molecular combing showing the mutated allele. Wild-type allele is not shown. Fluorescent images were taken at ×40 magnification level. Validated signal with labeled genes from left to right: red, *KCNT2* (1); cyan/green, *CFH* (2); blue, intronic region (5); yellow/blue, *CFHR4* (6); green/red, *CFHR2* (7); magenta, *CFHR5* (8); green, *F13B* + *ASPM* (9). **C:** Breakpoint identification using PCR and Sanger sequencing (primer: Table 1). **Red arrow**, last nucleotide that identifies the *CFH* sequence; **yellow arrows**, first nucleotides that identify the *CFHR1* sequence. Breakpoint region (**gray boxed area**). **D:** Schematic view of the breakpoint region. *CFH* sequence of the breakpoint region (green). *CFHR1* sequence of the breakpoint region (yellow). Breakpoints occur within the homologous region (gray). Scale bar = 20 μm (**B**).

detection indicated a heterozygous loss of exons 22 and 23 of *CFH*, of *CFHR3*, and of the first four exons of *CFHR1* (Figure 6A). Using molecular combing, the presence of a structural aberration could be confirmed in the patient, which resembled either a *CFH/CFHR1* hybrid gene or the common *CFHR3/CFHR1* deletion (Figure 6B). Breakpoint mapping using Sanger sequencing revealed the presence of the rare *CFH/CFHR1* hybrid gene and confirmed the breakpoints to be in a homologous region of 53 bp between *CFH* and *CFHR1*, identical to the hybrid gene reported by Venables et al[40] (Figure 6, C and D).

Discussion

Molecular diagnostics of patients with abnormalities in the *CFH* gene cluster can be challenging. The disease spectrum is genetically heterogeneous and characterized by a broad range of clinical manifestations, spanning from early to late onset of disease. Reduced penetrance is frequently noted in autosomal dominant forms. There are also large differences in the reported diagnostic yield, ranging from 60% to 70%[31,42,43] to in our experience much lower numbers in even purely pediatric cohorts despite comprehensive testing.

One particular disadvantage is that the routinely used methods for SV detection [ie, bioinformatic CNV detection (based on short-read NGS data) and CNV detection by MLPA] are incomplete and do not give precise structural information. Although MLPA has potential advantages compared with bioinformatic CNV analysis to uncover smaller deletions/duplications (encompassing single exons), the commercially available MLPA kit for the *CFH* gene cluster is incomplete (missing probes for all genes of the

Table 1 *CFH* Gene Cluster and Structural Aberration PCR Primer Pairs

Structural aberration	Forward primer	Reverse primer	PCR product, bp
CFH/CFHR1 hybrid gene	5′-CGGGCGGTATATTGTAACTGTTATC-3′	5′-CTGGTTTCCCTTACTCCATCTCTATT-3′	749
CFH/CFHR1 hybrid gene*	5′-CGGGCGGTATATTGTAACTGTTATC-3′	5′-CCTCTGTCATTTATTTGTTTCTGTCTG-3′	1017
CFH/CFHR3 hybrid gene	5′-CAATGGTCAGAACCACCAAAAT-3′	5′-GAAACCCACAAGGTCAGAATGAC-3′	975

*Different primer design for Patient F15.

cluster) and rearrangements without copy number changes will not be identified by either method.

For the aHUS spectrum, the exact genetic diagnosis is of utmost importance to determine the therapeutic strategy. Cost of (permanent) complement inhibition and substantial risk involved with this treatment require careful consideration of who will benefit from the expensive therapy and who will not. Genetic rearrangements in the *CFH/CFHR* gene cluster are highly correlated to post-transplant recurrence of aHUS.[8,10,40] Eculizumab, a monoclonal antibody that inhibits the cleavage of C5 into C5a and C5b and thereby blocks the formation of the membrane attack complex, has been reported to prevent the recurrence of aHUS[44,45] and has been proven beneficial in patients with aHUS caused by *CFHR3/CFHR1* deletion (DEAP-HUS),[46] *CFH/CFHR1* hybrid gene,[32] *CFHR1/CFH* hybrid gene,[7,44] and *CFH/CFHR3* hybrid gene.[9] Eculizumab as treatment in patients with the *CFHR4/CFHR1* deletion and/or *CFHR4/CFHR1* deletion in *trans* with the *CFHR3/CFHR1* deletion has not been reported yet. An overview of SVs identified in aHUS, SLE, C3G, and dense-deposit disease and available information on the use of eculizumab/complement inhibition have been summarized in Supplemental Table S2.[7,9,13–15,22,32,44,46–55]

In this study, we performed full-length structural analysis of the *CFH/CFHR* gene cluster using a multistep analysis starting with NGS, including bioinformatic CNV analysis followed by single DNA strand visualization using the molecular combing fluorescent *in situ* hybridization technique and (if applicable) finalized the in-depth screening by breakpoint identification of the *CFHR3/CFHR1* and *CFHR4/CFHR1* deletion by cost-efficient target enrichment for long read using the Xdrop targeted sequence capture instead of expensive whole-genome long-read sequencing, and succeeded in identifying new breakpoint regions, thus contributing to the growing number of deletions in the complex *CFH* gene cluster.

The most common structural aberration of the *CFH* gene cluster is the *CFHR3/CFHR1* deletion. In Patient F18, breakpoints of the common *CFHR3/CFHR1* deletion differ from the previously published breakpoints, suggesting that these vary between the individuals.[4,16,19,21] Cantsilieris et al[4] refine the breakpoints of the common *CFHR3/CFHR1* deletion to a region of 489 bp of long interspersed nuclear element repeats. The breakpoints described in this study are located approximately 6 kb upstream from the breakpoints found in our aHUS patient and approximately 10 kb upstream from the 1618-bp breakpoint region described by Hughes et al.[19] Zhao et al[16] describe the *CFHR3/CFHR1* deletion within the SLE-associated block of approximately 146 kb starting from intron 9 of *CFH* and ending downstream of *CFHR1* (chromosome 1:196,686,918-196,824,773; GRCh37/hg19) incorporating the *CFHR3/CFHR1* deletion, identified in this study as well. They presented evidence that strongly suggests the *CFHR3/CFHR1* deletion to cause an increase of SLE risk in a dosage-dependent manner by showing that homozygous individuals have a higher risk of SLE than heterozygous ones.[16]

The *CFHR4/CFHR1* deletion breakpoints (chromosome 1:196,783,258-196,905,541; GRCh37/hg19), identified in F18 and resulting in an approximately 122-kb deletion, differ from the three *CFHR4/CFHR1* deletions described by Cantsilieris et al.[4] The compound-heterozygous *CFHR3/CFHR1* and *CFHR4/CFHR1* deletion has previously been described in three patients by Moore et al,[22] who also developed factor H autoantibodies (DEAP-HUS). Antibody testing in Patient F18 yielded no pathologic findings.

Other rarely found SVs involving the CFH-related proteins have been associated with dense-deposit disease and C3G.[13,14,54] Most of these are fusion proteins that are not

Table 2 Samplx Xdrop Sequence Capture PCR Primer and Enrichment Validation qPCR Primer for the *CFHR3/CFHR1* and *CFHR4/CFHR1* Deletion

Structural aberration	Assay	Forward primer	Reverse primer
CFHR3/CFHR1 deletion	Droplet PCR	5′-ATTCTCTTGCGTCGCATCCA-3′	5′-GTCCTTCACCCGAACAGAGG-3′
	qPCR	5′-CACGGACTCCAAAAGCCACT-3′	5′-AGCTAGGAATTGTGATGCCCAA-3′
CFHR4/CFHR1 deletion	Droplet PCR	5′-ACTCCTCAAGGACTGCCAGA-3′	5′-ATCCGTGTTCTTAAAGGAAACCAC-3′
	qPCR	5′-GCTGCTTGTATTGCATTCCGT-3′	5′-GGTCTGATTCTCCTGACGCT-3′

Designed using the primer designing tool provided by Samplix (Birkerød, Denmark).
qPCR, real-time quantitative PCR.

described yet in the other pathologies, like age-related macular degeneration, SLE, or aHUS (except the *CFH/CFHR1* hybrid gene). In theory, the described SVs would have been detectable with the first-line NGS gene panel and CNV analysis and validated using the molecular combing screening approach.

In Patient F3, a *CFH/CFHR1* hybrid gene was found with the same breakpoint region to the previously reported *CFH/CFHR1* hybrid gene.[40] Maga et al[8] described a *CFH/CFHR1* hybrid gene with a different breakpoint region that resulted in an identical fusion protein. In addition, we present a third breakpoint region (in between the known breakpoint regions) resulting in yet another identical *CFH/CFHR1* fusion protein found in Patient F15. This hybrid gene is presumably generated by nonallelic or interlocus gene conversion in which exons 22 and 23 of *CFH* serve as the acceptor sequence, which is replaced by a copy of the exons 5 and 6 of *CFHR1* (donor sequence). The donor sequence, including the gene *CFHR3*, which is located between *CFH* and *CFHR1*, remains fully intact (Figure 3E). This mechanism is described in more detail by Chen et al.[56] All recombination events occur in a highly homologous region in intron 21 (ENST00000367429.9: intron 20) of *CFH* and result in the same fusion protein, suggesting a hotspot for structural recombination events. MLPA results from Patient F19 (data not shown) suggest that the breakpoints are located in intron 21 (ENST00000367429.9: intron 20) of *CFH*, similar to the other *CFH/CFHR1* hybrid genes found in this study.

Although there is no proof of clinically relevant mosaicism in aHUS at the moment, we see the technical advantage to uncover somatic structural aberrations that would remain beyond the means of detection for most currently used diagnostic methods, such as MLPA or Southern blot analysis. The principle feature of mosaicism detection has already been proven in other disease (eg, the clinical diagnostics of facio-scapulo-humeral dystrophy).[57] In addition, molecular combing allows the direct visual localization of structural variants within the gene cluster (even without loss or gain of DNA material), whereas MLPA and Southern blot analysis are limited to identify that a deletion/insertion has occurred but lacking information about the genomic localization.

This study shows that combined NGS and SV detection by molecular combing is able to enhance the detection of structural variants and can provide a more precise resolution of SVs in the genomic context, which might become important for genotype/phenotype correlations of diseases associated with the gene cluster. A cost estimation of the authors for molecular combing compared with other diagnostic methods is given in Supplemental Table S3.

Current probe design of molecular combing fails to distinguish between the frequent *CFHR3/CFHR1* deletion (which is rarely of clinical relevance) and the rare, high-penetrance *CFH/CFHR1* hybrid gene. This limitation is due to the fact that the C-terminal regions of *CFH* and *CFHR1* both are highly homologous to allow differential fluorescent labeling (Figure 1, both regions labeled in green), and can easily be resolved by a simple PCR with Sanger sequencing of the amplicon. Apart from this gap, molecular combing allows comprehensive haplotype views of the gene cluster. Visualization of single DNA molecules may help detect a wider range of structural variants for both alleles of the *CFH* gene cluster.

Acknowledgments

We thank Genomic Vision (Bagneux, France) for helping with their expertise on the custom *CFH* gene cluster probe design and molecular combing protocol. Flow cytometry experiments were performed in the FACS and Imaging Core Facility at the Max Planck Institute for Biology of Aging. Next-generation sequencing analyses were performed at the production site West German Genome Center (WGGC) Cologne.

Supplemental Data

Supplemental material for this article can be found at *http://doi.org/10.1016/j.jmoldx.2022.02.006*.

References

1. Zipfel PF, Skerka C, Hellwage J, Jokiranta ST, Meri S, Brade V, Kraiczy P, Noris M, Remuzzi G: Factor H family proteins: on complement, microbes and human diseases. Biochem Soc Trans 2002, 30(Pt 6):971−978
2. Heinen S, Sanchez-Corral P, Jackson MS, Strain L, Goodship JA, Kemp EJ, Skerka C, Jokiranta TS, Meyers K, Wagner E, Robitaille P, Esparza-Gordillo J, Rodriguez de Cordoba S, Zipfel PF, Goodship TH: De novo gene conversion in the RCA gene cluster (1q32) causes mutations in complement factor H associated with atypical hemolytic uremic syndrome. Hum Mutat 2006, 27:292−293
3. Díaz-Guillén MA, Rodríguez de Córdoba S, Heine-Suñer D: A radiation hybrid map of complement factor H and factor H-related genes. Immunogenetics 1999, 49:549−552
4. Cantsilieris S, Nelson BJ, Huddleston J, Baker C, Harshman L, Penewit K, Munson KM, Sorensen M, Welch AE, Dang V, Grassmann F, Richardson AJ, Guymer RH, Graves-Lindsay TA, Wilson RK, Weber BHF, Baird PN, Allikmets R, Eichler EE: Recurrent structural variation, clustered sites of selection, and disease risk for the complement factor H (CFH) gene family. Proc Natl Acad Sci U S A 2018, 115:E4433−E4442
5. Józsi M, Licht C, Strobel S, Zipfel SL, Richter H, Heinen S, Zipfel PF, Skerka C: Factor H autoantibodies in atypical hemolytic uremic syndrome correlate with CFHR1/CFHR3 deficiency. Blood 2008, 111:1512−1514
6. Pérez-Caballero D, González-Rubio C, Gallardo ME, Vera M, López-Trascasa M, Rodríguez de Córdoba S, Sánchez-Corral P: Clustering of missense mutations in the C-terminal region of factor H in atypical hemolytic uremic syndrome. Am J Hum Genet 2001, 68:478−484
7. Valoti E, Alberti M, Tortajada A, Garcia-Fernandez J, Gastoldi S, Besso L, Bresin E, Remuzzi G, Rodriguez de Cordoba S, Noris M: A novel atypical hemolytic uremic syndrome-associated hybrid CFHR1/CFH gene encoding a fusion protein that antagonizes factor H-dependent complement regulation. J Am Soc Nephrol 2015, 26:209−219

8. Maga TK, Meyer NC, Belsha C, Nishimura CJ, Zhang Y, Smith RJ: A novel deletion in the RCA gene cluster causes atypical hemolytic uremic syndrome. Nephrol Dial Transpl 2011, 26:739–741
9. Challis RC, Araujo GS, Wong EK, Anderson HE, Awan A, Dorman AM, Waldron M, Wilson V, Brocklebank V, Strain L, Morgan BP, Harris CL, Marchbank KJ, Goodship TH, Kavanagh D: A de novo deletion in the regulators of complement activation cluster producing a hybrid complement factor H/complement factor H-related 3 gene in atypical hemolytic uremic syndrome. J Am Soc Nephrol 2016, 27:1617–1624
10. Francis NJ, McNicholas B, Awan A, Waldron M, Reddan D, Sadlier D, Kavanagh D, Strain L, Marchbank KJ, Harris CL, Goodship TH: A novel hybrid CFH/CFHR3 gene generated by a microhomology-mediated deletion in familial atypical hemolytic uremic syndrome. Blood 2012, 119:591–601
11. Noris M, Remuzzi G: Overview of complement activation and regulation. Semin Nephrol 2013, 33:479–492
12. Zipfel PF, Wiech T, Stea ED, Skerka C: CFHR gene variations provide insights in the pathogenesis of the kidney diseases atypical hemolytic uremic syndrome and C3 glomerulopathy. J Am Soc Nephrol 2020, 31:241–256
13. Piras R, Breno M, Valoti E, Alberti M, Iatropoulos P, Mele C, Bresin E, Donadelli R, Cuccarolo P, Smith RJH, Benigni A, Remuzzi G, Noris M: CFH and CFHR copy number variations in C3 glomerulopathy and immune complex-mediated membranoproliferative glomerulonephritis. Front Genet 2021, 12:670727
14. Malik TH, Lavin PJ, Goicoechea de Jorge E, Vernon KA, Rose KL, Patel MP, de Leeuw M, Neary JJ, Conlon PJ, Winn MP, Pickering MC: A hybrid CFHR3-1 gene causes familial C3 glomerulopathy. J Am Soc Nephrol 2012, 23:1155–1160
15. Chen Q, Wiesener M, Eberhardt HU, Hartmann A, Uzonyi B, Kirschfink M, Amann K, Buettner M, Goodship T, Hugo C, Skerka C, Zipfel PF: Complement factor H-related hybrid protein deregulates complement in dense deposit disease. J Clin Invest 2014, 124:145–155
16. Zhao J, Wu H, Khosravi M, Cui H, Qian X, Kelly JA, et al: Association of genetic variants in complement factor H and factor H-related genes with systemic lupus erythematosus susceptibility. PLoS Genet 2011, 7:e1002079
17. Patel N, Adewoyin T, Chong NV: Age-related macular degeneration: a perspective on genetic studies. Eye (Lond) 2008, 22:768–776
18. Hageman GS, Hancox LS, Taiber AJ, Gehrs KM, Anderson DH, Johnson LV, Radeke MJ, Kavanagh D, Richards A, Atkinson J, Meri S, Bergeron J, Zernant J, Merriam J, Gold B, Allikmets R, Dean M; AMD Clinical Study Group: Extended haplotypes in the complement factor H (CFH) and CFH-related (CFHR) family of genes protect against age-related macular degeneration: characterization, ethnic distribution and evolutionary implications. Ann Med 2006, 38:592–604
19. Hughes AE, Orr N, Esfandiary H, Diaz-Torres M, Goodship T, Chakravarthy U: A common CFH haplotype, with deletion of CFHR1 and CFHR3, is associated with lower risk of age-related macular degeneration. Nat Genet 2006, 38:1173–1177
20. Sivakumaran TA, Igo RP Jr, Kidd JM, Itsara A, Kopplin LJ, Chen W, et al: Correction: A 32 kb critical region excluding Y402H in CFH mediates risk for age-related macular degeneration. PLoS One 2018, 13:e0209943
21. Zipfel PF, Edey M, Heinen S, Józsi M, Richter H, Misselwitz J, Hoppe B, Routledge D, Strain L, Hughes AE, Goodship JA, Licht C, Goodship TH, Skerka C: Deletion of complement factor H-related genes CFHR1 and CFHR3 is associated with atypical hemolytic uremic syndrome. PLoS Genet 2007, 3:e41
22. Moore I, Strain L, Pappworth I, Kavanagh D, Barlow PN, Herbert AP, Schmidt CQ, Staniforth SJ, Holmes LV, Ward R, Morgan L, Goodship TH, Marchbank KJ: Association of factor H autoantibodies with deletions of CFHR1, CFHR3, CFHR4, and with mutations in CFH, CFI, CD46, and C3 in patients with atypical hemolytic uremic syndrome. Blood 2010, 115: 379–387
23. Gharavi AG, Kiryluk K, Choi M, Li Y, Hou P, Xie J, et al: Genome-wide association study identifies susceptibility loci for IgA nephropathy. Nat Genet 2011, 43:321–327
24. Zhang C, Lv Q, Fan W, Tang W, Yi Z: Influence of CFH gene on symptom severity of schizophrenia. Neuropsychiatr Dis Treat 2017, 13:697–706
25. Nursal AF, Aydin PC, Pehlivan M, Sever U, Pehlivan S: UCP2 and CFH gene variants with genetic susceptibility to schizophrenia in Turkish population. Endocr Metab Immune Disord Drug Targets 2020, 21:2084–2089
26. Tang W, Liu H, Chen L, Zhao K, Zhang Y, Zheng K, Zhu C, Zheng T, Liu J, Wang D, Yu L, Fang X, Zhang C, Su KP: Inflammatory cytokines, complement factor H and anhedonia in drug-naïve major depressive disorder. Brain Behav Immun 2021, 95:238–244
27. Fakhouri F, Zuber J, Frémeaux-Bacchi V, Loirat C: Haemolytic uraemic syndrome. Lancet 2017, 390:681–696
28. Loirat C, Saland J, Bitzan M: Management of hemolytic uremic syndrome. Presse Med 2012, 41:115–135
29. Sethi S, Fervenza FC: Pathology of renal diseases associated with dysfunction of the alternative pathway of complement: C3 glomerulopathy and atypical hemolytic uremic syndrome (aHUS). Semin Thromb Hemost 2014, 40:416–421
30. Goicoechea de Jorge E, Tortajada A, García SP, Gastoldi S, Merinero HM, García-Fernández J, Arjona E, Cao M, Remuzzi G, Noris M, Rodríguez de Córdoba S: Factor H competitor generated by gene conversion events associates with atypical hemolytic uremic syndrome. J Am Soc Nephrol 2018, 29:240–249
31. Noris M, Caprioli J, Bresin E, Mossali C, Pianetti G, Gamba S, Daina E, Fenili C, Castelletti F, Sorosina A, Piras R, Donadelli R, Maranta R, van der Meer I, Conway EM, Zipfel PF, Goodship TH, Remuzzi G: Relative role of genetic complement abnormalities in sporadic and familial aHUS and their impact on clinical phenotype. Clin J Am Soc Nephrol 2010, 5:1844–1859
32. Nester C, Stewart Z, Myers D, Jetton J, Nair R, Reed A, Thomas C, Smith R, Brophy P: Pre-emptive eculizumab and plasmapheresis for renal transplant in atypical hemolytic uremic syndrome. Clin J Am Soc Nephrol 2011, 6:1488–1494
33. Hofer J, Janecke AR, Zimmerhackl LB, Riedl M, Rosales A, Giner T, Cortina G, Haindl CJ, Petzelberger B, Pawlik M, Jeller V, Vester U, Gadner B, van Husen M, Moritz ML, Würzner R, Jungraithmayr T; German-Austrian HUS Study Group: Complement factor H-related protein 1 deficiency and factor H antibodies in pediatric patients with atypical hemolytic uremic syndrome. Clin J Am Soc Nephrol 2013, 8: 407–415
34. Dragon-Durey MA, Loirat C, Cloarec S, Macher MA, Blouin J, Nivet H, Weiss L, Fridman WH, Frémeaux-Bacchi V: Anti-factor H autoantibodies associated with atypical hemolytic uremic syndrome. J Am Soc Nephrol 2005, 16:555–563
35. Hackl A, Erger F, Skerka C, Wenzel A, Tschernoster N, Ehren R, Burgmaier K, Riehmer V, Licht C, Kirschfink M, Weber LT, Altmueller J, Zipfel PF, Habbig S: Long-term data on two sisters with C3GN due to an identical, homozygous CFH mutation and autoantibodies. Clin Nephrol 2020, 94:197–206
36. Madsen EB, Höijer I, Kvist T, Ameur A, Mikkelsen MJ: Xdrop: targeted sequencing of long DNA molecules from low input samples using droplet sorting. Hum Mutat 2020, 41:1671–1679
37. Li H: Minimap2: pairwise alignment for nucleotide sequences. Bioinformatics 2018, 34:3094–3100
38. Li H, Handsaker B, Wysoker A, Fennell T, Ruan J, Homer N, Marth G, Abecasis G, Durbin R; 1000 Genome Project Data

Processing Subgroup: The sequence alignment/Map format and SAMtools. Bioinformatics 2009, 25:2078–2079
39. Robinson JT, Thorvaldsdóttir H, Winckler W, Guttman M, Lander ES, Getz G, Mesirov JP: Integrative genomics viewer. Nat Biotechnol 2011, 29:24–26
40. Venables JP, Strain L, Routledge D, Bourn D, Powell HM, Warwicker P, Diaz-Torres ML, Sampson A, Mead P, Webb M, Pirson Y, Jackson MS, Hughes A, Wood KM, Goodship JA, Goodship TH: Atypical haemolytic uraemic syndrome associated with a hybrid complement gene. PLoS Med 2006, 3:e431
41. Rodríguez de Córdoba S, Esparza-Gordillo J, Goicoechea de Jorge E, Lopez-Trascasa M, Sánchez-Corral P: The human complement factor H: functional roles, genetic variations and disease associations. Mol Immunol 2004, 41:355–367
42. Fremeaux-Bacchi V, Fakhouri F, Garnier A, Bienaimé F, Dragon-Durey MA, Ngo S, Moulin B, Servais A, Provot F, Rostaing L, Burtey S, Niaudet P, Deschênes G, Lebranchu Y, Zuber J, Loirat C: Genetics and outcome of atypical hemolytic uremic syndrome: a nationwide French series comparing children and adults. Clin J Am Soc Nephrol 2013, 8:554–562
43. Rodríguez de Córdoba S, Hidalgo MS, Pinto S, Tortajada A: Genetics of atypical hemolytic uremic syndrome (aHUS). Semin Thromb Hemost 2014, 40:422–430
44. Eyler SJ, Meyer NC, Zhang Y, Xiao X, Nester CM, Smith RJ: A novel hybrid CFHR1/CFH gene causes atypical hemolytic uremic syndrome. Pediatr Nephrol 2013, 28:2221–2225
45. Valoti E, Alberti M, Noris M: Posttransplant recurrence of atypical hemolytic uremic syndrome. J Nephrol 2012, 25:911–917
46. Zipfel PF, Mache C, Müller D, Licht C, Wigger M, Skerka C; European DEAP-HUS Study Group: DEAP-HUS: deficiency of CFHR plasma proteins and autoantibody-positive form of hemolytic uremic syndrome. Pediatr Nephrol 2010, 25:2009–2019
47. de Holanda MI, Pôrto LC, Wagner T, Christiani LF, Palma LMP: Use of eculizumab in a systemic lupus erythemathosus patient presenting thrombotic microangiopathy and heterozygous deletion in CFHR1-CFHR3: a case report and systematic review. Clin Rheumatol 2017, 36:2859–2867
48. Torres EA, Chang Y, Desai S, Chang I, Zuckerman JE, Burwick R, Kalantar-Zadeh K, Hanna RM: Complement-mediated thrombotic microangiopathy associated with lupus nephritis treated with eculizumab: a case report. Case Rep Nephrol Dial 2021, 11:95–102
49. Valoti E, Alberti M, Iatropoulos P, Piras R, Mele C, Breno M, Cremaschi A, Bresin E, Donadelli R, Alizzi S, Amoroso A, Benigni A, Remuzzi G, Noris M: Rare functional variants in complement genes and anti-FH autoantibodies-associated aHUS. Front Immunol 2019, 10:853
50. Breville G, Zamberg I, Sadallah S, Stephan C, Ponte B, Seebach JD: Case report: severe complement-mediated thrombotic microangiopathy in IgG4-related disease secondary to anti-factor H IgG4 autoantibodies. Front Immunol 2021, 11:604759
51. Togarsimalemath SK, Sethi SK, Duggal R, Le Quintrec M, Jha P, Daniel R, Gonnet F, Bansal S, Roumenina LT, Fremeaux-Bacchi V, Kher V, Dragon-Durey MA: A novel CFHR1-CFHR5 hybrid leads to a familial dominant C3 glomerulopathy. Kidney Int 2017, 92:876–887
52. Xiao X, Ghossein C, Tortajada A, Zhang Y, Meyer N, Jones M, Borsa NG, Nester CM, Thomas CP, de Córdoba SR, Smith RJ: Familial C3 glomerulonephritis caused by a novel CFHR5-CFHR2 fusion gene. Mol Immunol 2016, 77:89–96
53. Tortajada A, Yébenes H, Abarrategui-Garrido C, Anter J, García-Fernández JM, Martínez-Barricarte R, Alba-Domínguez M, Malik TH, Bedoya R, Cabrera Pérez R, López Trascasa M, Pickering MC, Harris CL, Sánchez-Corral P, Llorca O, Rodríguez de Córdoba S: C3 glomerulopathy-associated CFHR1 mutation alters FHR oligomerization and complement regulation. J Clin Invest 2013, 123:2434–2446
54. Gale DP, de Jorge EG, Cook HT, Martinez-Barricarte R, Hadjisavvas A, McLean AG, Pusey CD, Pierides A, Kyriacou K, Athanasiou Y, Voskarides K, Deltas C, Palmer A, Frémeaux-Bacchi V, de Cordoba SR, Maxwell PH, Pickering MC: Identification of a mutation in complement factor H-related protein 5 in patients of Cypriot origin with glomerulonephritis. Lancet 2010, 376:794–801
55. Medjeral-Thomas N, Malik TH, Patel MP, Toth T, Cook HT, Tomson C, Pickering MC: A novel CFHR5 fusion protein causes C3 glomerulopathy in a family without Cypriot ancestry. Kidney Int 2014, 85:933–937
56. Chen JM, Cooper DN, Chuzhanova N, Férec C, Patrinos GP: Gene conversion: mechanisms, evolution and human disease. Nat Rev Genet 2007, 8:762–775
57. Nguyen K, Walrafen P, Bernard R, Attarian S, Chaix C, Vovan C, Renard E, Dufrane N, Pouget J, Vannier A, Bensimon A, Lévy N: Molecular combing reveals allelic combinations in facioscapulohumeral dystrophy. Ann Neurol 2011, 70:627–633

Long-read sequencing identifies a common transposition haplotype predisposing for *CLCNKB* deletions

Nikolai Tschernoster, Florian Erger, Stefan Kohl, Björn Reusch, Andrea Wenzel, Stephen Walsh, Holger Thiele, Christian Becker, Marek Franitza, Malte P Bartram, Martin Kömhoff Lena Schumacher, Christian Kukat, Tatiana Borodina, Claudia Quedenau, Peter Nürnberg, Markus M Rinschen, Jan H Driller, Bjørn P Pedersen, Karl P Schlingmann, Bruno Hüttel, Detlef Bockenhauer, Bodo Beck, Janine Altmüller

Submitted to the Journal of Genome Medicine on 22.03.2023. Under review since 30.03.2023

Author contributions:

NT: data generation, data analysis, figure design, and manuscript writing; FE: data analysis, data analysis tools, and manuscript writing; SK: clinical care, sample collection, and manuscript writing; BR: data generation; AW: data generation; SW: clinical care and sample collection; HT: data generation; CB: data generation; MF: data generation; MPB: clinical care and sample collection; MK: clinical care and sample collection; LS: data generation; CK: data generation TB: data generation; CQ: data generation; PN: data generation MMR: clinical care and sample collection; KPS: clinical care and sample collection; JHD; data generation, manuscript writing; BPP; data generation, manuscript writing; BH: data generation; DB: clinical care and sample collection; BB: study conception, sample collection, and manuscript writing; JA: study conception, data generation, and manuscript writing. All authors read and approved the final manuscript.

Supplementary Material is listed in Supplementary Material Manuscript 3.

Abstract

Background

Long-read sequencing is increasingly used to uncover structural variants in the human genome, both functionally neutral and deleterious. Structural variants occur more frequently in regions with a high homology or repetitive segments, and one rearrangement may predispose to additional events. Bartter syndrome type 3 (BS 3) is a monogenic tubulopathy caused by deleterious variants in the chloride channel gene *CLCNKB*, a high proportion of these being large gene deletions. Multiplex ligation-dependent probe amplification, the current diagnostic gold standard for this type of mutation, will indicate a simple homozygous gene deletion in biallelic deletion carriers. However, since the phenotypic spectrum of BS 3 is broad even among biallelic deletion carriers, we undertook a more detailed analysis of precise breakpoint regions and genomic structure.

Methods

Structural variants in 33 BS 3 patients with *CLCNKB* deletions were investigated using long-read and synthetical long-read sequencing, as well as targeted long-read sequencing approaches.

Results

We report a ~3 kb duplication of 3'-UTR *CLCNKB* material transposed to the corresponding locus of the neighbouring *CLCNKA* gene, also found on ~50 % of alleles in healthy control individuals. This previously unknown common haplotype is significantly enriched in our cohort of patients with *CLCNKB* deletions (45 of 51 alleles with haplotype information, $p=9.16x10^{-9}$). Breakpoint coordinates for the *CLCNKB* deletion were identifiable in 28 patients, with three being compound heterozygous. In total, eight different alleles were found, one of them a complex rearrangement with three breakpoint regions. Two patients had different *CLCNKA/CLCNKB* hybrid genes encoding a predicted *CLCNKA/CLCNKB* hybrid protein with likely residual function.

Conclusions

The presence of multiple different deletion alleles in our cohort suggests that large *CLCNKB* gene deletions originated from many independently recurring genomic events clustered in a few hot spots. The uncovered, strongly associated sequence transposition haplotype apparently predisposes to these additional events.

The spectrum of *CLCNKB* deletion alleles is broader than expected and likely still incomplete, but represents an obvious candidate for future genotype/phenotype association studies.

We suggest a sensitive and cost-efficient approach, consisting of indirect sequence capture and long-read sequencing, to analyse disease-relevant structural variant hotspots in general.

Keywords:
Bartter Syndrome type 3, salt-wasting tubulopathy, Long-read Sequencing, Target enrichment, *CLCNKA*, *CLCNKB*, Structural variant, Risk haplotype, Next-Generation Sequencing, HiFi-Sequencing

Abbreviations
BS: Bartter Syndrome; BS3: Bartter Syndrome type 3; BS 4b: Bartter Syndrome type 4b; NAHR: Non-allelic homologous recombination; TAL: Thick ascending limb; DCT: distal convoluted tubule; GS: Gitelman Syndrome; CKD: Chronic kidney disease; MLPA: Multiplex ligation-dependent probe amplification; NGS: Next-Generation Sequencing; LRS: Long-read third Generation Sequencing; HMW: High molecular weight; EDTA: Ethylenediaminetetraacetic acid; WES: Whole-Exome Sequencing; WGS: Whole-Genome Sequencing; CNV: Copy number variation; MAF: Minor allele frequency; ROI: Region of interest; PCR: Polymerase chain reaction; ONT: Oxford Nanopore Technology; ROH: Region of homozygosity; UTR: Untranslated region; SV: Structural variant; AA: Amino-acid; bp: Base-pairs; AF: Alphafold; RMSD: Root-Mean-Square Deviation

Introduction

Bartter Syndrome (BS), first reported in 1962 (BARTTER et al. 1962), is unarguably the prototypic Mendelian salt-losing tubulopathy, characterized by defective salt reabsorption in the thick ascending limb (TAL) of Henle and/or the distal convoluted tubule (DCT), resulting in chronic hypokalaemia, hypochloraemia, metabolic alkalosis, and hyperreninaemic hyperaldosteronism with low or normal blood pressure (Kleta and Bockenhauer 2018). BS forms a clinically heterogenous spectrum with variable onset and severity manifesting from antenatal life to adulthood with variable clinical signs (with/without nephrocalcinosis), and sometimes extrarenal findings like sensorineural deafness (BARTTER et al. 1962; Rodríguez-Soriano 1998; Gitelman et al. 1966). Today, the BS spectrum is genetically classified into five subtypes (type 1-5) and Gitelman syndrome (GS; phenotypically defined by hypomagnesemia and hypocalciuria in addition to hypokalaemic metabolic alkalosis), however, there is wide phenotypic overlap between the BS and the GS (like) spectrum (Kleta and Bockenhauer 2018). With the exception of *MAGED2* associated BS 5 (X-linked recessive), all other BS types (with digenic loss of *CLCNKB* and *CLCNKA* in the ultra-rare BS 4b) and *SLC12A3*-associated GS constitute autosomal recessive disorders (Table 1).

Table 1: Bartter syndrome subtypes and Gitelman syndrome classification: AR, autosomal recessive; DR, digenic recessive; XLR, X-linked recessive; a Prevalence in patients with antenatal BS, reported by Legrand et al. (Legrand et al. 2018); b Estimated incidence of GS reported by Kondo et al. (Kondo et al. 2021).

Bartter subtype	Gene	OMIM	Related Protein	Inheritance	prevalence	Reference
Type I	*SLC12A1*	601678	NKCC2	AR	Rare disease with unknown prevalence. More common BS type. Accounts for 24 % of antenatal BS cases[a]	(Simon et al. 1996a)
Type II	*KCNJ1*	241200	ROMK	AR	Rare disease with unknown prevalence. More common BS type. Accounts for 25 % of antenatal BS cases[a]	(Simon et al. 1996b)
Type III	*CLCNKB*	607364	ClC-Kb	AR	Rare disease with unknown prevalence. Maybe the most common type of BS worldwide. Accounts for 19 % of antenatal BS cases[a]	(BARTTER et al. 1962; Simon et al. 1997)

Type IV A	*BSND*	602522	Barttin	AR	Rare disease with unknown prevalence. Less common BS type. Accounts for 8 % of antenatal BS cases[a]	(Seyberth et al. 1985; Birkenhäger et al. 2001)
Type IV B	*CLCNKA + CLCNKB*	613090	ClC-Ka + ClC-Kb	DR	ultrarare BS type	(Schlingmann et al. 2004)
Type V	*MAGED2*	300971	MAGED2	XLR	Rare disease with unknown prevalence. Less common BS type. Accounts for 9 % of antenatal BS cases[a]	(Engels, A., Gordjani, N., Nolte, S., Seyberth, H. W. 1991; Laghmani et al. 2016)
Gitelman	*SLC12A3*	263800	NCCT	AR	Most common tubulopathy worldwide ca. 1:5000[b]	(Gitelman et al. 1966; Simon et al. 1996c)

BS 3 is caused by biallelic pathogenic variants in the *CLCNKB* gene encoding the ClC-Kb chloride channel (Simon et al. 1997). There are more than 140 different causative sequence variants reported in the *CLCNKB* gene (HGMD database accessed in 12/2022), but complete deletions of *CLCNKB* account for more than 50 % of all BS 3 disease alleles, often found in a homozygous state (Simon et al. 1997; Konrad et al. 2000; Han et al. 2017; Han et al. 2020; Seys et al. 2017; Najafi et al. 2019). The *CLCNKB* gene is directly adjacent to the highly homologous *CLCNKA* gene, presumably as a result of an ancient gene duplication. This genomic structure likely predisposes the locus to meiotic rearrangements, as is known to happen to other similar structured loci (e.g. the *CYP11B1/CYP11B2* locus (Lifton et al. 1992)).

Clinically, the BS 3 phenotype seems the most variable of all BS types, ranging from antenatal/neonatal BS (30 %), classic infantile/childhood BS (44 %), to a GS-like phenotype (26 %) (Matsunoshita et al. 2016; Seys et al. 2017; Brochard et al. 2009; Jeck et al. 2000; Konrad et al. 2000) of the 115 patients analysed in a recent retrospective French study (Seys et al. 2017). Patients with BS 3 are at risk to develop chronic kidney disease (CKD), which can progress to end-stage renal disease in some cases. Preliminary data on genotype/phenotype

correlations for BS 3 indicate that deletions and truncating mutations are associated with earlier diagnosis and higher risk for CKD (Seys et al. 2017; Matsunoshita et al. 2016). Currently, genetic diagnosis is commonly performed with Multiplex Ligation-dependent Probe Amplification (MLPA), a method that does not allow to determine the concrete expansion and detection of breakpoint regions of the deletion.

In this study, using a combination of synthetic long-read sequencing and Nanopore/PacBio Long-read Third Generation Sequencing (LRS), we performed an in-depth structural investigation of the *CLCNKA*/*CLCNKB* locus. Analysing 32 patients with *CLCNKB* deletion-associated BS 3, and one patient with digenic BS 4b (P17), we shed new light on the genomic complexity of this rearrangement-prone region.

Methods

Patients

Patients with a diagnosis of BS due to *CLCNKB* gene deletion were recruited from the departments of nephrology and paediatric nephrology at the University Hospital of Cologne, the department of paediatrics at the University of Marburg, the department of general paediatrics at the University Children's Hospital of Münster, and from Great Ormond Street Hospital in London.

High molecular weight DNA isolation

High molecular weight (HMW) genomic DNA isolation for linked read and Xdrop applications was performed using the MagAttract HMW DNA Kit (Cat. No. 67563) for 200 µl fresh EDTA blood input according to the manufacturer's specifications (Qiagen, Hilden, Germany).

Whole Exome Sequencing (WES)

WES was performed using Agilent SureSelect Whole Exome v7 enrichment (Agilent Technologies, Santa Clara, California, USA), followed by NGS on an Illumina NovaSeq 6000 platform (Illumina, San Diego, California, USA). Data analysis and NGS-based CNV detection were performed using the Cologne Center for Genomics Varbank2 application v.3.3 (Cologne Center for Genomics, Cologne, Germany). In particular, we filtered for high-quality (coverage >15-fold; Phred-scaled quality >25), rare (minor allele frequency (MAF) ≤0.01) variants. To exclude pipeline-related artefacts, we additionally filtered against common variants from in-house WES datasets.

10x Genomics linked-read analysis

High molecular weight DNA was extracted for library preparation following the Chromium Genome Reagent Kit standard protocol (CG00022 RevA) using the Chromium Genome Chip Kit PN-120216 (10× Genomics, Pleasanton, USA) and the Genome Library, Gel Bead & Multi- plex V1 Kit PN-120229 (10× Genomics) with the modification of using 0.9 ng of genomic DNA input. The fragment size of the prepared library was assessed using Tapestation 4200 (Agilent Technologies). The library was sequenced on a NovaSeq6000 sequencer (Illumina), which generated $1.63x10^9$ paired-end reads. Assembly was performed using the de novo genome assemblies setting of the Long Ranger v.2.2.2 genome assembler and visualized using the Loupe Browser v.2.1.1 (10x Genomics). 96.4 % of reads were mapped, reaching a mean coverage depth of 70.3x.

Samplix Xdrop indirect sequence capture and ONT long-read sequencing

The Xdrop indirect sequence capture allows the isolation of specific genomic DNA fragments which contain a region of interest (ROI) and enriches these fragments for long-read sequencing applications. Essentially, a small known genomic sequence of ~ 150 bp (detection sequence) is used near the ROI to select genomic high molecular weight DNA fragments of up to 50 kb spanning the breakpoint region or other structural variants of interest. To identify the breakpoint regions of the *CLCNKB* deletion, Xdrop indirect sequence capture was performed in selected patients (Suppl. Table 1). High molecular DNA is encapsulated with a PCR reaction mix (Samplix, Birkerød, Denmark). The short fluorescence-labelled detection sequence (forward primer; 5'-ATCCTGACACAGCCATCTGC-3' and reverse primer; 5'-TGATCACGCAGAACCCTCAG-3') is used to mark our ROI (suppl. Figure 1). Droplets containing the genomic ROI were enriched using a FACS Aria IIIu (BD Biosciences, Franklin Lakes, USA) using the 100-micron nozzle at 20 psi pressure, gating based on forward scatter pulse height, side scatter pulse height, and droplet fluorescence pulse height. Droplets were sorted using the "Yield" precision mode for the best possible recovery of droplets of interest. The sorting of droplets is described in more detail by Madsen et al. (Madsen et al. 2020). Before sequencing, the evaluation sequence (forward primer; 5'-GCCCAGAAGAGTTATGTGGCT-3' and reverse primer; 5'-GAGCCCTTGGAAAGCGAGTA-3') (Suppl. Figure 1) is used to assess the enrichment factor as quality control. DNA is released from the isolated droplets and encapsulated again containing a multiple displacement amplification mix for target enrichment followed by long-read sequencing using a GridIon sequencing device from Oxford Nanopore (Oxford Nanopore Technologies, Oxford, UK). Sequencing reads were aligned using the minimap2 software v2.17 (Li 2018), with the pre-specified map-ont parameter. The resulting alignment files were sorted and indexed using samtools v1.7 (Li et al. 2009), and visualized in the Integrative Genomics Viewer software v.2.10.2 (Robinson et al. 2011).

Long-range polymerase chain reaction (PCR) and amplicon-based SMRT sequencing

Specific forward primer 5'-AGATACTGGTTTTCCGTCATCTC-3' and reverse primer 5'-TACCTTTGTGGATATTTCCTCCTAC-3' were designed to exclusively amplify a ~6450 bp region covering the *CLCNKB* breakpoint regions previously identified by Xdrop targeted enrichment as described above. PCR was performed with 100 ng gDNA and 0.4 µM of primers using the LA-Taq polymerase and 2xGC PCR-Buffer I according to manufacturer protocols (Takara Bio Inc., Kusatsu, Japan).

PacBio whole genome long-read sequencing (Single-molecule real-time SMRT-Seq)

Libraries were prepared using the SMRTbell Express Template Prep Kit 2.0 (PN 101-853-100, Pacific Biosciences, Menlo Park, California, USA). Briefly, 5 µg of the genomic DNA was sheared to 15 kbp (Megaruptor 3, Diagenode, Denville, New York, USA), followed by performing damage repair, end repair, A-tailing and hairpin adapter ligation and final exonuclease treatment. All libraries were size selected using BluePippin (Sage Sciences, Beverly, Massachusetts, USA) running with a size cut-off of 10000 bp. AMPure PB magnetic beads (Pacific Biosciences) were used for all purification steps. Library size and quality were assessed using Fragment Analyzer (Agilent Technologies) and Qubit fluorometer with Quant-iT dsDNA HS Assay Kits (Invitrogen, Waltham, Massachusetts, USA).

Sequencing primer v5 and Sequel 2.2 DNA Polymerase were annealed and bound, respectively, to the final SMRTbell library. Libraries were loaded at an on-plate concentration of 80 pM and sequencing was performed using 8M SMRT cells on the Sequel II System with Sequel II Sequencing Plate 2.0 for 24h movie time. Secondary Analysis (HiFi reads) was performed using Pacific Biosciences SMRT Link v10.2. The sequencing data were then processed and analysed as described above.

ClC-Kb/ClC-Ka hybrid protein structure predictions

Protein structures of reference and hybrid ClC protein sequences were predicted using the ParaFold (Zhong et al. 2021) version of Alphafold2 (Jumper et al. 2021) using default parameters. Since ClC channels are homodimeric, the homodimeric states were generated using the multimer pre-set (n=2).

Results

Genetic workup of Family P1

Family P1 first presented in the paediatric nephrology department in 2018 with three male siblings with hypokalaemic metabolic alkalosis, hypochloraemia, hyperuricaemia and progressive chronic kidney disease (Figure 1A-F).

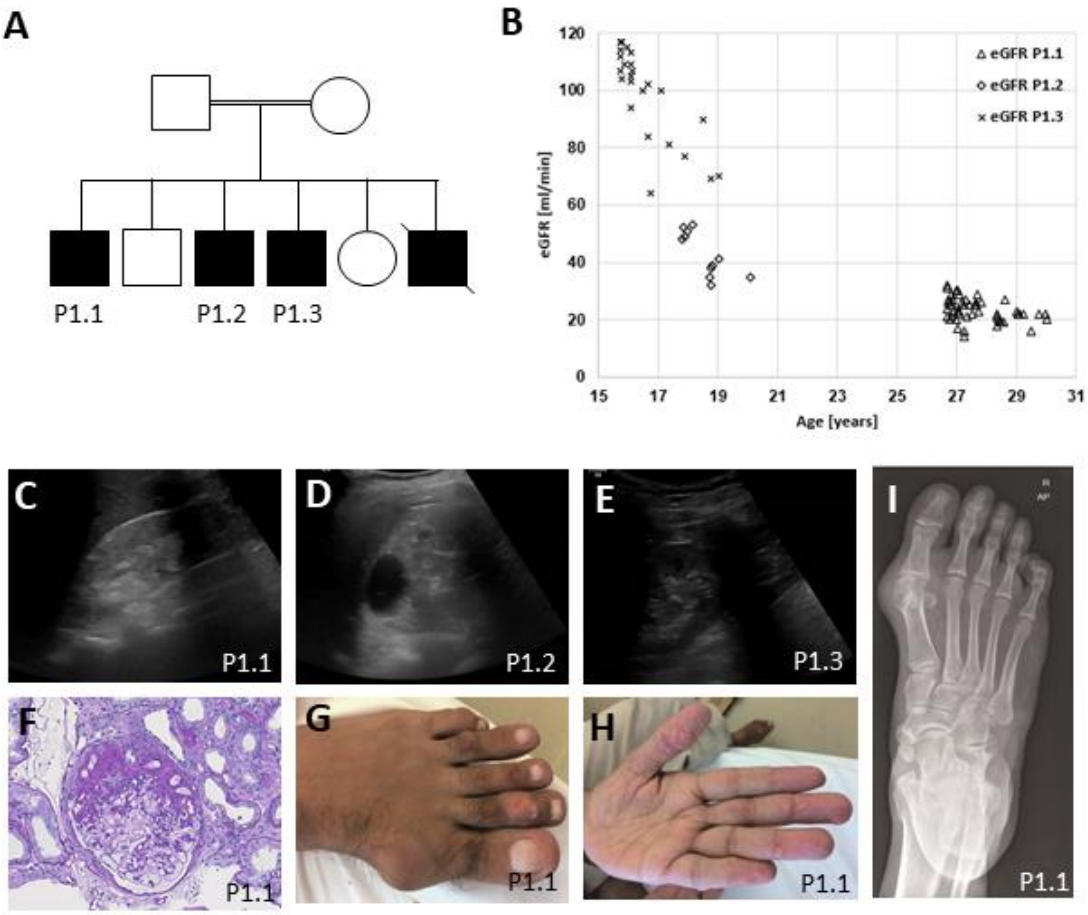

Figure 1: Clinical findings and pedigree in severely affected family P1

***A** Pedigree of family P1. **B** Estimated glomerular filtration rate (eGFR) in all brothers over a 15 years' timeline. Note that eGFR declines over age in all brothers. C-E Discordant kidney sonograms. **C** Increased echogenicity, nephrocalcinosis, and reduced cortico-medullary differentiation. **D** Increased echogenicity, nephrocalcinosis and multiple large cysts. **E**: Mildly increased echogenicity. **F** Histologic slide of kidney biopsy showing unspecific focal segmental glomerulosclerosis in P1.1. **G-I** Destructive gouty arthritis and multiple gout tophi in P1.1.*

WES of the three patients revealed no causative single nucleotide variants, but WES-based CNV detection suggested a homozygous deletion of *CLCNKB* (Figure 2A). A region of homozygosity (ROH) value of 389 Mb confirmed the reported consanguinity. Due to the unusually severe clinical presentation of the oldest sibling with intradermal tophi and gouty arthritis (Figure 1G-I), we performed breakpoint detection using linked-read whole genome sequencing. We identified an unusual pattern consisting of a large homozygous deletion encompassing *CLCNKB* and two smaller adjacent deletions nearby, but the precise genomic architecture remained unclear due to discontinuous sequencing reads (Figure 2B). As our attempts to identify breakpoints by PCR were unsuccessful, we used Xdrop indirect sequence capture and subsequent ONT long-read sequencing in patient P1.2. Here, we identified three breakpoint regions of 30-410 bp size that could not be further narrowed down because of their sequence homology (Figure 2C). The genomic architecture was then reconstructed as shown in Figure 2D. Based on the peculiar genomic findings in Family P1, we initiated a more detailed characterisation of the complete locus in a cohort of *CLCNKB* deletion patients.

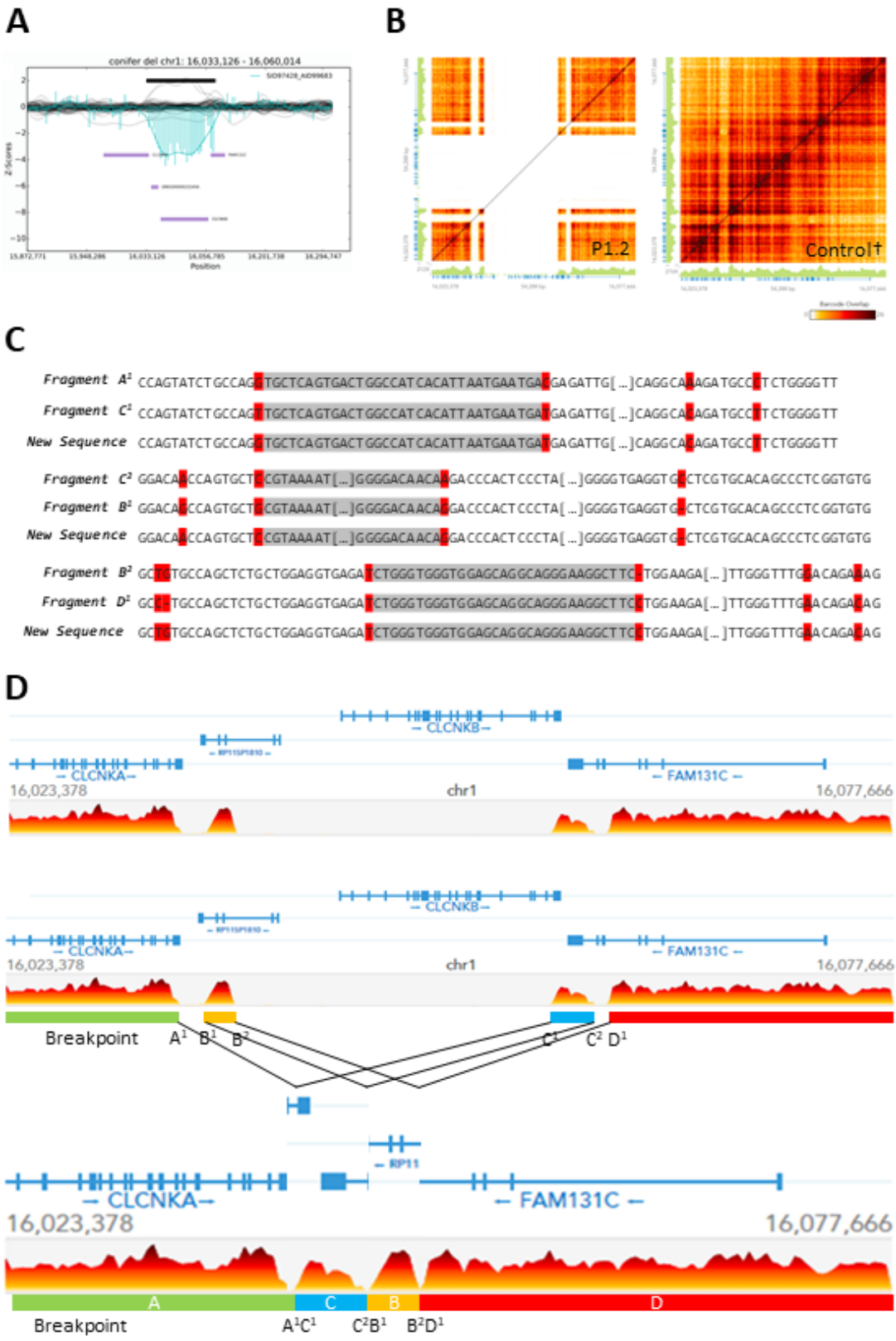
A
conifer del chr1: 16,033,126 - 16,060,014
Z-Scores
Position
B
P1.2
Control
C
Fragment A1 CCAGTATCTGCCAGGTGCTCAGTGACTGGCCATCACATTAATGAATGAAGAGATTG[...]CAGGCAAAGATGCCTTCTGGGGTT
Fragment C1 CCAGTATCTGCCAGTTGCTCAGTGACTGGCCATCACATTAATGAATGAAGAGATTG[...]CAGGCAAAGATGCCTTCTGGGGTT
New Sequence CCAGTATCTGCCAGGTGCTCAGTGACTGGCCATCACATTAATGAATGAAGAGATTG[...]CAGGCAAAGATGCCTTCTGGGGTT
Fragment C2 GGACAACCAGTGCTCCGTAAAAT[...]GGGGACAACAAGACCCACTCCCTA[...]GGGGTGAGGTGGCTCGTGCACAGCCCTCGGTGTG
Fragment B1 GGACAACCAGTGCTCCGTAAAAT[...]GGGGACAACAAGACCCACTCCCTA[...]GGGGTGAGGTGGCTCGTGCACAGCCCTCGGTGTG
New Sequence GGACAACCAGTGCTCCGTAAAAT[...]GGGGACAACAAGACCCACTCCCTA[...]GGGGTGAGGTGGCTCGTGCACAGCCCTCGGTGTG
Fragment B2 GCTGTGCCAGCTCTGCTGGAGGTGAGATCTGGGTGGGTGGAGCAGGCAGGGAAGGCTTCCTGGAAGA[...]TTGGGTTTGGACAGAAAG
Fragment D1 GCCTGCCAGCTCTGCTGGAGGTGAGATCTGGGTGGGTGGAGCAGGCAGGGAAGGCTTCCTGGAAGA[...]TTGGGTTTGGACAGAAAG
New Sequence GCTGTGCCAGCTCTGCTGGAGGTGAGATCTGGGTGGGTGGAGCAGGCAGGGAAGGCTTCCTGGAAGA[...]TTGGGTTTGGACAGAAAG
D
CLCNKB
RP11SP1810
CLCNKA
FAM131C
16,023,378
chr1
16,077,666
Breakpoint
A1 B1 B2
C1 C2 D1
RP11
A
C
B
D
A1C1
C2B1
B2D1

Figure 2: Results of the WGS and linked-read WGS analysis from patient P1.2.

***A** Varbank2 implemented conifer CNV analysis tool showing results from the WGS dataset. Z-scores from patient P1.2 in cyan coloured bars and also as extrapolated curve. Affected region is indicated by the black horizontal bar. Genes in this region are indicated by purple horizontal bars. The markers are evenly distributed among the positional X-axis. The black curves represent the control collective, consisting of a fixed set of samples for the given enrichment kit. **B** Linked-read Loupe browser v.2.1.1 haplotype resolved SV results for patient P1.2 compared to a control sample (matrix view). Genomic region chr1:16.023.378-16.077.660 (hg38) is displayed on y- and x-axis for both alleles, respectively. Number of reads is indicated by green vertical bars. Sequence coverage (barcode overlap) is indicated by the heat map ranging from zero coverage (white) to high coverage (black). **C** Xdrop indirect sequence capture and ONT long-read sequencing results for patient P1.2. Gene-specific nucleotides are indicated by red background, breakpoint regions are indicated by grey background. Long stretches of homologous genomic DNA sequence have been shortened, indicated by […]. **D** Reconstruction of the genomic structural rearrangement of patient P1.2. The three breakpoint regions result in a rearrangement of fragment B and fragment C and the deletion of the genomic DNA in-between these fragments. Genomic DNA Fragments were rearranged according to the identified breakpoints. New genomic rearrangement consisting of fragment A-C-B-D. The common sequence transposition haplotype equates to the transposition of fragment C. Genes are indicated in blue with exons as blue vertical bars. Gene orientation is indicated by blue arrows. Colour coding of genomic fragments A (green), B (orange), C (blue) and D (red). Genomic sequence coordinates refer to the hg38 human reference. † Linked-read control carries the CLCNKA 3' UTR sequence transposition haplotype heterozygously.*

Results of the genomic workup of the cohort

Long-range PCR containing a ~6450 bp DNA fragment covering the genomic breakpoint regions found in patient P1.2 was performed, and 29 additional patients with *CLCNKB* deletion-associated BS 3, and one patient with BS 4b were analysed. The long-range PCR yielded an amplicon in 25 of the 33 patients. For a summary of the molecular genetic analyses performed on each patient, see Suppl. Table 1. Clinical data for all patients included in this study are summarized in Table 2.

Table 2: Patient cohort. ABS, antenatal BS; CBS, classical BS, GLS, Gitelmann like syndrome; lower case letters in the country of origin column indicate c, consanguineous; familial (f); sporadic (s) case; wk, week; mo, months; y, years; nd, no data. a patient has been previously reported in Giri et al. 2020. b Patients have been previously reported in Konrad et al. 2000. c Patient has been previously reported in Schlingmann et al. 2004.

Family Patient ID	sex	age at study	age at definite diagnosis	country of origin	phenotype	Other complications, remarks	eGFR (ml/min/1.73m²) or serum creatinine (mg/dl) on last follow up	Deletion alleles (letter code)
P1.1	male	31	0	Syria; c	ABS	destructive gouty arthritis	<15 (age 31 y)	C
P1.2	male	22	0	Syria; c	ABS	Hyperuricemia	35 (age 22 y)	C
P1.3	male	20	0	Syria; c	ABS	Hyperuricemia, seizures (normal EEG)	70 (age 19 y)	C
P2	female	46	nd	UK-Asian	CBS	Short statue	27	E
P3	female	18	1	UK-Asian	CBS	(polyhydramnios, but born 42 wks Presented with critical collapse with multisystem organ failure age 1 y in the context of enteroviral infection	70 (age 17 y)	E
P4	male	15	7	UK-Asian	CBS	Childhood, initially presented age 2 y with growth failure, referred to nephrology age 7 y with persistent hypokalaemia	140 (age 8 y)	A
P5	male	15	8	UK-black	GS	Childhood, presented age 7 y with abdominal pain and blood tests showed hypokalaemia/hypomagnesaemia	155 (age 10 y)	F
P6	female	10	3	UK-Asian	CBS	Childhood, presented age 3 y with growth failure and noted to have hypokalaemia and alkalosis	180 (age 10 y)	H
P7	female	32	~6	Italy	CBS, GS	Presented initially in Italy, notes only say that she presented initially as CBS, but then looked more and more like GS, so that BS3 was suspected.	102 (age 17 y)	B
P8	male	18	2	Sri Lanka	ABS	Antenatal, (polyhydramnios, born at term), 3 siblings died in infancy of unclear cause in Sri Lanka	60 (age 17 y)	B
P9	male	29	1	UK-black	ABS	Antenatal, (27 wk gestation), nephrocalcinosis, nephrotic range proteinuria (first noted age 13), quantified as 3.3 g/d	67 (age 16 y)	B, F
P10[a]	female	10	1	UK-white	nd	Born 34 wk (no polyhydramnios) presented age 4 days with weight loss, found to have HSD3B2 deficiency.	120 (age 1 y)	D
P11	male	nd	1	Italy	ABS	Antenatal, (polyhydramnios with 4 amnioreductions, born at term), intrauterine growth restriction, birthweight 2130g. In neonatal period noted to have hypoklaemic alkalosis	95 (age 3 y)	G
P12	female	17	1	UK-Iranian	ABS	Antenatal, (polyhydramnios, but born at term), presented at age 3 months with growth failure and severe electrolyte abnormalities: Na 120, K: 1.0)	50 (age 17 y)	E
P13	male	29	7	Iran	CBS	Childhood, pre-school age presentation with growth failure, polyuria, hypokalaemia history of previous fetal loss with polyhydramnios	15 (creatinine 350, age 18 y)	E
P14	female	3	1	UK-black	CBS	Presentation age 2 months with growth failure, noticed to have hypokalaemia	110 (age 3 y)	B, F
P15.1[b]	male	nd	nd	German, f	nd	5 wk	nd	A
P15.2[b]	male	nd	nd	German, f	nd	Childhood, age 4 years	nd	A
P16[b]	male	nd	nd	Turk, f	nd	5 wk	nd	nd
P17[b, c]	female	34	nd	Turk, c	ABS	Antenatal, (polyhydramnios, born at 28 wks gestation), polyuria, hypokalaemia, metabolic alkalosis, sensorineural deafness, digenic BS 4b	nd	B
P18	female	29	22 mo	Congo, s	CBS	Childhood, pre-school age presentation with growth failure	90 (age 27 y)	F
P19	female	27	2.5 mo	Turk, c	CBS	Infantile onset	Creatinine 1.3 (age 4.5 y)	nd
P20	male	nd	nd	Turk, c	nd	nd	nd	B
P21	male	23	3 wk	Turk, c	CBS	Antenatal, (34 wk gestation) vomiting, hypokalaemic alkalosis	Creatinine 0.9 (age 14 y)	E

P22	male	21	5 mo	Tamil	CBS	Infantile onset, vomiting, hypokalaemic alkalosis	Creatinine 0.3-0.4 (age 1 y)	nd
P23	female	24	9 mo	France, s	CBS	Infantile onset, failure to thrive, polyuria	nd	F
P24	female	20	5 wk	Arabia, c	CBS	Infantile onset	Creatinine 0.4 (age 2 mo)	E
P25	female	32	nd	Rwanda, s	nd	nd	nd	nd
P26	female	19	6 mo	Afghanistan, c	CBS	nd	nd	nd
P27	male	18	2 mo	Turk, c	CBS	Failure to thrive	nd	E
P28	female	16	nd	Turk, c	ABS	nd	nd	E
P29	female	nd	nd	Turk, c	nd	nd	nd	E
P30	male	nd	nd	Africa, s	CBS	nd	nd	B

Patient P11 with no long-range PCR product was first analysed using Xdrop targeted DNA enrichment and long-read sequencing, identifying the breakpoint regions. In this patient, the first breakpoint region is located upstream of the long-range PCR forward primer resulting in the loss of the PCR forward primer binding site. Of the other seven patients with no long-read PCR amplicons, two patients (P6 and P10) were subsequently analysed using whole genome long-read sequencing, which identified the cause of amplification failure. In patient P10, one breakpoint region is located 1727 bp downstream of the long-range PCR reverse primer binding site, thus, deleting the binding site. In patient P6, a single breakpoint region located 302 bp upstream of the long-range PCR forward primer binding site resulted in the loss of the binding site. Taken together, we identified the breakpoint regions in 28 of the 33 patients with *CLCNKB* deletions. Whereas we initially hypothesised that the deletions in the *CLCNKA*/*CLCNKB* locus largely represent complex events, our investigation of the larger cohort and healthy controls revealed the presence of a common, but previously unreported structural haplotype. In most patients, we detected a transposition of a 2.2-3.0 kb long segment of the human genome reference *CLCNKB* 3' untranslated region (UTR) to the corresponding region in the *CLCNKA* 3' UTR. In NGS datasets aligned against the reference genome, this results in an apparent loss of *CLCNKA* 3' UTR sequence with a concomitant gain of *CLCNKB* 3' UTR genetic material (see Figure 3). 45 (88.2 %) of the structurally characterized deletion alleles for which a haplotype determination could be made (alleles A-F, n=51) lie on the variant haplotype. Additionally, we reviewed the *CLCNKA*/*CLCNKB* gene cluster in the new T2T CHM13-v2.0 human reference genome (Nurk et al. 2022) on a random selection of our patients and confirmed both the sequence transposition haplotype as well as the different deletion alleles (data not shown).

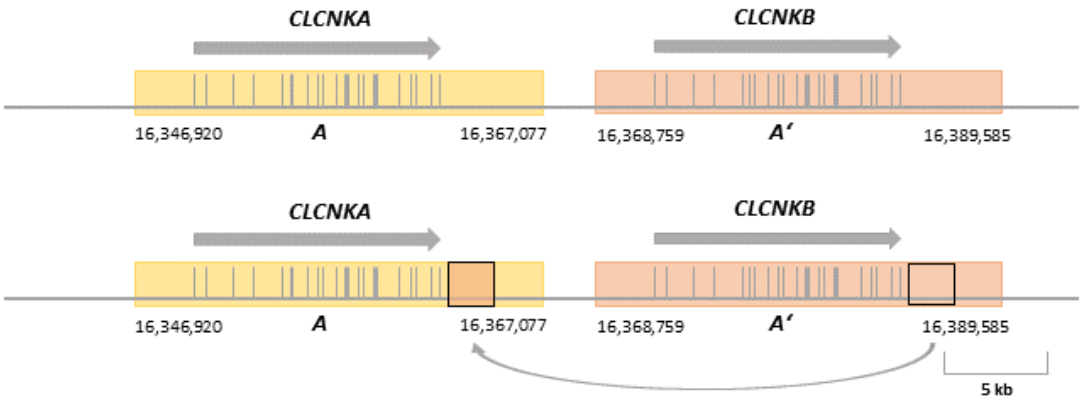

Figure 3: Genomic CLCNKA/CLCNKB locus and the common CLCNKA 3' UTR sequence transposition haplotype on chromosome 1p36.13.

The genomic environment surrounding the CLCNKA/CLCNKB gene locus contains two highly homologous genomic regions (A and A', sequence homology approx. 80 %). A and A' are indicated by the yellow and orange boxes, respectively. The homologous region A stretches over 20.157 bp from chr1:16,346,920-16,367,077 (GRCh37/Hg19), region A' stretches over 20.827 bp from chr1:16,368,759-16,389,585 (GRCh37/Hg19). The exonic sequence homology of CLCNKA and CLCNKB is 94 % (Simon et al. 1997). In the alternative transposition haplotype, a 2.2-3 kb large DNA fragment of the CLCNKA 3' UTR (small orange box, arrow head) is replaced by the homologous fragment from the 3' UTR of CLCNKB (small orange box, arrow tail), resulting in the loss of the genomic material downstream of CLCNKA and an extra copy of the DNA fragment duplicated from the CLCNKB 3' UTR. Gene length and orientation of CLCNKA and CLCNKB are indicated by the grey arrows. Exons are indicated as grey bars.

In our review of short-read and long-read in-house control datasets, we found this sequence transposition haplotype on nearly half of all alleles. Based on coverage data from more than 76,000 whole genome sequencing analyses in the gnomAD v3.1.2 dataset, we estimate the worldwide allele frequency of the variant haplotype at approximately 50 % (Suppl. Figure 2). To investigate whether the human reference haplotype or the transposition haplotype is the ancestral haplotype, we compared the human reference sequence to the rhesus monkeys' and other, more distantly related species' reference sequences. While the rhesus monkey reference sequence corresponds to the human reference sequence in 40 of the allele-defining 69 nucleotides (58 %), a meaningful comparison was not feasible in other studied species, likely due to larger genetic distance. The moderate reference sequence similarity between human and rhesus monkey does not currently prove or rule out the presence of either haplotype in the rhesus monkey population, and we thus cannot determine the ancestral haplotype.

Altogether, we found eight different deletion alleles (termed here A-H; Figure 4). At least five of the eight deletion alleles (B, C, D, E, F) derive from the variant haplotype (Figure 4). Allele A derives from the reference haplotype. The origin of deletion alleles G and H cannot be determined with certainty based on sequence data, as the transposed segment lies within the deletion. Interestingly, we could detect alleles of various complexity ranging from simple single breakpoint regions to more complex interlaced "scattered" alleles with three breakpoint regions (allele G). Deletion alleles C and E are defined by the same breakpoint region but differ in the length of the variant haplotype sequence transposition segment in the *CLCNKA* 3' UTR (2.2 kb vs. 3.0 kb). A summary of each patient's breakpoint region coordinates can be found in Suppl. Table 2. The breakpoint region in alleles C and E is the most common breakpoint region identified in this study (24 of 56 alleles), with allele E being the single most common allele (18 of 56). All SVs found in this study are in a homozygous state, except for patients P9, P14, and P18. P9 and P14 both carry the deletion alleles B and F compound heterozygously (Figure 4A). Patient P18 was previously diagnosed with a presumably hemizygous 5 bp deletion in exon 9 of *CLCNKB* resulting in a frameshift (c.847_851delTTCTT; p.Phe284Cysfs*38, Suppl. Figure 3). Patient P17 has previously been reported by Schlingmann et al. with digenic BS 4b (Schlingmann et al. 2004). Sequence overviews of all deletion alleles found in our cohort are shown in Suppl. Figure 4.

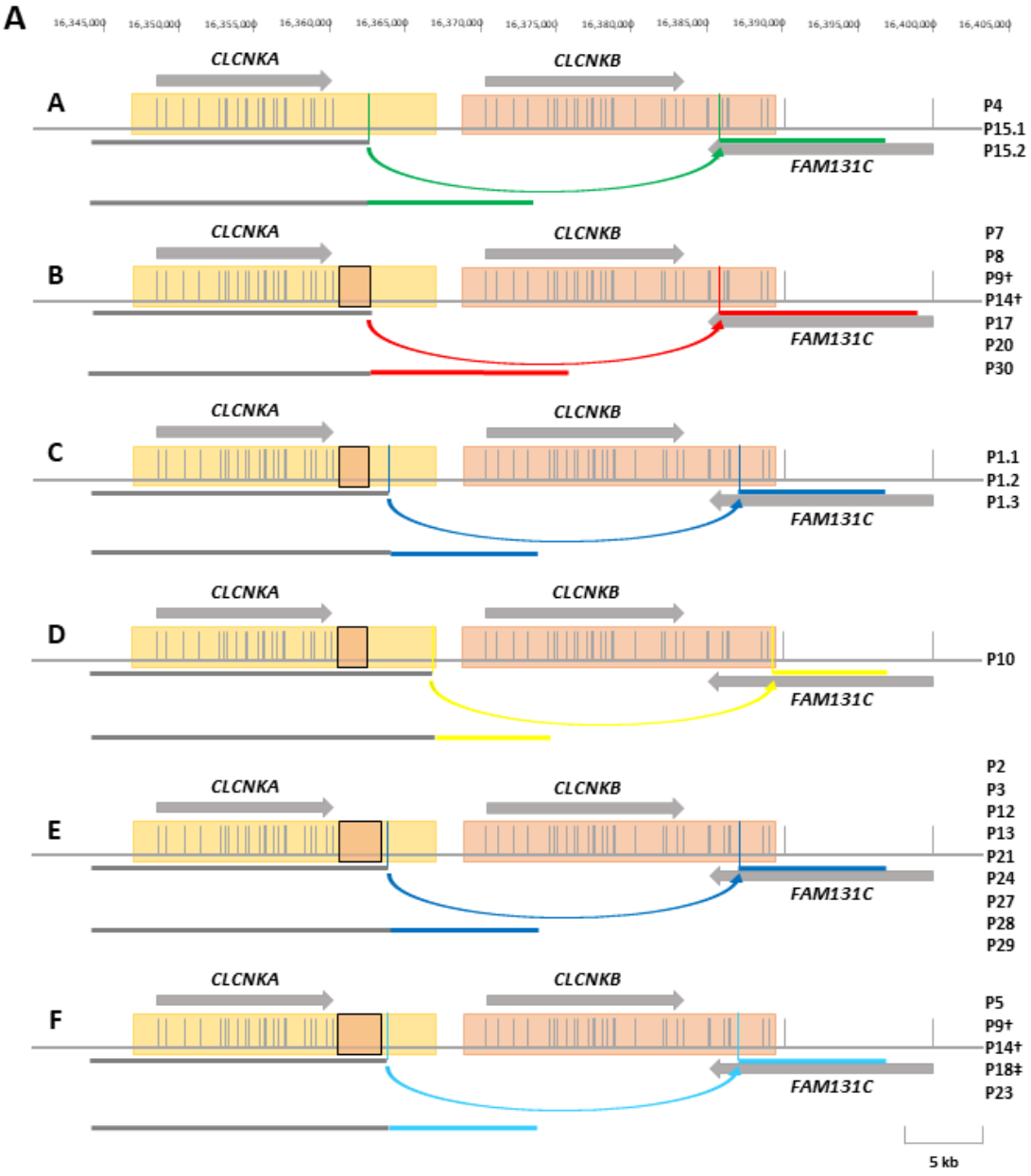
A
16,345,000
16,350,000
16,355,000
16,360,000
16,365,000
16,370,000
16,375,000
16,380,000
16,385,000
16,390,000
16,395,000
16,400,000
16,405,000
CLCNKA
CLCNKB
A
P4
P15.1
P15.2
FAM131C
CLCNKA
CLCNKB
B
P7
P8
P9†
P14†
P17
P20
P30
FAM131C
CLCNKA
CLCNKB
C
P1.1
P1.2
P1.3
FAM131C
CLCNKA
CLCNKB
D
P10
FAM131C
CLCNKA
CLCNKB
E
P2
P3
P12
P13
P21
P24
P27
P28
P29
FAM131C
CLCNKA
CLCNKB
F
P5
P9†
P14†
P18‡
P23
FAM131C
5 kb

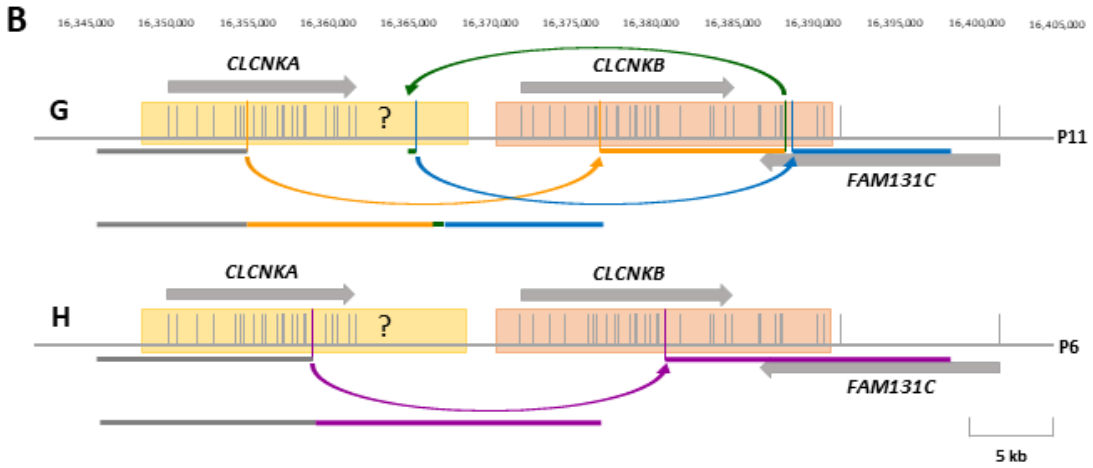

Figure 4: Summary of the CLCNKB deletion alleles identified in this study.

Breakpoint regions are indicated by coloured arrows. Identical breakpoint regions are coloured in the same colour. Two common CLCNKA 3' UTR sequence transpositions identified in this study are indicated by the orange box within the yellow box of CLCNKA. Breakpoint region coordinates of the 2.2 kb and 3 kb sized sequence transpositions are listed in Suppl. Table 2. Exons are indicated as vertical bars. Orientation and length of CLCNKA and CLCNKB are indicated by grey arrows. The gene FAM131C, located on the negative strand, is only partially visualized. ***A*** *Deletion allele A is derived from the reference haplotype. Deletion alleles B, C and D are derived from the smaller 2.2 kb sized sequence transposition haplotype. Deletion alleles E and F are derived from the larger 3 kb sized sequence transposition haplotype. Adjacent breakpoint region coordinates that discriminate the deletion alleles E and F are listed in Suppl. Table 2. All patients show the corresponding deletion allele in a homozygous state if not indicated otherwise.* ***B*** *Deletion alleles G and H that result in CLCNKA/CLCNKB hybrid genes. Since the haplotype-defining genomic sequence is deleted on these alleles, a haplotype determination could not be made. † Patients, compound heterozygous for the deletion alleles B and F; ‡ Heterozygous deletion allele. This patient carries a 5 bp deletion in exon 9 in trans.*

CLCNKA/CLCNKB hybrid gene

In two patients we found breakpoint regions affecting the coding sequence of both *CLCNKA* and *CLCNKB*. Patient P11 carries a complex deletion allele G with three breakpoint regions. The first breakpoint region is located in a homologous region of 53 bp in intron 7/8 of *CLCNKA* and intron 7/8 of *CLCNKB* resulting in an in-frame fusion of *CLCNKA* exons 1-7 to *CLCNKB* exons 8-20. Patient P6 carries a single breakpoint in a homologous region of 144 bp in intron 14/15 of *CLCNKA* and intron 15/16 of *CLCNKB* resulting in an in-frame hybrid gene composed of exons 1-15 of *CLCNKA* and exons 16-20 of *CLCNKB* (Figure 4B).

Predicted ClC-Ka/ClC-Kb hybrid proteins

ClC-Ka and ClC-Kb channels share a high sequence identity of 91.3%. The hybrid genes identified in patients P6 and P11 result in two different ClC-Ka/ClC-Kb hybrid proteins. In patient P11 the predicted hybrid protein is composed of amino-acids (AA) 1-218 of ClC-Ka and AA 219-687 of ClC-Kb (Figure 5A, 6A). Due to the high sequence identity between ClC-Ka and ClC-Kb, this hybrid protein differs in 43 AA positions from the wildtype ClC-Ka protein. In patient P6 the breakpoint is located at Gly541, behind the last transmembrane helix of ClC-Ka. The predicted hybrid protein is composed of AA 1-540 of ClC-Ka and AA 541-687 of ClC-Kb altering the ClC-Ka AA-sequence by 16 AA (Figure 5B, 6B).

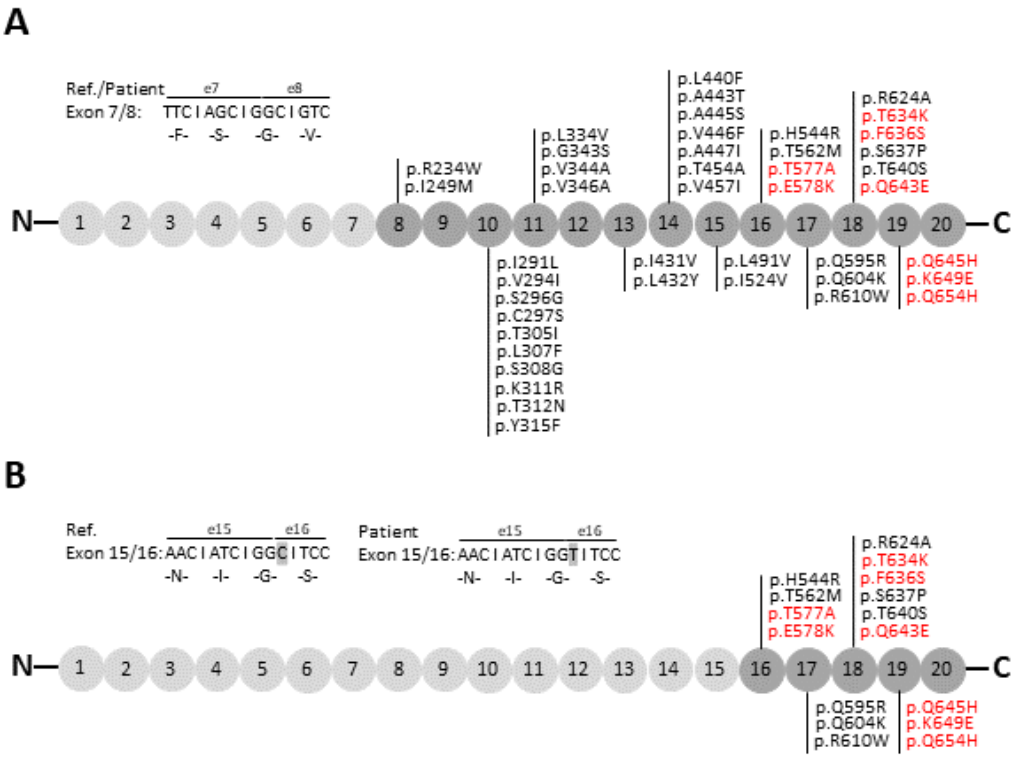

Figure 5: Workup of the ClC-Ka/ClC-Kb hybrid genes in patients P6 and P11.

ClC-Ka AA-sequence is indicated in light grey; ClC-Kb AA-sequence is indicated in dark grey; AA changes between wildtype ClC-Ka and ClC-Ka/ClC-Kb hybrid protein are annotated in the corresponding exon. AA changes analysed in detail in Figure 6 are shown in red. ***A*** *Hybrid gene in patient P11. Breakpoint region in intron 7/8. Genomic sequence at the border between exon 7 and exon 8 divided into triplets and the corresponding AA are shown. Ser218 is the last AA encoded by exon 7 before the breakpoint region.* ***B*** *Hybrid gene in patient P6. Breakpoint region in intron 15/16. Genomic sequence at the border between exon 15 and exon 16 divided into triplets and the corresponding AA are shown. I540 is the last AA encoded by exon 15 before the breakpoint region. AA G541 is encoded by the last two nucleotides of exon 15 and the first nucleotide of exon 16. In the hybrid gene the first nucleotide in exon 16 encoded by CLCNKB has changed from C>T but the corresponding AA G541 remains unchanged in the hybrid protein.*

As no frameshifts are introduced or deletions occur in the hybrid genes, the overall topology of the ClC-K channel is retained in these hybrids and we assume that the hybrid genes express stable proteins. We predicted the structures of ClC-Ka, ClC-Kb as well as the two hybrids in a homodimeric state using Alphafold2 (AF) (Jumper et al. 2021; Zhong et al. 2021). The AF predictions show minimal difference between the two homologs and the two hybrids with a Root-Mean-Square Deviation (RMSD) between Cα atoms of the structures of 0.3Å (see Figure 6A, B). We checked the validity of the predictions by comparing to the cryo-EM structure of ClC-K from Bos Taurus (PDB ID: 5TQQ, 84,3% seq. ID to ClC-Ka and ClC-Kb). The predictions were found to be highly similar to the Bos Taurus ClC-Channel with an RMSD of 0.5 Å, supporting that the predictions are correct (Park et al. 2017)(see Figure 6A-C). As AA variations in the hybrid proteins arise from the two endogenous proteins, most AA variations exhibit the same sidechain properties (e.g. hydrophobic:hydrophobic, polar:polar) within the membrane helices. Since the tunnel of the protein is not affected by any AA variation between ClC-Ka and ClC-Kb, interference with channel function would thus not be expected (Figure 6D).

Interestingly, both hybrids contain the cytoplasmic cystathionine beta synthase (CBS) domain of the ClC-Kb channel, which are known regulators in ClC proteins via binding to adenosine nucleotides thereby activating or inhibiting channel function (Accardi and Picollo 2010). This suggests that the activity of the hybrid proteins is regulated as the ClC-Kb would be. The CBS domains of ClC-Ka and ClC-Kb show distinct differences in the putative adenosine nucleotide binding side (577 Thr(A)/Ala(B), 578 Glu(A)/Lys(B), 654 Gln(A)/His (B)) when superimposing the ATP bound in ClC-7 (RCSB Protein database 7jm7) to the predicted structures (Figure 6E). Binding of ATP in ClC-7 is however also supported by the N-terminal region of the protein, which is missing here (Schrecker et al. 2020). It is currently still unknown if ClC-K proteins are regulated by adenosine nucleotides as other ClC proteins are. Several interesting AA changes can also be found in the CBS domain interface with the membrane region (Figure 6F) and the CBS dimerization interface (Figure 6G).

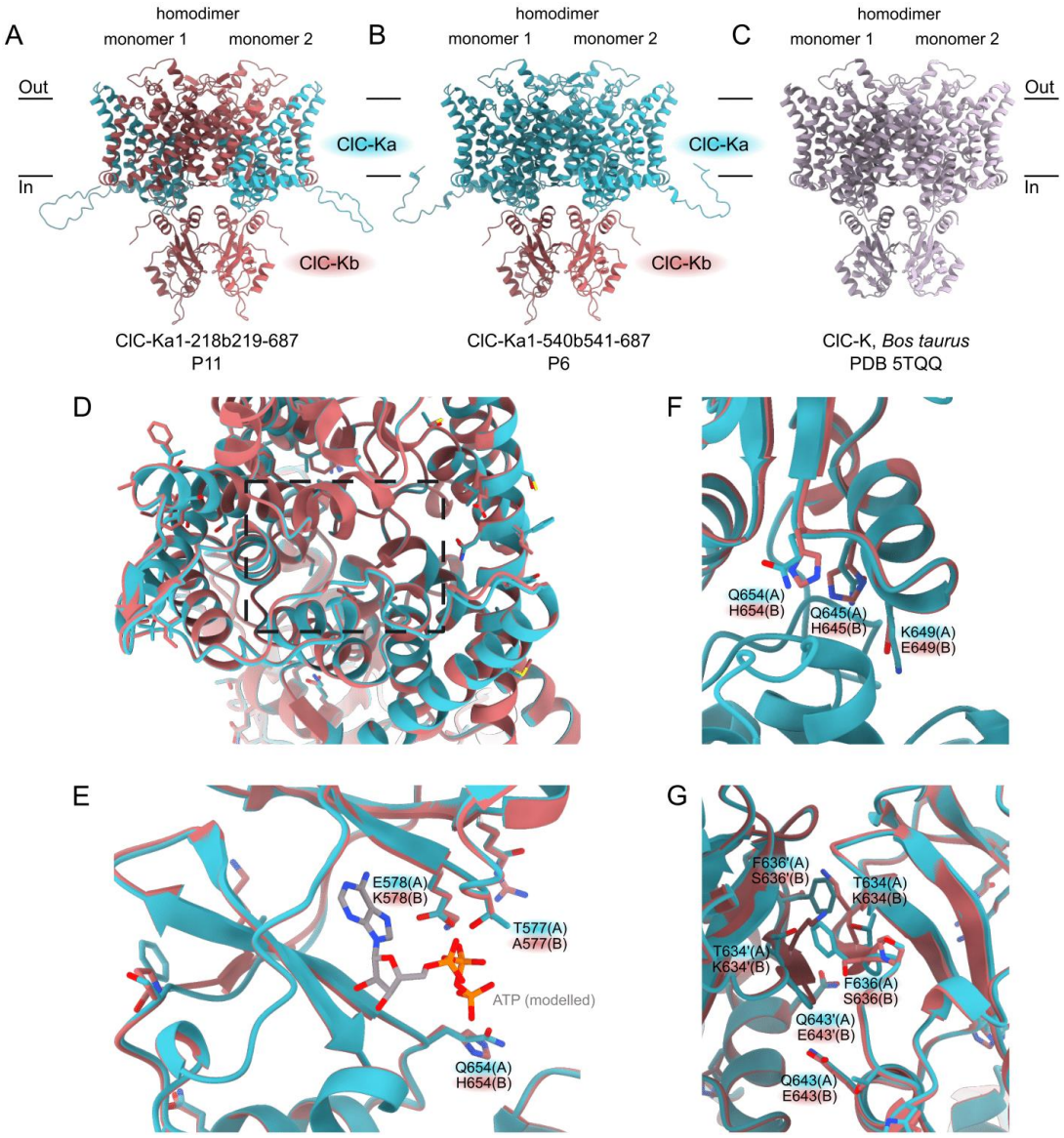

Figure 6: Predicted ClC-Ka/ClC-Kb hybrid proteins in patients P6 and P11.

***A** AlphaFold2 prediction of the ClC-Ka1-218b219-687 hybrid homodimer (P11). **B** AlphaFold2 prediction of the ClC-Ka1-540b541-687 hybrid homodimer (P6). **C** Cryo-EM structure of the ClC-K homodimer from Bos taurus (PDB ID: 5TQQ, 84,3% seq ID to ClC-Ka and ClC-Kb). **D** View on the membrane region of ClC-Ka (teal) and ClC-Kb (pastel red) with the amino acid variations shown in sticks shows no significant changes in the ion tunnel between the variants ClC-Ka and ClC-Kb. **E** Putative adenosine nucleotide binding site in ClC-Ka and ClC-Kb superimposed with an ATP bound in ClC-7 structure (Protein data base: 7jm7). **F** Interface between the cytosolic CBS domains of the ClC-Ka and ClC-Kb proteins. **G** Dimerization interface of the CBS domains in the ClC-Ka and ClC-Kb shows distinct differences.*

Discussion

CLCNKB deletions are the leading cause of Bartter syndrome type 3 worldwide (Simon et al. 1997; Han et al. 2020; Han et al. 2017; Najafi et al. 2019).

In this study, we report the *CLCNKB* deletion breakpoint region coordinates of 27 patients from 25 families with BS 3 and one patient with BS 4b. We characterize the deletion alleles utilizing long-read sequencing and detected eight different *CLCNKB* deletion alleles, which are likely caused by non-allelic homologous recombination (NAHR) with homologous flanking regions >200 bp as suggested by Ebert et al. (Ebert et al. 2021). For the remaining five patients with no long-read PCR amplicons, additional molecular genetic workup was not performed. For two of these patients the DNA quality was very low, which could explain the failure to generate a long-range PCR product. Given the number of different deletion alleles detected in this study, the probability of additional genotypes is high.

Based on these results, we estimate that the long-range PCR reported here is capable of identifying about 75 % (49/65) of the deletion alleles, assuming that all patients with a single deletion allele type are homozygous for this deletion allele. This procedure cannot exclude compound heterozygosity for a “long-range PCR positive” deletion allele with a “long-range PCR negative” deletion allele. However, such a constellation was not detected in any patient analysed by whole-genome LRS or indirect sequence capture LRS. The discrimination between two different “long-range PCR positive” deletion alleles in the same patient (as in patients P9 and P14) is possible. A fully sensitive and specific as well as allele-agnostic method is the indirect sequence capture approach by Xdrop followed by LRS, or alternatively whole-genome LRS – the latter being cost-prohibitive in most settings. In our view, a reasonable procedure to precisely detect breakpoint alleles is to start with a screening long-range PCR followed by indirect sequence capture LRS if no PCR product can be derived.

The presence of multiple different deletion alleles in our cohort suggests that *CLCNKB* whole gene deletions originated from many independently recurring genomic events.

This in-depth approach characterizing *CLCNKB* deletion alleles may prove useful for the investigation of genotype/phenotype correlations in BS 3 patients, who show a remarkable phenotypic variability that currently remains largely unexplained. Approximately 1/3 of patients carrying biallelic *CLCNKB* deletions present antenatally with polyhydramnios (Simon et al. 1997; Konrad et al. 2000; Brochard et al. 2009; Schurman et al. 2001). This observation

is consistent with the clinical data of our cohort, in which 34 % (9 of 26) of patients for which phenotype data is available, also had an antenatal onset of disease (see Table 2). Whether the precise determination of the deletion allele could have an impact on patient care or could allow a better prognosis of the severity and disease progression (e.g. renal failure) cannot yet be predicted given our cohort size. This question needs to be revisited when more exact genotype-phenotype data becomes available in larger cohorts. The *CLCNKB* deletions also include parts of the 3' UTR of *FAM131C*. The size of the *FAM131C* 3' UTR deletion was not associated with the differences concerning the clinical phenotype in our cohort. Furthermore, no monogenic disease caused by mutations in *FAM131C* is known to date and *FAM131C* has not been attributed to any particular function.

CLCNKB full gene deletions are most often described as homozygous (Konrad et al. 2000; Han et al. 2017; Han et al. 2020; Schurman et al. 2001; Najafi et al. 2019; Giri et al. 2020). Only a few studies reported cases with heterozygous whole *CLCNKB* gene deletions in combination with other mutations (Nozu et al. 2007; Han et al. 2020; Zhao et al. 2022). Cases of two different whole gene *CLCNKB* deletion alleles have not been reported until now. This is most likely because previous studies have utilised MLPA, PCR or WES to identify deletions, which are not sensitive to small breakpoint region differences in the two alleles. Only through long-read sequencing it has become possible to completely characterize these structural variants.

Our deep genotype analysis identified two patients with different *CLCNKA*/*CLCNKB* hybrid genes. Rare *CLCNKA*/*CLCNKB* hybrid genes have been reported previously, but always in a heterozygous state (Sahbani et al. 2020; Nozu et al. 2008; Konrad et al. 2000). Here we report two novel hybrid genes in a homozygous state that presumably lead to the expression of hybrid ClC-Ka/ClC-Kb proteins under the *CLCNKA* promotor. Complete loss of ClC-Ka and ClC-Kb function would result in hearing loss in addition to salt-wasting tubulopathy (BS 4b) (Schlingmann et al. 2004). Interestingly, our patients have no hearing impairment, suggesting an at least partially functional ClC-Ka/ClC-Kb hybrid protein that still can accommodate functions of ClC-Ka. This deduction is further supported by the structure predictions of the hybrid proteins and the fact that the proteins share a very high sequence similarity, with basically no AA variations within the transport pathway of the transmembrane region. Although we find district differences between the cytosolic CBS domains in ClC-Ka and ClC-Kb, that are present in the hybrid proteins (Figure 6A, B), proteins seem to retain partial

functionality. Therefore, further work is needed to elucidate the possible functional changes of these differences between ClC-Ka, ClC-Kb and their hybrid proteins.

In this study, we characterize a novel variant haplotype of the *CLCNKA*/*CLCNKB* genomic region defined by a ~3 kb *CLCNKA* 3' UTR sequence transposition. This haplotype is significantly associated with structural aberrations in the *CLCNKA*/*CLCNKB* locus and likely represents a predisposing factor for their occurrence. Given an estimated allele frequency of 45-50 % in the general population, the frequency of the variant haplotype in our cohort is significantly enriched ($p= 9.16x10^{-9}$, binominal test). This transposition thus constitutes another example of a common structural polymorphism that predisposes to additional genomic reconstruction relevant for human disease as discussed by Poubsky et al. (Porubsky et al. 2022).

Conclusions

In conclusion, we show that the genomic region encompassing *CLCNKA* and *CLCNKB* can give rise to complex structural variants due to high sequence similarity, and emphasize that *CLCNKB* deletions are more diverse than routine diagnostics are able to discriminate. Further larger studies are needed to determine whether the precise genomic architecture of the deletion allele has a relevant impact on clinical phenotype and management.

Declarations

Ethics approval and consent to participate

This study was approved by the ethics committee of the Medical Faculty of the University of Cologne (ID 15-215), the Medical Faculty of Marburg (ID 65/94), the Medical Faculty of Münster (ID 2012-373-f-S), and an NHS Research Ethics Committee. The research conforms with the principles of the Declaration of Helsinki.

Consent for publication

All patients gave written informed consent for their participation in this study.

Availability of data and materials

The datasets used and/or analyzed during the current study are available from the corresponding author upon reasonable request.

Competing interests

The authors declare that they have no competing interests.

Funding

This work was supported by the Deutsche Forschungsgemeinschaft (DFG, German Research Foundation) - Clinical research unit [KFO 329, AL901/2-1 and AL901/3-1] to JA and Clinical research unit [KFO 329, BE6072/2-1 and BE6072/3-1] to BB.

This work was supported by the DFG Research Infrastructure as part of the Next Generation Sequencing Competence Network [project 423957469]. NGS analyses were carried out at the production site WGGC Cologne and the Genomics Technology Platform of MDC and BIH in Berlin.

Acknowledgement

We thank Samplix for helping us with their expertise on the custom *CLCNKB* probe design and targeted sequence capture protocol. Samplix, Bregnerødvej 96, 3460 Birkerød, Denmark

Flow cytometry experiments were performed in the FACS & Imaging Core Facility at the Max Planck Institute for Biology of Ageing.

Gökhan Yigit kindly shared linked-read data from healthy individuals for comparison.

Several authors of this publication are members of the European Reference Network for Rare Kidney Diseases (ERKNet).

Publication bibliography

Accardi, Alessio; Picollo, Alessandra (2010): CLC channels and transporters: proteins with borderline personalities. In *Biochimica et biophysica acta* 1798 (8), pp. 1457–1464. DOI: 10.1016/j.bbamem.2010.02.022.

BARTTER, F. C.; PRONOVE, P.; GILL, J. R., JR; MACCARDLE, R. C. (1962): Hyperplasia of the juxtaglomerular complex with hyperaldosteronism and hypokalemic alkalosis. A new syndrome. In *The American journal of medicine* 33, pp. 811–828. DOI: 10.1016/0002-9343(62)90214-0.

Birkenhäger, R.; Otto, E.; Schürmann, M. J.; Vollmer, M.; Ruf, E. M.; Maier-Lutz, I. et al. (2001): Mutation of BSND causes Bartter syndrome with sensorineural deafness and kidney failure. In *Nature genetics* 29 (3), pp. 310–314. DOI: 10.1038/ng752.

Brochard, Karine; Boyer, Olivia; Blanchard, Anne; Loirat, Chantal; Niaudet, Patrick; Macher, Marie-Alice et al. (2009): Phenotype-genotype correlation in antenatal and neonatal variants of Bartter syndrome. In *Nephrology, dialysis, transplantation : official publication of the European Dialysis and Transplant Association - European Renal Association* 24 (5), pp. 1455–1464. DOI: 10.1093/ndt/gfn689.

Ebert, Peter; Audano, Peter A.; Zhu, Qihui; Rodriguez-Martin, Bernardo; Porubsky, David; Bonder, Marc Jan et al. (2021): Haplotype-resolved diverse human genomes and integrated analysis of structural variation. In *Science (New York, N.Y.)* 372 (6537). DOI: 10.1126/science.abf7117.

Engels, A., Gordjani, N., Nolte, S., Seyberth, H. W. (1991): Angeborene passagere hyperprostaglandinurische Tubulopathie bei zwei fruhgeborenen Geschwistern. In *Mschr. Kinderheilk* (139), 185 only.

Giri, Dinesh; Bockenhauer, Detlef; Deshpande, Charu; Achermann, John C.; Taylor, Norman F.; Rumsby, Gill et al. (2020): Co-Existence of Congenital Adrenal Hyperplasia and Bartter Syndrome due to Maternal Uniparental Isodisomy of HSD3B2 and CLCNKB Mutations. In *Hormone research in paediatrics* 93 (2), pp. 137–142. DOI: 10.1159/000507577.

Gitelman, H. J.; Graham, J. B.; Welt, L. G. (1966): A new familial disorder characterized by hypokalemia and hypomagnesemia. In *Transactions of the Association of American Physicians* 79, pp. 221–235.

Han, Yue; Cheng, Hai; Shao, Shihong; Lang, Yanhua; Zhao, Xiangzhong; Lin, Yi et al. (2020): Thirteen novel CLCNKB variants and genotype/phenotype association study in 42 Chinese patients with Bartter syndrome type 3. In *Endocrine* 68 (1), pp. 192–202. DOI: 10.1007/s12020-019-02156-9.

Han, Yue; Lin, Yi; Sun, Qing; Wang, Shujuan; Gao, Yanxia; Shao, Leping (2017): Mutation spectrum of Chinese patients with Bartter syndrome. In *Oncotarget* 8 (60), pp. 101614–101622. DOI: 10.18632/oncotarget.21355.

Jeck, N.; Konrad, M.; Peters, M.; Weber, S.; Bonzel, K. E.; Seyberth, H. W. (2000): Mutations in the chloride channel gene, CLCNKB, leading to a mixed Bartter-Gitelman phenotype. In *Pediatric research* 48 (6), pp. 754–758. DOI: 10.1203/00006450-200012000-00009.

Jumper, John; Evans, Richard; Pritzel, Alexander; Green, Tim; Figurnov, Michael; Ronneberger, Olaf et al. (2021): Highly accurate protein structure prediction with AlphaFold. In *Nature* 596 (7873), pp. 583–589. DOI: 10.1038/s41586-021-03819-2.

Kleta, Robert; Bockenhauer, Detlef (2018): Salt-Losing Tubulopathies in Children: What's New, What's Controversial? In *Journal of the American Society of Nephrology : JASN* 29 (3), pp. 727–739. DOI: 10.1681/ASN.2017060600.

Konrad, Martin; Vollmer, Martin; Lemmink, Henny H.; VAN DEN Heuvel, Lambertus P W J; Jeck, Nikola; Vargas-Poussou, Rosa et al. (2000): Mutations in the chloride channel gene CLCNKB as a cause of classic Bartter syndrome. In *Journal of the American Society of Nephrology : JASN* 11 (8), pp. 1449–1459. DOI: 10.1681/ASN.V1181449.

Laghmani, Kamel; Beck, Bodo B.; Yang, Sung-Sen; Seaayfan, Elie; Wenzel, Andrea; Reusch, Björn et al. (2016): Polyhydramnios, Transient Antenatal Bartter's Syndrome, and MAGED2 Mutations. In *The New England journal of medicine* 374 (19), pp. 1853–1863. DOI: 10.1056/NEJMoa1507629.

Li, Heng (2018): Minimap2: pairwise alignment for nucleotide sequences. In *Bioinformatics (Oxford, England)* 34 (18), pp. 3094–3100. DOI: 10.1093/bioinformatics/bty191.

Li, Heng; Handsaker, Bob; Wysoker, Alec; Fennell, Tim; Ruan, Jue; Homer, Nils et al. (2009): The Sequence Alignment/Map format and SAMtools. In *Bioinformatics (Oxford, England)* 25 (16), pp. 2078–2079. DOI: 10.1093/bioinformatics/btp352.

Lifton, R. P.; Dluhy, R. G.; Powers, M.; Rich, G. M.; Cook, S.; Ulick, S.; Lalouel, J. M. (1992): A chimaeric 11 beta-hydroxylase/aldosterone synthase gene causes glucocorticoid-remediable aldosteronism and human hypertension. In *Nature* 355 (6357), pp. 262–265. DOI: 10.1038/355262a0.

Madsen, Esben B.; Höijer, Ida; Kvist, Thomas; Ameur, Adam; Mikkelsen, Marie J. (2020): Xdrop: Targeted sequencing of long DNA molecules from low input samples using droplet sorting. In *Human mutation* 41 (9), pp. 1671–1679. DOI: 10.1002/humu.24063.

Matsunoshita, Natsuki; Nozu, Kandai; Shono, Akemi; Nozu, Yoshimi; Fu, Xue Jun; Morisada, Naoya et al. (2016): Differential diagnosis of Bartter syndrome, Gitelman syndrome, and pseudo-Bartter/Gitelman syndrome based on clinical characteristics. In *Genetics in medicine : official journal of the American College of Medical Genetics* 18 (2), pp. 180–188. DOI: 10.1038/gim.2015.56.

Najafi, Maryam; Kordi-Tamandani, Dor Mohammad; Behjati, Farkhondeh; Sadeghi-Bojd, Simin; Bakey, Zeineb; Karimiani, Ehsan Ghayoor et al. (2019): Mimicry and well known genetic friends: molecular diagnosis in an Iranian cohort of suspected Bartter syndrome and proposition of an algorithm for clinical differential diagnosis. In *Orphanet journal of rare diseases* 14 (1), p. 41. DOI: 10.1186/s13023-018-0981-5.

Nozu, K.; Inagaki, T.; Fu, X. J.; Nozu, Y.; Kaito, H.; Kanda, K. et al. (2008): Molecular analysis of digenic inheritance in Bartter syndrome with sensorineural deafness. In *Journal of medical genetics* 45 (3), pp. 182–186. DOI: 10.1136/jmg.2007.052944.

Nozu, Kandai; Fu, Xue Jun; Nakanishi, Koichi; Yoshikawa, Norishige; Kaito, Hiroshi; Kanda, Kyoko et al. (2007): Molecular analysis of patients with type III Bartter syndrome: picking up large heterozygous deletions with semiquantitative PCR. In *Pediatric research* 62 (3), pp. 364–369. DOI: 10.1203/PDR.0b013e318123fb90.

Nurk, Sergey; Koren, Sergey; Rhie, Arang; Rautiainen, Mikko; Bzikadze, Andrey V.; Mikheenko, Alla et al. (2022): The complete sequence of a human genome. In *Science (New York, N.Y.)* 376 (6588), pp. 44–53. DOI: 10.1126/science.abj6987.

Park, Eunyong; Campbell, Ernest B.; MacKinnon, Roderick (2017): Structure of a CLC chloride ion channel by cryo-electron microscopy. In *Nature* 541 (7638), pp. 500–505. DOI: 10.1038/nature20812.

Porubsky, David; Höps, Wolfram; Ashraf, Hufsah; Hsieh, PingHsun; Rodriguez-Martin, Bernardo; Yilmaz, Feyza et al. (2022): Recurrent inversion polymorphisms in humans associate with genetic instability and genomic disorders. In *Cell* 185 (11), 1986-2005.e26. DOI: 10.1016/j.cell.2022.04.017.

Robinson, James T.; Thorvaldsdóttir, Helga; Winckler, Wendy; Guttman, Mitchell; Lander, Eric S.; Getz, Gad; Mesirov, Jill P. (2011): Integrative genomics viewer. In *Nature biotechnology* 29 (1), pp. 24–26. DOI: 10.1038/nbt.1754.

Rodríguez-Soriano, J. (1998): Bartter and related syndromes: the puzzle is almost solved. In *Pediatric nephrology (Berlin, Germany)* 12 (4), pp. 315–327. DOI: 10.1007/s004670050461.

Sahbani, Dalila; Strumbo, Bice; Tedeschi, Silvana; Conte, Elena; Camerino, Giulia Maria; Benetti, Elisa et al. (2020): Functional Study of Novel Bartter's Syndrome Mutations in ClC-Kb and Rescue by the Accessory Subunit Barttin Toward Personalized Medicine. In *Frontiers in pharmacology* 11, p. 327. DOI: 10.3389/fphar.2020.00327.

Schlingmann, Karl P.; Konrad, Martin; Jeck, Nikola; Waldegger, Petra; Reinalter, Stephan C.; Holder, Martin et al. (2004): Salt wasting and deafness resulting from mutations in two chloride channels. In *The New England journal of medicine* 350 (13), pp. 1314–1319. DOI: 10.1056/NEJMoa032843.

Schrecker, Marina; Korobenko, Julia; Hite, Richard K. (2020): Cryo-EM structure of the lysosomal chloride-proton exchanger CLC-7 in complex with OSTM1. In *eLife* 9. DOI: 10.7554/eLife.59555.

Schurman, S. J.; Perlman, S. A.; Sutphen, R.; Campos, A.; Garin, E. H.; Cruz, D. N.; Shoemaker, L. R. (2001): Genotype/phenotype observations in African Americans with Bartter syndrome. In *The Journal of pediatrics* 139 (1), pp. 105–110. DOI: 10.1067/mpd.2001.115020.

Seyberth, H. W.; Rascher, W.; Schweer, H.; Kühl, P. G.; Mehls, O.; Schärer, K. (1985): Congenital hypokalemia with hypercalciuria in preterm infants: a hyperprostaglandinuric tubular syndrome different from Bartter syndrome. In *The Journal of pediatrics* 107 (5), pp. 694–701. DOI: 10.1016/s0022-3476(85)80395-4.

Seys, Elsa; Andrini, Olga; Keck, Mathilde; Mansour-Hendili, Lamisse; Courand, Pierre-Yves; Simian, Christophe et al. (2017): Clinical and Genetic Spectrum of Bartter Syndrome Type 3.

In *Journal of the American Society of Nephrology : JASN* 28 (8), pp. 2540–2552. DOI: 10.1681/ASN.2016101057.

Simon, D. B.; Bindra, R. S.; Mansfield, T. A.; Nelson-Williams, C.; Mendonca, E.; Stone, R. et al. (1997): Mutations in the chloride channel gene, CLCNKB, cause Bartter's syndrome type III. In *Nature genetics* 17 (2), pp. 171–178. DOI: 10.1038/ng1097-171.

Simon, D. B.; Karet, F. E.; Hamdan, J. M.; DiPietro, A.; Sanjad, S. A.; Lifton, R. P. (1996a): Bartter's syndrome, hypokalaemic alkalosis with hypercalciuria, is caused by mutations in the Na-K-2Cl cotransporter NKCC2. In *Nature genetics* 13 (2), pp. 183–188. DOI: 10.1038/ng0696-183.

Simon, D. B.; Karet, F. E.; Rodriguez-Soriano, J.; Hamdan, J. H.; DiPietro, A.; Trachtman, H. et al. (1996b): Genetic heterogeneity of Bartter's syndrome revealed by mutations in the K+ channel, ROMK. In *Nature genetics* 14 (2), pp. 152–156. DOI: 10.1038/ng1096-152.

Simon, D. B.; Nelson-Williams, C.; Bia, M. J.; Ellison, D.; Karet, F. E.; Molina, A. M. et al. (1996c): Gitelman's variant of Bartter's syndrome, inherited hypokalaemic alkalosis, is caused by mutations in the thiazide-sensitive Na-Cl cotransporter. In *Nature genetics* 12 (1), pp. 24–30. DOI: 10.1038/ng0196-24.

Zhao, Qianying; Xiang, Qinqin; Tan, Yu; Xiao, Xiao; Xie, Hanbing; Wang, He et al. (2022): A novel CLCNKB variant in a Chinese family with classic Bartter syndrome and prenatal genetic diagnosis. In *Molecular genetics & genomic medicine*, e2027. DOI: 10.1002/mgg3.2027.

Zhong, Bozitao; Su, Xiaoming; Wen, Minhua; Zuo, Sichen; Hong, Liang; Lin, James (2021): ParaFold: Paralleling AlphaFold for Large-Scale Predictions. Available online at https://arxiv.org/pdf/2111.06340.

General Discussion

Today over 6000 rare disease entities have been identified (orpha.net: assessed on 11.04.2023). About 600 genes are associated with Mendelian forms of kidney and genitourinary disorders, most of which with prevalence's of less than one affected patient per 2000 individuals (Rasouly et al. 2019). Following the development, improvement of accessibility and costs, the application of next-generation sequencing has increased the accuracy of diagnosing rare renal diseases. Genetic counselling and genetic testing have become more accessible to a larger number of families and definite genetic determination carries considerable prognostic significance in certain ailments (Groopman et al. 2019; Jayasinghe et al. 2021). In the future, the number of people that have gone through genetic testing will keep increasing, and even larger datasets will enhance the statistical power of forthcoming research. Gained genetic knowledge frequently allows quick transformation into molecular mechanistic insights of rare diseases. This strategy has already led to new targeted treatment options like the use of eculizumab in aHUS.

Expanding the Spectrum of FAT1 Nephropathies by Novel Mutations That Affect Hippo Signaling

The first study focused on a small group of four patients from three families with novel mutations in the *FAT1* gene resulting in *FAT1*-associated nephropathy. Mutations were found using a custom-made gene panel including 122 monogenetic nephropathy and proteinuria disease genes and WES. Together with state of the art NGS technology, this gene panel provides a broad and fast method to reliably identify all of the standard SNVs and small SVs affecting the coding region of the genes for most of the genes widely associated to diseases with renal involvement. FAT1 mutations cause glomerulotubular nephropathy and CKD characterized by SRNS, FSGS, proteinuria, podocyte food process malformation, ocular features (ptosis, coloboma, microphthalmia), feed syndactyly, tubular dilation, tubular fibrosis, and tubular basement membrane dysplasia that may progress to ESRD (Gee et al. 2016; Sethi et al. 2022; Lahrouchi et al. 2019). In this study, we confirmed the functional relevance of these mutations by showing, that loss of FAT1 affects Hippo signaling pathway effector proteins YAP/TAZ that results in subsequently upregulation of target genes. If Hippo signaling is active, the core kinase MST and LATS are phosphorylated, resulting in

phosphorylation (inactivation) of the effector proteins YAP and TAZ that remain in the cytoplasm. YAP and TAZ translocate into the nucleus and induce expression of various target genes such as *AREG*, *CCND2*, *MUC1*, *IL6* or *GADD45B* if Hippo signaling is inactive. As FAT1 was known as an upstream regulator of Hippo signaling, we analysed this pathway in isolated primary urine-derived renal epithelial cells from patients with mutations in FAT1. We could indeed show, that one of the Hippo core kinases; MST1/2, is inactivated as shown by decreased phosphorylation. In line with this, YAP is activated and translocated into the nucleus in these cells, where it acts as a transcriptional co-activator to upregulate the transcription of target genes. The findings of our study correlate with the previous knowledge about FAT1 and hippo signaling. Additionally, our study substantially expanded the genotype/phenotype data of patients with FAT1 nephropathy. As shown before, missense mutations in FAT1 result in an SRNS-like phenotype

The findings of this study are significant in the context of rare kidney disease, as they expand the spectrum of global FAT1 nephropathies significantly. FAT1 nephropathy is an extremely rare disease with only 14 affected individuals from 8 families worldwide. The mutations identified in this study can provide a better understanding of the pathogenesis of this disease, as well as new targets for developing therapeutic strategies and suggests Hippo signaling as a diagnostic measure in FAT1-associated disease.

Unraveling Structural Rearrangements of the CFH Gene Cluster in Atypical Hemolytic Uremic Syndrome Patients Using Molecular Combing and Long-Fragment Targeted Sequencing

While the first study widened the spectrum of slit diaphragm FAT1 mutations resulting in FAT1 nephropathy identified by short-read NGS technology, the second study focused on patients with atypical haemolytic uremic syndrome caused by structural variants in the complement regulating gene CFH, analysed with molecular combing and LRS. aHUS is characterized by haemolytic anaemia, thrombocytopenia, and renal impairment (Noris and Remuzzi 2005). CKD is a common manifestation of aHUS patients. Approximately half of the patients develop ESRD (Constantinescu et al. 2004; Taylor et al. 2004). Here, we analysed 15 patients with aHUS and 6 patients with C3GN that were negative for NGS-based gene-panel sequencing in the most common rTMA genes *DGKE, CFH, CFI,* and *CD46,* including one family with two siblings carrying the same *CFH* mutation but developed different courses of disease. CFH is one of the major regulating proteins of the alternative pathway of the complement system and CFH deficiency plays a crucial role in the development of aHUS (Rodríguez de Córdoba et al. 2004). None of the other genes associated with aHUS are prone to structural aberrations. This phenomenon is highly likely due to the high sequence homology between the proteins in the *CFH/CFHR* gene cluster that formed during evolutional segmental duplication events. Between 3-8 % of aHUS cases result from SVs and fusion genes of the CFH protein family (Venables et al. 2006; Piras et al. 2022). Multiple different SVs have been reported until now. In this study, we benchmarked the method of molecular combing to reliably identify structural aberrations in the *CFH/CFHR* gene cluster, identified novel *CFH/CFHR1* hybrid genes, *CFHR4/CFHR1* deletions and, found the common *CFHR3/CFHR1* deletion risk factor in high frequencies among our aHUS cohort. We suggest, that the rearrangements are likely responsible for the development of the disease in our patients. The large *CFH*/*CFHR* gene cluster, approximately 360 kb in length, was investigated using the molecular combing technique. In this fibre FISH technology, long genomic DNA strands are attached onto a glass surface, and the individual genes of the cluster are fluorescently labelled and analysed with a fluorescence microscope. Molecular combing has an accurate resolution range from ~ 1kb to up to ~ 1 Mb. Therefore, molecular combing is appropriate for rather large genomic structural rearrangements and

deletions/insertions of whole genes than for small variations within single genes. The most important advantage of the method of molecular combing is the ability to identify somatic genomic mosaic variants which remain out of reach for classical diagnostic methods such as MLPA or Southern blot. Additionally, molecular combing allows the visual localization of structural variants within the gene cluster whereas MLPA and southern blot are limited to identify the presence of an SV without exact localization information.

For analyses on a single base pair resolution level, we used Samplix's targeted long-fragment enrichment and LRS. The possibility to focus on specific regions in the genome has improved the costly method of LRS by generating only data that contains the genetic information you are interested in when whole exome or whole genome long-read sequencing is not necessary. This can either be achieved using kits and methods for target DNA enrichment or utilizing the real-time sequencing capabilities of the long-read sequencer to select the specific DNA fragments in real-time during sequencing by recognizing the right sequence and discarding the other fragments during sequencing (Payne et al. 2021).

This study is significant because it provides an effective tool for identifying structural rearrangements in the *CFH* gene cluster in aHUS patients. Identification of the underlying genetic cause in the context of aHUS is of utmost importance as therapeutic decisions will depend on this information. In the case of CFH-associated aHUS with renal failure, isolated kidney transplantation will result in quick graft failure since the defective fluid phase glycoprotein CFH is produced in the liver. This is illustrated by the two quick graft failures of the patient in our study with the previously unrecognized *CFH*/*CFHR1* hybrid gene who could ultimately receive successful kidney transplantation under Eculizumab medication. The recombinant, fully humanized monoclonal complement component 5 (C5) antibody Eculizumab is a powerful suppressor of the alternative complement pathway, inhibiting the cleavage of C5 into C5a and C5b, thus preventing the formation of the membrane attack complex. Researchers found that eculizumab medication resulted in disease remission in the majority of the participants and noticed a significant enhancement of renal performance (Zuber et al. 2012).

The results from our study contribute to a more comprehensive understanding of the genetic basis of *CFH/CFHR* gene cluster-associated aHUS. Furthermore, the study expands the current literature on genetic aHUS diagnostics and suggests that molecular combing and long-

fragment targeted sequencing can be useful tools for identifying structural rearrangements in the *CFH* gene cluster.

Long-read sequencing identifies a common transposition haplotype predisposing for *CLCNKB* deletions

The third study focused on patients with *CLCNKB* deletion-associated Bartter syndrome identified by targeted enrichment and LRS. BS, in general, is characterized by defects in sodium, potassium and chloride homeostasis, resulting in hypokalemic, hypochloremic metabolic alkalosis, and high renin and aldosterone levels (BARTTER et al. 1962; Goodman et al. 1969). FSGS has also been reported in BS (BARTTER et al. 1962; Su et al. 2000). In BS patients, FSGS may occur as a secondary lesion due to adaptation to long-term salt loss and chronic activation of the renin-angiotensin-system (Hanevold et al. 2006; Akil et al. 2010). In general, kidney biopsies are not commonly required for diagnosis of BS and clinical diagnosis is mainly based on biochemical parameters and renal functional tests. Diagnosis is usually confirmed by molecular genetic analyses (e.g. sequencing, MLPA) to define the precise subtype (Konrad et al. 2021). Here, we analysed 28 patients with *CLCNKB* deletion-associated BS 3 and identified eight different *CLCNKB* deletion alleles. 88 % of the deletion alleles originated from a previously unknown structural haplotype that is also present in ~ 50 % of alleles in the general population. This alternative haplotype constitutes a transposition of a 2.2-3 kb sequence fragment from the *CLCNKB* 3' UTR to the homologous genomic region in the *CLCNKA* 3' UTR. With 45 out of the 51 alleles, of which a haplotype determination could be made, the transposition haplotype is significantly enriched in our patients compared to controls ($p=9.16x10^{-9}$, binominal test). Taken together this transposition haplotype might predispose to the SV events resulting in *CLCNKB* deletions, and may explain the relatively high allelic frequency of *CLCNKB* deletion observed in BS 3 patients. Using a combination of specifically designed long-read PCR, targeted long DNA fragment enrichment followed by LRS and whole genome LRS we were able to unravel in great detail the genomic complexity and heterogeneity of the *CLCNKA*/*CLNKB* gene cluster on a single base-pair resolution. Using LRS, we were the first to identify a very common structural sequence transposition polymorphism and to establish a link between sequence transposition and *CLCNKB* deletions. LRS, in contrast to NGS, allows one to connect genomic alterations that are clearly distant from each other and broadens the view on genomic loci.

Additionally, there is strong evidence to assume that the transposition haplotype and the *CLCNKB* deletion would have been identifiable using the molecular combing technology as

well. The 2-3 kb transposition haplotype, the ~ 23 kb *CLCNKB* deletion and the two *CLCNKA*/*CLCNKB* hybrid genes fit into the resolution capabilities of molecular combing and could have been nicely visualized if *CLCNKA* and *CLCNKB* including their respective 3' UTRs would have been hybridized using different coloured probes.

Next to the deletion alleles we could also identify two BS 3 patients with different *CLCNKA*/*CLCNKB* hybrid genes, that may result in ClC-Ka/ClC-Kb hybrid proteins. Loss of both genes *CLCNKA* and *CLCNKB* would manifest in BS with hearing loss (Schlingmann et al. 2004), which was not observed in our patients. We assumed, that the hybrid genes result in putative hybrid proteins with residual function. To further assess this assumption, we analysed the putative hybrid proteins using the Alphafold software. Prediction of the AA changes in the hybrid proteins suggest at least partial functional chloride channels.

In conclusion, this study reveals the complexity of the *CLCNKA*/*CLCNKB* gene cluster and provides a suitable protocol for *CLCNKB* deletion allele identification which might enable genotype-phenotype correlations in the future. To test this, more deletion allele screening of the existing, or upcoming cohorts needs to be done.

Conclusion

Rare kidney disease has become a prominent topic in the field of disease development and prevention, especially in children who require repeated kidney transplantation in case of ESRD. RKD affects 3.5-5.9 % of the population worldwide. More and more genes and pathways get identified contributing to the complexity of RKD, but also providing insight into fundamental processes associated with CKD. Due to the high heterogeneity and growing identification of causal genes, the number of people affected by the respective diseases is very small. Pathways are largely not yet fully understood and cohort numbers are statistically too small to make significant comparisons (e.g. genotype/phenotype correlations). The wide phenotypical spectrum makes clear clinical diagnostics difficult and exact disease subtypes can often only be precisely determined by genotyping. However, a large number of cases still remain unexplained and further research is needed to clarify these cases at some point. It is therefore even more important to analyse these few patients in the best possible way, as each individual patient makes up a large proportion of the overall cohort, and this patient can provide the missing link to a better understanding of the molecular bases of kidney disease. New molecular genetic methods are constantly being developed or improved enhancing the diagnostic yield of the disease and closing the gap of genetic information that is still challenging to analyse. Studies like mine are essential in advancing research and patient care. To identify the underlying genetic cause of the disease and to transfer new insights back into disease pathophysiology. This way has proven suitable to develop simpler and more accurate molecular diagnostics. This work provides new insights into current state of the art of genomics in three important areas of rare kidney disease. Our findings have already led to improved patient care in those patients we could provide with a definite diagnosis and likely provide new stimuli for further research on the genetic basis of kidney disease.

Publication bibliography

Accardi, Alessio; Picollo, Alessandra (2010): CLC channels and transporters: proteins with borderline personalities. In *Biochimica et biophysica acta* 1798 (8), pp. 1457–1464. DOI: 10.1016/j.bbamem.2010.02.022.

Ahmed, Abdulrzag F.; Bock, Charles E. de; Lincz, Lisa F.; Pundavela, Jay; Zouikr, Ihssane; Sontag, Estelle et al. (2015): FAT1 cadherin acts upstream of Hippo signalling through TAZ to regulate neuronal differentiation. In *Cellular and molecular life sciences : CMLS* 72 (23), pp. 4653–4669. DOI: 10.1007/s00018-015-1955-6.

Akil, Ipek; Ozen, Serkan; Kandiloglu, Ali Riza; Ersoy, Betul (2010): A patient with Bartter syndrome accompanying severe growth hormone deficiency and focal segmental glomerulosclerosis. In *Clinical and experimental nephrology* 14 (3), pp. 278–282. DOI: 10.1007/s10157-009-0262-7.

Akilesh, S. (2014): Normal Kidney Function and Structure. In Linda M. McManus, Richard N. Mitchell (Eds.): Pathobiology of Human Disease. San Diego: Academic Press, pp. 2716–2733. Available online at https://www.sciencedirect.com/science/article/pii/B9780123864567054022.

Ansari, Daniel; Ohlsson, Henrik; Althini, Carl; Bauden, Monika; Zhou, Qimin; Hu, Dingyuan; Andersson, Roland (2019): The Hippo Signaling Pathway in Pancreatic Cancer. In *Anticancer research* 39 (7), pp. 3317–3321. DOI: 10.21873/anticanres.13474.

Ares, Gustavo R.; Caceres, Paulo S.; Ortiz, Pablo A. (2011): Molecular regulation of NKCC2 in the thick ascending limb. In *American journal of physiology. Renal physiology* 301 (6), F1143-59. DOI: 10.1152/ajprenal.00396.2011.

Armento, Angela; Ueffing, Marius; Clark, Simon J. (2021): The complement system in age-related macular degeneration. In *Cellular and molecular life sciences : CMLS* 78 (10), pp. 4487–4505. DOI: 10.1007/s00018-021-03796-9.

Babar, Faizan; Cohen, Scott D. (2018): Thrombotic Microangiopathies with Rheumatologic Involvement. In *Rheumatic diseases clinics of North America* 44 (4), pp. 635–649. DOI: 10.1016/j.rdc.2018.06.010.

Bailey, J. A.; Yavor, A. M.; Massa, H. F.; Trask, B. J.; Eichler, E. E. (2001): Segmental duplications: organization and impact within the current human genome project assembly. In *Genome research* 11 (6), pp. 1005–1017. DOI: 10.1101/gr.gr-1871r.

Barker, D. F.; Hostikka, S. L.; Zhou, J.; Chow, L. T.; Oliphant, A. R.; Gerken, S. C. et al. (1990): Identification of mutations in the COL4A5 collagen gene in Alport syndrome. In *Science (New York, N.Y.)* 248 (4960), pp. 1224–1227. DOI: 10.1126/science.2349482.

BARTTER, F. C.; PRONOVE, P.; GILL, J. R., JR; MACCARDLE, R. C. (1962): Hyperplasia of the juxtaglomerular complex with hyperaldosteronism and hypokalemic alkalosis. A new syndrome. In *The American journal of medicine* 33, pp. 811–828. DOI: 10.1016/0002-9343(62)90214-0.

Beck, Bodo B.; van Spronsen, FrancJan; Diepstra, Arjan; Berger, Rolf M. F.; Kömhoff, Martin (2017): Renal thrombotic microangiopathy in patients with cblC defect: review of an under-

recognized entity. In *Pediatric nephrology (Berlin, Germany)* 32 (5), pp. 733–741. DOI: 10.1007/s00467-016-3399-0.

Bensimon, A.; Simon, A.; Chiffaudel, A.; Croquette, V.; Heslot, F.; Bensimon, D. (1994): Alignment and sensitive detection of DNA by a moving interface. In *Science (New York, N.Y.)* 265 (5181), pp. 2096–2098. DOI: 10.1126/science.7522347.

Bettinelli, Alberto; Borsa, Nicolò; Bellantuono, Rosa; Syrèn, Marie-Louise; Calabrese, Raffaele; Edefonti, Alberto et al. (2007): Patients with biallelic mutations in the chloride channel gene CLCNKB: long-term management and outcome. In *American journal of kidney diseases : the official journal of the National Kidney Foundation* 49 (1), pp. 91–98. DOI: 10.1053/j.ajkd.2006.10.001.

Birkenhäger, R.; Otto, E.; Schürmann, M. J.; Vollmer, M.; Ruf, E. M.; Maier-Lutz, I. et al. (2001): Mutation of BSND causes Bartter syndrome with sensorineural deafness and kidney failure. In *Nature genetics* 29 (3), pp. 310–314. DOI: 10.1038/ng752.

Boopathy, Gandhi T. K.; Hong, Wanjin (2019): Role of Hippo Pathway-YAP/TAZ Signaling in Angiogenesis. In *Frontiers in cell and developmental biology* 7, p. 49. DOI: 10.3389/fcell.2019.00049.

Boute, N.; Gribouval, O.; Roselli, S.; Benessy, F.; Lee, H.; Fuchshuber, A. et al. (2000): NPHS2, encoding the glomerular protein podocin, is mutated in autosomal recessive steroid-resistant nephrotic syndrome. In *Nature genetics* 24 (4), pp. 349–354. DOI: 10.1038/74166.

Brochard, Karine; Boyer, Olivia; Blanchard, Anne; Loirat, Chantal; Niaudet, Patrick; Macher, Marie-Alice et al. (2009a): Phenotype-genotype correlation in antenatal and neonatal variants of Bartter syndrome. In *Nephrology, dialysis, transplantation : official publication of the European Dialysis and Transplant Association - European Renal Association* 24 (5), pp. 1455–1464. DOI: 10.1093/ndt/gfn689.

Brochard, Karine; Boyer, Olivia; Blanchard, Anne; Loirat, Chantal; Niaudet, Patrick; Macher, Marie-Alice et al. (2009b): Phenotype-genotype correlation in antenatal and neonatal variants of Bartter syndrome. In *Nephrology, dialysis, transplantation : official publication of the European Dialysis and Transplant Association - European Renal Association* 24 (5), pp. 1455–1464. DOI: 10.1093/ndt/gfn689.

Brown, A. L., JR (1966): The structure of the nephron. In *The Medical clinics of North America* 50 (4), pp. 927–935. DOI: 10.1016/s0025-7125(16)33140-6.

Bu, Fengxiao; Maga, Tara; Meyer, Nicole C.; Wang, Kai; Thomas, Christie P.; Nester, Carla M.; Smith, Richard J. H. (2014): Comprehensive genetic analysis of complement and coagulation genes in atypical hemolytic uremic syndrome. In *Journal of the American Society of Nephrology : JASN* 25 (1), pp. 55–64. DOI: 10.1681/ASN.2013050453.

Büscher, Anja K.; Beck, Bodo B.; Melk, Anette; Hoefele, Julia; Kranz, Birgitta; Bamborschke, Daniel et al. (2016): Rapid Response to Cyclosporin A and Favorable Renal Outcome in Nongenetic Versus Genetic Steroid-Resistant Nephrotic Syndrome. In *Clinical journal of the American Society of Nephrology : CJASN* 11 (2), pp. 245–253. DOI: 10.2215/CJN.07370715.

Butt, Linus; Unnersjö-Jess, David; Höhne, Martin; Edwards, Aurelie; Binz-Lotter, Julia; Reilly, Dervla et al. (2020): A molecular mechanism explaining albuminuria in kidney disease. In *Nature metabolism* 2 (5), pp. 461–474. DOI: 10.1038/s42255-020-0204-y.

Cai, Jing; Song, Xuewen; Wang, Wei; Watnick, Terry; Pei, York; Qian, Feng; Pan, Duojia (2018): A RhoA-YAP-c-Myc signaling axis promotes the development of polycystic kidney disease. In *Genes & development* 32 (11-12), pp. 781–793. DOI: 10.1101/gad.315127.118.

Caprioli, Jessica; Noris, Marina; Brioschi, Simona; Pianetti, Gaia; Castelletti, Federica; Bettinaglio, Paola et al. (2006): Genetics of HUS: the impact of MCP, CFH, and IF mutations on clinical presentation, response to treatment, and outcome. In *Blood* 108 (4), pp. 1267–1279. DOI: 10.1182/blood-2005-10-007252.

Carter, Simon A.; Mistry, Shilan; Fitzpatrick, Jessica; Banh, Tonny; Hebert, Diane; Langlois, Valerie et al. (2020): Prediction of Short- and Long-Term Outcomes in Childhood Nephrotic Syndrome. In *Kidney international reports* 5 (4), pp. 426–434. DOI: 10.1016/j.ekir.2019.12.015.

Cavero, Teresa; Auñón, Pilar; Caravaca-Fontán, Fernando; Trujillo, Hernando; Arjona, Emi; Morales, Enrique et al. (2022): Thrombotic microangiopathy in patients with malignant hypertension. In *Nephrology, dialysis, transplantation : official publication of the European Dialysis and Transplant Association - European Renal Association*. DOI: 10.1093/ndt/gfac248.

Chaisson, Mark J. P.; Sanders, Ashley D.; Zhao, Xuefang; Malhotra, Ankit; Porubsky, David; Rausch, Tobias et al. (2019): Multi-platform discovery of haplotype-resolved structural variation in human genomes. In *Nature communications* 10 (1), p. 1784. DOI: 10.1038/s41467-018-08148-z.

Chan, Eunice H. Y.; Nousiainen, Marjaana; Chalamalasetty, Ravindra B.; Schäfer, Anja; Nigg, Erich A.; Silljé, Herman H. W. (2005): The Ste20-like kinase Mst2 activates the human large tumor suppressor kinase Lats1. In *Oncogene* 24 (12), pp. 2076–2086. DOI: 10.1038/sj.onc.1208445.

Chaplin, H., JR (2005): Review: the burgeoning history of the complement system 1888-2005. In *Immunohematology* 21 (3), pp. 85–93.

Chen, Lihe; Higgins, Paul J.; Zhang, Wenzheng (2017): Development and Diseases of the Collecting Duct System. In *Results and problems in cell differentiation* 60, pp. 165–203. DOI: 10.1007/978-3-319-51436-9_7.

Cheong, Hae Il (2020): Genetic tests in children with steroid-resistant nephrotic syndrome. In *Kidney research and clinical practice* 39 (1), pp. 7–16. DOI: 10.23876/j.krcp.20.001.

Cheung, Priscilla; Xiol, Jordi; Dill, Michael T.; Yuan, Wei-Chien; Panero, Riccardo; Roper, Jatin et al. (2020): Regenerative Reprogramming of the Intestinal Stem Cell State via Hippo Signaling Suppresses Metastatic Colorectal Cancer. In *Cell stem cell* 27 (4), 590-604.e9. DOI: 10.1016/j.stem.2020.07.003.

Clarke, James; Wu, Hai-Chen; Jayasinghe, Lakmal; Patel, Alpesh; Reid, Stuart; Bayley, Hagan (2009): Continuous base identification for single-molecule nanopore DNA sequencing. In *Nature nanotechnology* 4 (4), pp. 265–270. DOI: 10.1038/nnano.2009.12.

Cody, Ellen; Claes, Donna; Taylor, Veronica; Erkan, Elif (2022): Pregnancy associated TMA in 13-year-old patient successfully treated with Eculizumab: case report. In *BMC nephrology* 23 (1), p. 147. DOI: 10.1186/s12882-022-02766-y.

Connaughton, Dervla M.; Hildebrandt, Friedhelm (2020): Personalized medicine in chronic kidney disease by detection of monogenic mutations. In *Nephrology, dialysis, transplantation : official publication of the European Dialysis and Transplant Association - European Renal Association* 35 (3), pp. 390–397. DOI: 10.1093/ndt/gfz028.

Conrad, D. H.; Carlo, J. R.; Ruddy, S. (1978): Interaction of beta1H globulin with cell-bound C3b: quantitative analysis of binding and influence of alternative pathway components on binding. In *The Journal of experimental medicine* 147 (6), pp. 1792–1805. DOI: 10.1084/jem.147.6.1792.

Costero, Olga; Picazo, Mari Luz; Zamora, Pilar; Romero, Sara; Martinez-Ara, Jorge; Selgas, Rafael (2010): Inhibition of tyrosine kinases by sunitinib associated with focal segmental glomerulosclerosis lesion in addition to thrombotic microangiopathy. In *Nephrology, dialysis, transplantation : official publication of the European Dialysis and Transplant Association - European Renal Association* 25 (3), pp. 1001–1003. DOI: 10.1093/ndt/gfp666.

Couser, William G. (2017): Primary Membranous Nephropathy. In *Clinical journal of the American Society of Nephrology : CJASN* 12 (6), pp. 983–997. DOI: 10.2215/CJN.11761116.

Delvaeye, Mieke; Noris, Marina; Vriese, Astrid de; Esmon, Charles T.; Esmon, Naomi L.; Ferrell, Gary et al. (2009): Thrombomodulin mutations in atypical hemolytic-uremic syndrome. In *The New England journal of medicine* 361 (4), pp. 345–357. DOI: 10.1056/NEJMoa0810739.

Devarajan, Prasad; Chertow, Glenn M.; Susztak, Katalin; Levin, Adeera; Agarwal, Rajiv; Stenvinkel, Peter et al. (2022): Emerging Role of Clinical Genetics in CKD. In *Kidney medicine* 4 (4), p. 100435. DOI: 10.1016/j.xkme.2022.100435.

Devuyst, Olivier; Knoers, Nine V A M; Remuzzi, Giuseppe; Schaefer, Franz (2014): Rare inherited kidney diseases: challenges, opportunities, and perspectives. In *Lancet (London, England)* 383 (9931), pp. 1844–1859. DOI: 10.1016/S0140-6736(14)60659-0.

Donoviel, D. B.; Freed, D. D.; Vogel, H.; Potter, D. G.; Hawkins, E.; Barrish, J. P. et al. (2001): Proteinuria and perinatal lethality in mice lacking NEPH1, a novel protein with homology to NEPHRIN. In *Molecular and cellular biology* 21 (14), pp. 4829–4836. DOI: 10.1128/MCB.21.14.4829-4836.2001.

Down, Michelle; Power, Maryanne; Smith, Shirley I.; Ralston, Kylie; Spanevello, Mark; Burns, Gordon F.; Boyd, Andrew W. (2005): Cloning and expression of the large zebrafish protocadherin gene, Fat. In *Gene expression patterns : GEP* 5 (4), pp. 483–490. DOI: 10.1016/j.modgep.2004.12.005.

Du, Xingrong; Wen, Jing; Wang, Yanyan; Karmaus, Peer W. F.; Khatamian, Alireza; Tan, Haiyan et al. (2018): Hippo/Mst signalling couples metabolic state and immune function of CD8α(+) dendritic cells. In *Nature* 558 (7708), pp. 141–145. DOI: 10.1038/s41586-018-0177-0.

Ebert, Peter; Audano, Peter A.; Zhu, Qihui; Rodriguez-Martin, Bernardo; Porubsky, David; Bonder, Marc Jan et al. (2021): Haplotype-resolved diverse human genomes and integrated analysis of structural variation. In *Science (New York, N.Y.)* 372 (6537). DOI: 10.1126/science.abf7117.

Eid, John; Fehr, Adrian; Gray, Jeremy; Luong, Khai; Lyle, John; Otto, Geoff et al. (2009): Real-time DNA sequencing from single polymerase molecules. In *Science (New York, N.Y.)* 323 (5910), pp. 133–138. DOI: 10.1126/science.1162986.

Engels, A., Gordjani, N., Nolte, S., Seyberth, H. W. (1991): Angeborene passagere hyperprostaglandinurische Tubulopathie bei zwei fruhgeborenen Geschwistern. In *Mschr. Kinderheilk* (139), 185 only.

Evang, Karl (1925): The sex-linked mutants vesiculated and semi-lethal in drosophila melanogaster. In *Z.Ver-erbungslehre* 39 (1), pp. 165–183. DOI: 10.1007/BF01961520.

Eyler, Stephen J.; Meyer, Nicole C.; Zhang, Yuzhou; Xiao, Xue; Nester, Carla M.; Smith, Richard J. H. (2013): A novel hybrid CFHR1/CFH gene causes atypical hemolytic uremic syndrome. In *Pediatric nephrology (Berlin, Germany)* 28 (11), pp. 2221–2225. DOI: 10.1007/s00467-013-2560-2.

Field, Michael J.; Harris, David C.; Pollock, Carol A. (Eds.) (2010): The Renal System (Second Edition). Second Edition: Churchill Livingstone.

Filler, Guido; Young, Elizabeth; Geier, Pavel; Carpenter, Blair; Drukker, Alfred; Feber, Janusz (2003): Is there really an increase in non-minimal change nephrotic syndrome in children? In *American journal of kidney diseases : the official journal of the National Kidney Foundation* 42 (6), pp. 1107–1113. DOI: 10.1053/j.ajkd.2003.08.010.

Francis, Nigel J.; McNicholas, Bairbre; Awan, Atif; Waldron, Mary; Reddan, Donal; Sadlier, Denise et al. (2012): A novel hybrid CFH/CFHR3 gene generated by a microhomology-mediated deletion in familial atypical hemolytic uremic syndrome. In *Blood* 119 (2), pp. 591–601. DOI: 10.1182/blood-2011-03-339903.

Frémeaux-Bacchi, Veronique; Miller, Elizabeth C.; Liszewski, M. Kathryn; Strain, Lisa; Blouin, Jacques; Brown, Alison L. et al. (2008): Mutations in complement C3 predispose to development of atypical hemolytic uremic syndrome. In *Blood* 112 (13), pp. 4948–4952. DOI: 10.1182/blood-2008-01-133702.

Fujimura, Junya; Nozu, Kandai; Yamamura, Tomohiko; Minamikawa, Shogo; Nakanishi, Keita; Horinouchi, Tomoko et al. (2019): Clinical and Genetic Characteristics in Patients With Gitelman Syndrome. In *Kidney international reports* 4 (1), pp. 119–125. DOI: 10.1016/j.ekir.2018.09.015.

Fukasawa, Hirotaka; Bornheimer, Scott; Kudlicka, Krystyna; Farquhar, Marilyn G. (2009): Slit diaphragms contain tight junction proteins. In *Journal of the American Society of Nephrology : JASN* 20 (7), pp. 1491–1503. DOI: 10.1681/ASN.2008101117.

Gadjeva, Mihaela (2014): The complement system. Overview. In *Methods in molecular biology (Clifton, N.J.)* 1100, pp. 1–9. DOI: 10.1007/978-1-62703-724-2_1.

García Castaño, Alejandro; Pérez de Nanclares, Gustavo; Madariaga, Leire; Aguirre, Mireia; Madrid, Álvaro; Chocrón, Sara et al. (2017): Poor phenotype-genotype association in a large series of patients with Type III Bartter syndrome. In *PloS one* 12 (3), e0173581. DOI: 10.1371/journal.pone.0173581.

Gast, Christine; Pengelly, Reuben J.; Lyon, Matthew; Bunyan, David J.; Seaby, Eleanor G.; Graham, Nikki et al. (2016): Collagen (COL4A) mutations are the most frequent mutations underlying adult focal segmental glomerulosclerosis. In *Nephrology, dialysis, transplantation : official publication of the European Dialysis and Transplant Association - European Renal Association* 31 (6), pp. 961–970. DOI: 10.1093/ndt/gfv325.

Gee, Heon Yung; Sadowski, Carolin E.; Aggarwal, Pardeep K.; Porath, Jonathan D.; Yakulov, Toma A.; Schueler, Markus et al. (2016): FAT1 mutations cause a glomerulotubular nephropathy. In *Nature communications* 7, p. 10822. DOI: 10.1038/ncomms10822.

Giri, Dinesh; Bockenhauer, Detlef; Deshpande, Charu; Achermann, John C.; Taylor, Norman F.; Rumsby, Gill et al. (2020): Co-Existence of Congenital Adrenal Hyperplasia and Bartter Syndrome due to Maternal Uniparental Isodisomy of HSD3B2 and CLCNKB Mutations. In *Hormone research in paediatrics* 93 (2), pp. 137–142. DOI: 10.1159/000507577.

Gitelman, H. J.; Graham, J. B.; Welt, L. G. (1966): A new familial disorder characterized by hypokalemia and hypomagnesemia. In *Transactions of the Association of American Physicians* 79, pp. 221–235.

Go, Alan S.; Tan, Thida C.; Chertow, Glenn M.; Ordonez, Juan D.; Fan, Dongjie; Law, David et al. (2021): Primary Nephrotic Syndrome and Risks of ESKD, Cardiovascular Events, and Death: The Kaiser Permanente Nephrotic Syndrome Study. In *Journal of the American Society of Nephrology : JASN* 32 (9), pp. 2303–2314. DOI: 10.1681/ASN.2020111583.

Goicoechea de Jorge, Elena; Harris, Claire L.; Esparza-Gordillo, Jorge; Carreras, Luis; Arranz, Elena Aller; Garrido, Cynthia Abarrategui et al. (2007): Gain-of-function mutations in complement factor B are associated with atypical hemolytic uremic syndrome. In *Proceedings of the National Academy of Sciences of the United States of America* 104 (1), pp. 240–245. DOI: 10.1073/pnas.0603420103.

Goodman, A. D.; Vagnucci, A. H.; Hartroft, P. M. (1969): Pathogenesis of Bartter's syndrome. In *The New England journal of medicine* 281 (26), pp. 1435–1439. DOI: 10.1056/NEJM196912252812601.

Gordon, D. L.; Kaufman, R. M.; Blackmore, T. K.; Kwong, J.; Lublin, D. M. (1995): Identification of complement regulatory domains in human factor H. In *Journal of immunology (Baltimore, Md. : 1950)* 155 (1), pp. 348–356.

Groopman, Emily E.; Marasa, Maddalena; Cameron-Christie, Sophia; Petrovski, Slavé; Aggarwal, Vimla S.; Milo-Rasouly, Hila et al. (2019): Diagnostic Utility of Exome Sequencing for Kidney Disease. In *The New England journal of medicine* 380 (2), pp. 142–151. DOI: 10.1056/NEJMoa1806891.

Han, Yue; Cheng, Hai; Shao, Shihong; Lang, Yanhua; Zhao, Xiangzhong; Lin, Yi et al. (2020): Thirteen novel CLCNKB variants and genotype/phenotype association study in 42 Chinese

patients with Bartter syndrome type 3. In *Endocrine* 68 (1), pp. 192–202. DOI: 10.1007/s12020-019-02156-9.

Han, Yue; Lin, Yi; Sun, Qing; Wang, Shujuan; Gao, Yanxia; Shao, Leping (2017): Mutation spectrum of Chinese patients with Bartter syndrome. In *Oncotarget* 8 (60), pp. 101614–101622. DOI: 10.18632/oncotarget.21355.

Hanevold, Coral; Mian, Ayesa; Dalton, Rory (2006): C1q nephropathy in association with Gitelman syndrome: a case report. In *Pediatric nephrology (Berlin, Germany)* 21 (12), pp. 1904–1908. DOI: 10.1007/s00467-006-0261-9.

Harambat, J.; Hogan, J.; Macher, M-Al; Couchoud, C. (2013): ESRD in children and adolescents. In *Nephrologie & therapeutique* 9 Suppl 1, S167-79. DOI: 10.1016/S1769-7255(13)70044-0.

Harris, P. C.; Ward, C. J.; Peral, B.; Hughes, J. (1995 Oct): Polycystic kidney disease. 1: Identification and analysis of the primary defect. United States.

Hashimoto, T.; Karasawa, T.; Saito, A.; Miyauchi, N.; Han, G. D.; Hayasaka, K. et al. (2007): Ephrin-B1 localizes at the slit diaphragm of the glomerular podocyte. In *Kidney international* 72 (8), pp. 954–964. DOI: 10.1038/sj.ki.5002454.

Hayashi, Shuichiro; Umeda, Tamami (2008): 35 years of Japanese policy on rare diseases. In *Lancet (London, England)* 372 (9642), pp. 889–890. DOI: 10.1016/S0140-6736(08)61393-8.

Heinen, Stefan; Sanchez-Corral, Pilar; Jackson, Michael S.; Strain, Lisa; Goodship, Judith A.; Kemp, Elizabeth J. et al. (2006): De novo gene conversion in the RCA gene cluster (1q32) causes mutations in complement factor H associated with atypical hemolytic uremic syndrome. In *Human mutation* 27 (3), pp. 292–293. DOI: 10.1002/humu.9408.

Hierholzer, K.; Wiederholt, M. (1976): Some aspects of distal tubular solute and water transport. In *Kidney international* 9 (2), pp. 198–213. DOI: 10.1038/ki.1976.21.

Hinkes, Bernward G.; Mucha, Bettina; Vlangos, Christopher N.; Gbadegesin, Rasheed; Liu, Jinhong; Hasselbacher, Katrin et al. (2007): Nephrotic syndrome in the first year of life: two thirds of cases are caused by mutations in 4 genes (NPHS1, NPHS2, WT1, and LAMB2). In *Pediatrics* 119 (4), e907-19. DOI: 10.1542/peds.2006-2164.

Hu, Xiaoling; Zhai, Yuanfang; Kong, Pengzhou; Cui, Heyang; Yan, Ting; Yang, Jian et al. (2017): FAT1 prevents epithelial mesenchymal transition (EMT) via MAPK/ERK signaling pathway in esophageal squamous cell cancer. In *Cancer letters* 397, pp. 83–93. DOI: 10.1016/j.canlet.2017.03.033.

Hunt, Ryan; Yalamanoglu, Ayla; Tumlin, James; Schiller, Tal; Baek, Jin Hyen; Wu, Andrew et al. (2017): A mechanistic investigation of thrombotic microangiopathy associated with IV abuse of Opana ER. In *Blood* 129 (7), pp. 896–905. DOI: 10.1182/blood-2016-08-736579.

Hureaux, Marguerite; Ashton, Emma; Dahan, Karin; Houillier, Pascal; Blanchard, Anne; Cormier, Catherine et al. (2019): High-throughput sequencing contributes to the diagnosis of tubulopathies and familial hypercalcemia hypocalciuria in adults. In *Kidney international* 96 (6), pp. 1408–1416. DOI: 10.1016/j.kint.2019.08.027.

Ichikawa, I.; Fogo, A. (1996): Focal segmental glomerulosclerosis. In *Pediatric nephrology (Berlin, Germany)* 10 (3), pp. 374–391. DOI: 10.1007/BF00866790.

Inoue, T.; Yaoita, E.; Kurihara, H.; Shimizu, F.; Sakai, T.; Kobayashi, T. et al. (2001): FAT is a component of glomerular slit diaphragms. In *Kidney international* 59 (3), pp. 1003–1012. DOI: 10.1046/j.1523-1755.2001.0590031003.x.

J. Gordon Betts; Kelly A. Young; James A. Wise; Eddie Johnson; Brandon Poe; Dean H. Kruse et al. (2013 // 2013-): Anatomy and Physiology // Anatomy & physiology. Houston, Texas: OpenStax; OpenStax College, Rice University.

Jayasinghe, Kushani; Stark, Zornitza; Kerr, Peter G.; Gaff, Clara; Martyn, Melissa; Whitlam, John et al. (2021): Clinical impact of genomic testing in patients with suspected monogenic kidney disease. In *Genetics in medicine : official journal of the American College of Medical Genetics* 23 (1), pp. 183–191. DOI: 10.1038/s41436-020-00963-4.

Jeck, N.; Konrad, M.; Peters, M.; Weber, S.; Bonzel, K. E.; Seyberth, H. W. (2000): Mutations in the chloride channel gene, CLCNKB, leading to a mixed Bartter-Gitelman phenotype. In *Pediatric research* 48 (6), pp. 754–758. DOI: 10.1203/00006450-200012000-00009.

Jokiranta, T. Sakari (2017): HUS and atypical HUS. In *Blood* 129 (21), pp. 2847–2856. DOI: 10.1182/blood-2016-11-709865.

Józsi, Mihály; Oppermann, Martin; Lambris, John D.; Zipfel, Peter F. (2007): The C-terminus of complement factor H is essential for host cell protection. In *Molecular immunology* 44 (10), pp. 2697–2706. DOI: 10.1016/j.molimm.2006.12.001.

Jumper, John; Evans, Richard; Pritzel, Alexander; Green, Tim; Figurnov, Michael; Ronneberger, Olaf et al. (2021): Highly accurate protein structure prediction with AlphaFold. In *Nature* 596 (7873), pp. 583–589. DOI: 10.1038/s41586-021-03819-2.

Kaartinen, Kati; Safa, Adrian; Kotha, Soumya; Ratti, Giorgio; Meri, Seppo (2019): Complement dysregulation in glomerulonephritis. In *Seminars in immunology* 45, p. 101331. DOI: 10.1016/j.smim.2019.101331.

Kallioniemi, A.; Kallioniemi, O. P.; Sudar, D.; Rutovitz, D.; Gray, J. W.; Waldman, F.; Pinkel, D. (1992): Comparative genomic hybridization for molecular cytogenetic analysis of solid tumors. In *Science (New York, N.Y.)* 258 (5083), pp. 818–821. DOI: 10.1126/science.1359641.

Kavanagh, David; Goodship, Tim H.; Richards, Anna (2013): Atypical hemolytic uremic syndrome. In *Seminars in nephrology* 33 (6), pp. 508–530. DOI: 10.1016/j.semnephrol.2013.08.003.

Kavanagh, David; Kemp, Elizabeth J.; Mayland, Elizabeth; Winney, Robin J.; Duffield, Jeremy S.; Warwick, Graham et al. (2005): Mutations in complement factor I predispose to development of atypical hemolytic uremic syndrome. In *Journal of the American Society of Nephrology : JASN* 16 (7), pp. 2150–2155. DOI: 10.1681/ASN.2005010103.

Kiran, B. Vijay; Barman, H.; Iyengar, A. (2014): Clinical profile and outcome of renal tubular disorders in children: A single center experience. In *Indian journal of nephrology* 24 (6), pp. 362–366. DOI: 10.4103/0971-4065.133002.

Kleta, Robert; Bockenhauer, Detlef (2018): Salt-Losing Tubulopathies in Children: What's New, What's Controversial? In *Journal of the American Society of Nephrology : JASN* 29 (3), pp. 727–739. DOI: 10.1681/ASN.2017060600.

Kokko, J. P. (1970): Sodium chloride and water transport in the descending limb of Henle. In *The Journal of clinical investigation* 49 (10), pp. 1838–1846. DOI: 10.1172/JCI106401.

Konrad, Martin; Nijenhuis, Tom; Ariceta, Gema; Bertholet-Thomas, Aurelia; Calo, Lorenzo A.; Capasso, Giovambattista et al. (2021): Diagnosis and management of Bartter syndrome: executive summary of the consensus and recommendations from the European Rare Kidney Disease Reference Network Working Group for Tubular Disorders. In *Kidney international* 99 (2), pp. 324–335. DOI: 10.1016/j.kint.2020.10.035.

Konrad, Martin; Vollmer, Martin; Lemmink, Henny H.; VAN DEN Heuvel, Lambertus P W J; Jeck, Nikola; Vargas-Poussou, Rosa et al. (2000): Mutations in the chloride channel gene CLCNKB as a cause of classic Bartter syndrome. In *Journal of the American Society of Nephrology : JASN* 11 (8), pp. 1449–1459. DOI: 10.1681/ASN.V1181449.

Koskimies, O.; Vilska, J.; Rapola, J.; Hallman, N. (1982): Long-term outcome of primary nephrotic syndrome. In *Archives of disease in childhood* 57 (7), pp. 544–548. DOI: 10.1136/adc.57.7.544.

Kunnen, Steven J.; Malas, Tareq B.; Formica, Chiara; Leonhard, Wouter N.; 't Hoen, Peter A C; Peters, Dorien J. M. (2018): Comparative transcriptomics of shear stress treated Pkd1(-/-) cells and pre-cystic kidneys reveals pathways involved in early polycystic kidney disease. In *Biomedicine & pharmacotherapy = Biomedecine & pharmacotherapie* 108, pp. 1123–1134. DOI: 10.1016/j.biopha.2018.07.178.

Laghmani, Kamel; Beck, Bodo B.; Yang, Sung-Sen; Seaayfan, Elie; Wenzel, Andrea; Reusch, Björn et al. (2016): Polyhydramnios, Transient Antenatal Bartter's Syndrome, and MAGED2 Mutations. In *The New England journal of medicine* 374 (19), pp. 1853–1863. DOI: 10.1056/NEJMoa1507629.

Lahrouchi, Najim; George, Aman; Ratbi, Ilham; Schneider, Ronen; Elalaoui, Siham C.; Moosa, Shahida et al. (2019): Homozygous frameshift mutations in FAT1 cause a syndrome characterized by colobomatous-microphthalmia, ptosis, nephropathy and syndactyly. In *Nature communications* 10 (1), p. 1180. DOI: 10.1038/s41467-019-08547-w.

Lai, Zhi-Chun; Wei, Xiaomu; Shimizu, Takeshi; Ramos, Edward; Rohrbaugh, Margaret; Nikolaidis, Nikolas et al. (2005): Control of cell proliferation and apoptosis by mob as tumor suppressor, mats. In *Cell* 120 (5), pp. 675–685. DOI: 10.1016/j.cell.2004.12.036.

Lander, E. S.; Linton, L. M.; Birren, B.; Nusbaum, C.; Zody, M. C.; Baldwin, J. et al. (2001): Initial sequencing and analysis of the human genome. In *Nature* 409 (6822), pp. 860–921. DOI: 10.1038/35057062.

Leach, John P.; Heallen, Todd; Zhang, Min; Rahmani, Mahdis; Morikawa, Yuka; Hill, Matthew C. et al. (2017): Hippo pathway deficiency reverses systolic heart failure after infarction. In *Nature* 550 (7675), pp. 260–264. DOI: 10.1038/nature24045.

Lee, Se Eun; Han, Kyoung Hee; Jung, Yun Hye; Lee, Hyun Kyung; Kang, Hee Gyung; Moon, Kyung Chul et al. (2011): Renal transplantation in a patient with Bartter syndrome and glomerulosclerosis. In *Korean journal of pediatrics* 54 (1), pp. 36–39. DOI: 10.3345/kjp.2011.54.1.36.

Lemaire, Mathieu; Frémeaux-Bacchi, Véronique; Schaefer, Franz; Choi, Murim; Tang, Wai Ho; Le Quintrec, Moglie et al. (2013): Recessive mutations in DGKE cause atypical hemolytic-uremic syndrome. In *Nature genetics* 45 (5), pp. 531–536. DOI: 10.1038/ng.2590.

Levy-Sakin, Michal; Ebenstein, Yuval (2013): Beyond sequencing: optical mapping of DNA in the age of nanotechnology and nanoscopy. In *Current opinion in biotechnology* 24 (4), pp. 690–698. DOI: 10.1016/j.copbio.2013.01.009.

Li, Heng (2018): Minimap2: pairwise alignment for nucleotide sequences. In *Bioinformatics (Oxford, England)* 34 (18), pp. 3094–3100. DOI: 10.1093/bioinformatics/bty191.

Li, Heng; Handsaker, Bob; Wysoker, Alec; Fennell, Tim; Ruan, Jue; Homer, Nils et al. (2009): The Sequence Alignment/Map format and SAMtools. In *Bioinformatics (Oxford, England)* 25 (16), pp. 2078–2079. DOI: 10.1093/bioinformatics/btp352.

Lifton, R. P.; Dluhy, R. G.; Powers, M.; Rich, G. M.; Cook, S.; Ulick, S.; Lalouel, J. M. (1992): A chimaeric 11 beta-hydroxylase/aldosterone synthase gene causes glucocorticoid-remediable aldosteronism and human hypertension. In *Nature* 355 (6357), pp. 262–265. DOI: 10.1038/355262a0.

Ling, Morris; Murali, Mandakolathur (2019): Analysis of the Complement System in the Clinical Immunology Laboratory. In *Clinics in laboratory medicine* 39 (4), pp. 579–590. DOI: 10.1016/j.cll.2019.07.006.

Lloyd, S. E.; Pearce, S. H.; Fisher, S. E.; Steinmeyer, K.; Schwappach, B.; Scheinman, S. J. et al. (1996): A common molecular basis for three inherited kidney stone diseases. In *Nature* 379 (6564), pp. 445–449. DOI: 10.1038/379445a0.

Loirat, Chantal; Frémeaux-Bacchi, Véronique (2011): Atypical hemolytic uremic syndrome. In *Orphanet journal of rare diseases* 6, p. 60. DOI: 10.1186/1750-1172-6-60.

Madsen, Esben B.; Höijer, Ida; Kvist, Thomas; Ameur, Adam; Mikkelsen, Marie J. (2020): Xdrop: Targeted sequencing of long DNA molecules from low input samples using droplet sorting. In *Human mutation* 41 (9), pp. 1671–1679. DOI: 10.1002/humu.24063.

Maga, Tara K.; Meyer, Nicole C.; Belsha, Craig; Nishimura, Carla J.; Zhang, Yuzhou; Smith, Richard J. H. (2011): A novel deletion in the RCA gene cluster causes atypical hemolytic uremic syndrome. In *Nephrology, dialysis, transplantation : official publication of the European Dialysis and Transplant Association - European Renal Association* 26 (2), pp. 739–741. DOI: 10.1093/ndt/gfq658.

Manenti, Lucio; Gnappi, Elisa; Vaglio, Augusto; Allegri, Landino; Noris, Marina; Bresin, Elena et al. (2013): Atypical haemolytic uraemic syndrome with underlying glomerulopathies. A case series and a review of the literature. In *Nephrology, dialysis, transplantation : official publication of the European Dialysis and Transplant Association - European Renal Association* 28 (9), pp. 2246–2259. DOI: 10.1093/ndt/gft220.

Mardis, Elaine R. (2013): Next-generation sequencing platforms. In *Annual review of analytical chemistry (Palo Alto, Calif.)* 6, pp. 287–303. DOI: 10.1146/annurev-anchem-062012-092628.

Margulies, Marcel; Egholm, Michael; Altman, William E.; Attiya, Said; Bader, Joel S.; Bemben, Lisa A. et al. (2005): Genome sequencing in microfabricated high-density picolitre reactors. In *Nature* 437 (7057), pp. 376–380. DOI: 10.1038/nature03959.

Mariot, Virginie; Roche, Stephane; Hourdé, Christophe; Portilho, Debora; Sacconi, Sabrina; Puppo, Francesca et al. (2015): Correlation between low FAT1 expression and early affected muscle in facioscapulohumeral muscular dystrophy. In *Annals of neurology* 78 (3), pp. 387–400. DOI: 10.1002/ana.24446.

Masliantsev, Konstantin; Karayan-Tapon, Lucie; Guichet, Pierre-Olivier (2021): Hippo Signaling Pathway in Gliomas. In *Cells* 10 (1). DOI: 10.3390/cells10010184.

Matsunoshita, Natsuki; Nozu, Kandai; Shono, Akemi; Nozu, Yoshimi; Fu, Xue Jun; Morisada, Naoya et al. (2016): Differential diagnosis of Bartter syndrome, Gitelman syndrome, and pseudo-Bartter/Gitelman syndrome based on clinical characteristics. In *Genetics in medicine : official journal of the American College of Medical Genetics* 18 (2), pp. 180–188. DOI: 10.1038/gim.2015.56.

Merle, Nicolas S.; Church, Sarah Elizabeth; Fremeaux-Bacchi, Veronique; Roumenina, Lubka T. (2015a): Complement System Part I - Molecular Mechanisms of Activation and Regulation. In *Frontiers in immunology* 6, p. 262. DOI: 10.3389/fimmu.2015.00262.

Merle, Nicolas S.; Noe, Remi; Halbwachs-Mecarelli, Lise; Fremeaux-Bacchi, Veronique; Roumenina, Lubka T. (2015b): Complement System Part II: Role in Immunity. In *Frontiers in immunology* 6, p. 257. DOI: 10.3389/fimmu.2015.00257.

Mevorach, D.; Mascarenhas, J. O.; Gershov, D.; Elkon, K. B. (1998): Complement-dependent clearance of apoptotic cells by human macrophages. In *The Journal of experimental medicine* 188 (12), pp. 2313–2320. DOI: 10.1084/jem.188.12.2313.

Mia, Masum M.; Singh, Manvendra K. (2022): New Insights into Hippo/YAP Signaling in Fibrotic Diseases. In *Cells* 11 (13). DOI: 10.3390/cells11132065.

Moon, Sohyeon; Hwang, Semi; Kim, Byeongseok; Lee, Siyoung; Kim, Hyoukjung; Lee, Giwan et al. (2022): Hippo Signaling in the Endometrium. In *International journal of molecular sciences* 23 (7). DOI: 10.3390/ijms23073852.

Moore, Iain; Strain, Lisa; Pappworth, Isabel; Kavanagh, David; Barlow, Paul N.; Herbert, Andrew P. et al. (2010): Association of factor H autoantibodies with deletions of CFHR1, CFHR3, CFHR4, and with mutations in CFH, CFI, CD46, and C3 in patients with atypical hemolytic uremic syndrome. In *Blood* 115 (2), pp. 379–387. DOI: 10.1182/blood-2009-05-221549.

Morinière, Vincent; Dahan, Karin; Hilbert, Pascale; Lison, Marieline; Lebbah, Said; Topa, Alexandra et al. (2014): Improving mutation screening in familial hematuric nephropathies through next generation sequencing. In *Journal of the American Society of Nephrology : JASN* 25 (12), pp. 2740–2751. DOI: 10.1681/ASN.2013080912.

Morris, Luc G. T.; Kaufman, Andrew M.; Gong, Yongxing; Ramaswami, Deepa; Walsh, Logan A.; Turcan, Şevin et al. (2013): Recurrent somatic mutation of FAT1 in multiple human cancers leads to aberrant Wnt activation. In *Nature genetics* 45 (3), pp. 253–261. DOI: 10.1038/ng.2538.

Müller, Roman-Ulrich; Schermer, Bernhard (2020): Hippo signaling-a central player in cystic kidney disease? In *Pediatric nephrology (Berlin, Germany)* 35 (7), pp. 1143–1152. DOI: 10.1007/s00467-019-04299-3.

Müller-Eberhard, H. J. (1986): The membrane attack complex of complement. In *Annual review of immunology* 4, pp. 503–528. DOI: 10.1146/annurev.iy.04.040186.002443.

Murray, Ian; Paolini, Michael A. (2022): Histology, Kidney and Glomerulus. In : StatPearls. Treasure Island (FL).

Najafi, Maryam; Kordi-Tamandani, Dor Mohammad; Behjati, Farkhondeh; Sadeghi-Bojd, Simin; Bakey, Zeineb; Karimiani, Ehsan Ghayoor et al. (2019): Mimicry and well known genetic friends: molecular diagnosis in an Iranian cohort of suspected Bartter syndrome and proposition of an algorithm for clinical differential diagnosis. In *Orphanet journal of rare diseases* 14 (1), p. 41. DOI: 10.1186/s13023-018-0981-5.

Najafi, Maryam; Riedhammer, Korbinian M.; Rad, Aboulfazl; Torbati, Paria Najarzadeh; Berutti, Riccardo; Schüle, Isabel et al. (2022): High detection rate for disease-causing variants in a cohort of 30 Iranian pediatric steroid resistant nephrotic syndrome cases. In *Frontiers in pediatrics* 10, p. 974840. DOI: 10.3389/fped.2022.974840.

Nester, Carla M.; Barbour, Thomas; Cordoba, Santiago Rodriquez de; Dragon-Durey, Marie Agnes; Fremeaux-Bacchi, Veronique; Goodship, Tim H. J. et al. (2015): Atypical aHUS: State of the art. In *Molecular immunology* 67 (1), pp. 31–42. DOI: 10.1016/j.molimm.2015.03.246.

Nguengang Wakap, Stéphanie; Lambert, Deborah M.; Olry, Annie; Rodwell, Charlotte; Gueydan, Charlotte; Lanneau, Valérie et al. (2020): Estimating cumulative point prevalence of rare diseases: analysis of the Orphanet database. In *European journal of human genetics : EJHG* 28 (2), pp. 165–173. DOI: 10.1038/s41431-019-0508-0.

Noris, Marina; Remuzzi, Giuseppe (2005): Hemolytic uremic syndrome. In *Journal of the American Society of Nephrology : JASN* 16 (4), pp. 1035–1050. DOI: 10.1681/ASN.2004100861.

Noris, Marina; Remuzzi, Giuseppe (2009): Atypical hemolytic-uremic syndrome. In *The New England journal of medicine* 361 (17), pp. 1676–1687. DOI: 10.1056/NEJMra0902814.

Nozu, K.; Inagaki, T.; Fu, X. J.; Nozu, Y.; Kaito, H.; Kanda, K. et al. (2008): Molecular analysis of digenic inheritance in Bartter syndrome with sensorineural deafness. In *Journal of medical genetics* 45 (3), pp. 182–186. DOI: 10.1136/jmg.2007.052944.

Nozu, Kandai; Fu, Xue Jun; Nakanishi, Koichi; Yoshikawa, Norishige; Kaito, Hiroshi; Kanda, Kyoko et al. (2007): Molecular analysis of patients with type III Bartter syndrome: picking up large heterozygous deletions with semiquantitative PCR. In *Pediatric research* 62 (3), pp. 364–369. DOI: 10.1203/PDR.0b013e318123fb90.

Nurk, Sergey; Koren, Sergey; Rhie, Arang; Rautiainen, Mikko; Bzikadze, Andrey V.; Mikheenko, Alla et al. (2022): The complete sequence of a human genome. In *Science (New York, N.Y.)* 376 (6588), pp. 44–53. DOI: 10.1126/science.abj6987.

Olsen, A. S.; Georgescu, A.; Johnson, S.; Carrano, A. V. (1996): Assembly of a 1-Mb restriction-mapped cosmid contig spanning the candidate region for Finnish congenital nephrosis (NPHS1) in 19q13.1. In *Genomics* 34 (2), pp. 223–225. DOI: 10.1006/geno.1996.0270.

Palazzo, Viviana; Raglianti, Valentina; Landini, Samuela; Cirillo, Luigi; Errichiello, Carmela; Buti, Elisa et al. (2022): Clinical and Genetic Characterization of Patients with Bartter and Gitelman Syndrome. In *International journal of molecular sciences* 23 (10). DOI: 10.3390/ijms23105641.

Pangburn, M. K.; Schreiber, R. D.; Müller-Eberhard, H. J. (1977): Human complement C3b inactivator: isolation, characterization, and demonstration of an absolute requirement for the serum protein beta1H for cleavage of C3b and C4b in solution. In *The Journal of experimental medicine* 146 (1), pp. 257–270. DOI: 10.1084/jem.146.1.257.

Park, Byoung Hee; Lee, Yong Hee (2011): Phosphorylation of SAV1 by mammalian ste20-like kinase promotes cell death. In *BMB reports* 44 (9), pp. 584–589. DOI: 10.5483/bmbrep.2011.44.9.584.

Park, Eunyong; Campbell, Ernest B.; MacKinnon, Roderick (2017): Structure of a CLC chloride ion channel by cryo-electron microscopy. In *Nature* 541 (7638), pp. 500–505. DOI: 10.1038/nature20812.

Patel, Samik; Tang, Jiaqi; Overstreet, Jessica M.; Anorga, Sandybell; Lian, Fei; Arnouk, Alex et al. (2019): Rac-GTPase promotes fibrotic TGF-β1 signaling and chronic kidney disease via EGFR, p53, and Hippo/YAP/TAZ pathways. In *FASEB journal : official publication of the Federation of American Societies for Experimental Biology* 33 (9), pp. 9797–9810. DOI: 10.1096/fj.201802489RR.

Payne, Alexander; Holmes, Nadine; Clarke, Thomas; Munro, Rory; Debebe, Bisrat J.; Loose, Matthew (2021): Readfish enables targeted nanopore sequencing of gigabase-sized genomes. In *Nature biotechnology* 39 (4), pp. 442–450. DOI: 10.1038/s41587-020-00746-x.

Pinkel, Daniel; Albertson, Donna G. (2005): Array comparative genomic hybridization and its applications in cancer. In *Nature genetics* 37 Suppl, S11-7. DOI: 10.1038/ng1569.

Piras, Rossella; Valoti, Elisabetta; Alberti, Marta; Bresin, Elena; Mele, Caterina; Breno, Matteo et al. (2022): CFH and CFHR structural variants in atypical Hemolytic Uremic Syndrome: Prevalence, genomic characterization and impact on outcome. In *Frontiers in immunology* 13, p. 1011580. DOI: 10.3389/fimmu.2022.1011580.

Porubsky, David; Höps, Wolfram; Ashraf, Hufsah; Hsieh, PingHsun; Rodriguez-Martin, Bernardo; Yilmaz, Feyza et al. (2022): Recurrent inversion polymorphisms in humans associate with genetic instability and genomic disorders. In *Cell* 185 (11), 1986-2005.e26. DOI: 10.1016/j.cell.2022.04.017.

Praskova, Maria; Xia, Fan; Avruch, Joseph (2008): MOBKL1A/MOBKL1B phosphorylation by MST1 and MST2 inhibits cell proliferation. In *Current biology : CB* 18 (5), pp. 311–321. DOI: 10.1016/j.cub.2008.02.006.

Radi, Zaher A. (2019): Kidney Pathophysiology, Toxicology, and Drug-Induced Injury in Drug Development. In *International journal of toxicology* 38 (3), pp. 215–227. DOI: 10.1177/1091581819831701.

Rasouly, Hila Milo; Groopman, Emily E.; Heyman-Kantor, Reuben; Fasel, David A.; Mitrotti, Adele; Westland, Rik et al. (2019): The Burden of Candidate Pathogenic Variants for Kidney and Genitourinary Disorders Emerging From Exome Sequencing. In *Annals of internal medicine* 170 (1), pp. 11–21. DOI: 10.7326/M18-1241.

Reiser, Jochen; Kriz, Wilhelm; Kretzler, Matthias; Mundel, Peter (2000): The glomerular slit diaphragm is a modified adherens junction. In *Journal of the American Society of Nephrology : JASN* 11 (1), pp. 1–8. DOI: 10.1681/ASN.V1111.

Rhoads, Anthony; Au, Kin Fai (2015): PacBio Sequencing and Its Applications. In *Genomics, proteomics & bioinformatics* 13 (5), pp. 278–289. DOI: 10.1016/j.gpb.2015.08.002.

Rice, William L.; van Hoek, Alfred N.; Păunescu, Teodor G.; Huynh, Chuong; Goetze, Bernhard; Singh, Bipin et al. (2013): High resolution helium ion scanning microscopy of the rat kidney. In *PloS one* 8 (3), e57051. DOI: 10.1371/journal.pone.0057051.

Richards, Anna; Kemp, Elizabeth J.; Liszewski, M. Kathryn; Goodship, Judith A.; Lampe, Anne K.; Decorte, Ronny et al. (2003): Mutations in human complement regulator, membrane cofactor protein (CD46), predispose to development of familial hemolytic uremic syndrome. In *Proceedings of the National Academy of Sciences of the United States of America* 100 (22), pp. 12966–12971. DOI: 10.1073/pnas.2135497100.

Riley, L. W.; Remis, R. S.; Helgerson, S. D.; McGee, H. B.; Wells, J. G.; Davis, B. R. et al. (1983): Hemorrhagic colitis associated with a rare Escherichia coli serotype. In *The New England journal of medicine* 308 (12), pp. 681–685. DOI: 10.1056/NEJM198303243081203.

Robinson, James T.; Thorvaldsdóttir, Helga; Winckler, Wendy; Guttman, Mitchell; Lander, Eric S.; Getz, Gad; Mesirov, Jill P. (2011): Integrative genomics viewer. In *Nature biotechnology* 29 (1), pp. 24–26. DOI: 10.1038/nbt.1754.

Rodríguez de Córdoba, Santiago; Esparza-Gordillo, Jorge; Goicoechea de Jorge, Elena; Lopez-Trascasa, Margarita; Sánchez-Corral, Pilar (2004): The human complement factor H: functional roles, genetic variations and disease associations. In *Molecular immunology* 41 (4), pp. 355–367. DOI: 10.1016/j.molimm.2004.02.005.

Rodríguez-Soriano, J. (1998): Bartter and related syndromes: the puzzle is almost solved. In *Pediatric nephrology (Berlin, Germany)* 12 (4), pp. 315–327. DOI: 10.1007/s004670050461.

Roselli, Séverine; Gribouval, Olivier; Boute, Nicolas; Sich, Mireille; Benessy, France; Attié, Tania et al. (2002): Podocin localizes in the kidney to the slit diaphragm area. In *The American journal of pathology* 160 (1), pp. 131–139. DOI: 10.1016/S0002-9440(10)64357-X.

Rosenthal, W.; Seibold, A.; Antaramian, A.; Lonergan, M.; Arthus, M. F.; Hendy, G. N. et al. (1992): Molecular identification of the gene responsible for congenital nephrogenic diabetes insipidus. In *Nature* 359 (6392), pp. 233–235. DOI: 10.1038/359233a0.

Roy, Ankita; Al-bataineh, Mohammad M.; Pastor-Soler, Núria M. (2015): Collecting duct intercalated cell function and regulation. In *Clinical journal of the American Society of Nephrology : CJASN* 10 (2), pp. 305–324. DOI: 10.2215/CJN.08880914.

Ruotsalainen, V.; Ljungberg, P.; Wartiovaara, J.; Lenkkeri, U.; Kestilä, M.; Jalanko, H. et al. (1999): Nephrin is specifically located at the slit diaphragm of glomerular podocytes. In *Proceedings of the National Academy of Sciences of the United States of America* 96 (14), pp. 7962–7967. DOI: 10.1073/pnas.96.14.7962.

Rybarczyk, Agnieszka; Klacz, Jakub; Wronska, Agata; Matuszewski, Marcin; Kmiec, Zbigniew; Wierzbicki, Piotr M. (2017): Overexpression of the YAP1 oncogene in clear cell renal cell carcinoma is associated with poor outcome. In *Oncology reports* 38 (1), pp. 427–439. DOI: 10.3892/or.2017.5642.

Sadowski, Carolin E.; Lovric, Svjetlana; Ashraf, Shazia; Pabst, Werner L.; Gee, Heon Yung; Kohl, Stefan et al. (2015): A single-gene cause in 29.5% of cases of steroid-resistant nephrotic syndrome. In *Journal of the American Society of Nephrology : JASN* 26 (6), pp. 1279–1289. DOI: 10.1681/ASN.2014050489.

Sahbani, Dalila; Strumbo, Bice; Tedeschi, Silvana; Conte, Elena; Camerino, Giulia Maria; Benetti, Elisa et al. (2020): Functional Study of Novel Bartter's Syndrome Mutations in ClC-Kb and Rescue by the Accessory Subunit Barttin Toward Personalized Medicine. In *Frontiers in pharmacology* 11, p. 327. DOI: 10.3389/fphar.2020.00327.

Saito, Akira; Miyauchi, Naoko; Hashimoto, Taeko; Karasawa, Tamaki; Han, Gi Dong; Kayaba, Mutsumi et al. (2011): Neurexin-1, a presynaptic adhesion molecule, localizes at the slit diaphragm of the glomerular podocytes in kidneys. In *American journal of physiology. Regulatory, integrative and comparative physiology* 300 (2), R340-8. DOI: 10.1152/ajpregu.00640.2009.

Sanger, F.; Nicklen, S.; Coulson, A. R. (1977): DNA sequencing with chain-terminating inhibitors. In *Proceedings of the National Academy of Sciences of the United States of America* 74 (12), pp. 5463–5467. DOI: 10.1073/pnas.74.12.5463.

Schifferli, J. A.; Ng, Y. C.; Peters, D. K. (1986): The role of complement and its receptor in the elimination of immune complexes. In *The New England journal of medicine* 315 (8), pp. 488–495. DOI: 10.1056/NEJM198608213150805.

Schlingmann, Karl P.; Konrad, Martin; Jeck, Nikola; Waldegger, Petra; Reinalter, Stephan C.; Holder, Martin et al. (2004): Salt wasting and deafness resulting from mutations in two chloride channels. In *The New England journal of medicine* 350 (13), pp. 1314–1319. DOI: 10.1056/NEJMoa032843.

Schrecker, Marina; Korobenko, Julia; Hite, Richard K. (2020): Cryo-EM structure of the lysosomal chloride-proton exchanger CLC-7 in complex with OSTM1. In *eLife* 9. DOI: 10.7554/eLife.59555.

Schröder-Braunstein, Jutta; Kirschfink, Michael (2019): Complement deficiencies and dysregulation: Pathophysiological consequences, modern analysis, and clinical management. In *Molecular immunology* 114, pp. 299–311. DOI: 10.1016/j.molimm.2019.08.002.

Schurman, S. J.; Perlman, S. A.; Sutphen, R.; Campos, A.; Garin, E. H.; Cruz, D. N.; Shoemaker, L. R. (2001): Genotype/phenotype observations in African Americans with Bartter syndrome. In *The Journal of pediatrics* 139 (1), pp. 105–110. DOI: 10.1067/mpd.2001.115020.

Schwarz, K.; Simons, M.; Reiser, J.; Saleem, M. A.; Faul, C.; Kriz, W. et al. (2001): Podocin, a raft-associated component of the glomerular slit diaphragm, interacts with CD2AP and nephrin. In *The Journal of clinical investigation* 108 (11), pp. 1621–1629. DOI: 10.1172/JCI12849.

Sethi, Sanjeev; Fervenza, Fernando C.; Zhang, Yuzhou; Smith, Richard J. H. (2012): Secondary focal and segmental glomerulosclerosis associated with single-nucleotide polymorphisms in the genes encoding complement factor H and C3. In *American journal of kidney diseases : the official journal of the National Kidney Foundation* 60 (2), pp. 316–321. DOI: 10.1053/j.ajkd.2012.04.011.

Sethi, Sanjeev; Madden, Benjamin; Casal Moura, Marta; Nasr, Samih H.; Klomjit, Nattawat; Gross, LouAnn et al. (2022): Hematopoietic Stem Cell Transplant-Membranous Nephropathy Is Associated with Protocadherin FAT1. In *Journal of the American Society of Nephrology : JASN* 33 (5), pp. 1033–1044. DOI: 10.1681/ASN.2021111488.

Seyberth, H. W.; Rascher, W.; Schweer, H.; Kühl, P. G.; Mehls, O.; Schärer, K. (1985): Congenital hypokalemia with hypercalciuria in preterm infants: a hyperprostaglandinuric tubular syndrome different from Bartter syndrome. In *The Journal of pediatrics* 107 (5), pp. 694–701. DOI: 10.1016/s0022-3476(85)80395-4.

Seyberth, Hannsjörg W. (2008): An improved terminology and classification of Bartter-like syndromes. In *Nature clinical practice. Nephrology* 4 (10), pp. 560–567. DOI: 10.1038/ncpneph0912.

Seyberth, Hannsjörg W.; Schlingmann, Karl P. (2011): Bartter- and Gitelman-like syndromes: salt-losing tubulopathies with loop or DCT defects. In *Pediatric nephrology (Berlin, Germany)* 26 (10), pp. 1789–1802. DOI: 10.1007/s00467-011-1871-4.

Seys, Elsa; Andrini, Olga; Keck, Mathilde; Mansour-Hendili, Lamisse; Courand, Pierre-Yves; Simian, Christophe et al. (2017): Clinical and Genetic Spectrum of Bartter Syndrome Type 3. In *Journal of the American Society of Nephrology : JASN* 28 (8), pp. 2540–2552. DOI: 10.1681/ASN.2016101057.

Shendure, Jay; Porreca, Gregory J.; Reppas, Nikos B.; Lin, Xiaoxia; McCutcheon, John P.; Rosenbaum, Abraham M. et al. (2005): Accurate multiplex polony sequencing of an evolved bacterial genome. In *Science (New York, N.Y.)* 309 (5741), pp. 1728–1732. DOI: 10.1126/science.1117389.

Shimkets, R. A.; Warnock, D. G.; Bositis, C. M.; Nelson-Williams, C.; Hansson, J. H.; Schambelan, M. et al. (1994): Liddle's syndrome: heritable human hypertension caused by

mutations in the beta subunit of the epithelial sodium channel. In *Cell* 79 (3), pp. 407–414. DOI: 10.1016/0092-8674(94)90250-x.

Simon, D. B.; Bindra, R. S.; Mansfield, T. A.; Nelson-Williams, C.; Mendonca, E.; Stone, R. et al. (1997): Mutations in the chloride channel gene, CLCNKB, cause Bartter's syndrome type III. In *Nature genetics* 17 (2), pp. 171–178. DOI: 10.1038/ng1097-171.

Simon, D. B.; Karet, F. E.; Hamdan, J. M.; DiPietro, A.; Sanjad, S. A.; Lifton, R. P. (1996a): Bartter's syndrome, hypokalaemic alkalosis with hypercalciuria, is caused by mutations in the Na-K-2Cl cotransporter NKCC2. In *Nature genetics* 13 (2), pp. 183–188. DOI: 10.1038/ng0696-183.

Simon, D. B.; Karet, F. E.; Rodriguez-Soriano, J.; Hamdan, J. H.; DiPietro, A.; Trachtman, H. et al. (1996b): Genetic heterogeneity of Bartter's syndrome revealed by mutations in the K+ channel, ROMK. In *Nature genetics* 14 (2), pp. 152–156. DOI: 10.1038/ng1096-152.

Simon, D. B.; Nelson-Williams, C.; Bia, M. J.; Ellison, D.; Karet, F. E.; Molina, A. M. et al. (1996c): Gitelman's variant of Bartter's syndrome, inherited hypokalaemic alkalosis, is caused by mutations in the thiazide-sensitive Na-Cl cotransporter. In *Nature genetics* 12 (1), pp. 24–30. DOI: 10.1038/ng0196-24.

Smith, Jodi M.; Stablein, Donald M.; Munoz, Ricardo; Hebert, Diane; McDonald, Ruth A. (2007): Contributions of the Transplant Registry: The 2006 Annual Report of the North American Pediatric Renal Trials and Collaborative Studies (NAPRTCS). In *Pediatric transplantation* 11 (4), pp. 366–373. DOI: 10.1111/j.1399-3046.2007.00704.x.

Smith, L. M.; Sanders, J. Z.; Kaiser, R. J.; Hughes, P.; Dodd, C.; Connell, C. R. et al. (1986): Fluorescence detection in automated DNA sequence analysis. In *Nature* 321 (6071), pp. 674–679. DOI: 10.1038/321674a0.

Smith, Richard J. H.; Appel, Gerald B.; Blom, Anna M.; Cook, H. Terence; D'Agati, Vivette D.; Fakhouri, Fadi et al. (2019): C3 glomerulopathy - understanding a rare complement-driven renal disease. In *Nature reviews. Nephrology* 15 (3), pp. 129–143. DOI: 10.1038/s41581-018-0107-2.

Soliman, Neveen A. (2012): Orphan kidney diseases. In *Nephron. Clinical practice* 120 (4), c194-9. DOI: 10.1159/000339785.

Somlo, S.; Mundel, P. (2000): Getting a foothold in nephrotic syndrome. In *Nature genetics* 24 (4), pp. 333–335. DOI: 10.1038/74139.

Stevens, Paul E.; Levin, Adeera (2013): Evaluation and management of chronic kidney disease: synopsis of the kidney disease: improving global outcomes 2012 clinical practice guideline. In *Annals of internal medicine* 158 (11), pp. 825–830. DOI: 10.7326/0003-4819-158-11-201306040-00007.

Stokman, Marijn F.; Renkema, Kirsten Y.; Giles, Rachel H.; Schaefer, Franz; Knoers, Nine V A M; van Eerde, Albertien M. (2016): The expanding phenotypic spectra of kidney diseases: insights from genetic studies. In *Nature reviews. Nephrology* 12 (8), pp. 472–483. DOI: 10.1038/nrneph.2016.87.

Su, I. H.; Frank, R.; Gauthier, B. G.; Valderrama, E.; Simon, D. B.; Lifton, R. P.; Trachtman, H. (2000): Bartter syndrome and focal segmental glomerulosclerosis: a possible link between two diseases. In *Pediatric nephrology (Berlin, Germany)* 14 (10-11), pp. 970–972. DOI: 10.1007/s004670050054.

Subramanya, Arohan R.; Ellison, David H. (2014): Distal convoluted tubule. In *Clinical journal of the American Society of Nephrology : CJASN* 9 (12), pp. 2147–2163. DOI: 10.2215/CJN.05920613.

Sun, Yuting; de Jin; Zhang, Ziwei; Di Jin; Xue, JiaoJiao; Duan, LiYun et al. (2022): The critical role of the Hippo signaling pathway in kidney diseases. In *Frontiers in pharmacology* 13, p. 988175. DOI: 10.3389/fphar.2022.988175.

Sun, Zhenqiang; Zhang, Qiuge; Yuan, Weitang; Li, Xiaoli; Chen, Chen; Guo, Yaxin et al. (2020): MiR-103a-3p promotes tumour glycolysis in colorectal cancer via hippo/YAP1/HIF1A axis. In *Journal of experimental & clinical cancer research : CR* 39 (1), p. 250. DOI: 10.1186/s13046-020-01705-9.

Tanoue, Takuji; Takeichi, Masatoshi (2005): New insights into Fat cadherins. In *Journal of cell science* 118 (Pt 11), pp. 2347–2353. DOI: 10.1242/jcs.02398.

Tapon, Nicolas; Harvey, Kieran F.; Bell, Daphne W.; Wahrer, Doke C. R.; Schiripo, Taryn A.; Haber, Daniel A.; Hariharan, Iswar K. (2002): salvador Promotes both cell cycle exit and apoptosis in Drosophila and is mutated in human cancer cell lines. In *Cell* 110 (4), pp. 467–478. DOI: 10.1016/s0092-8674(02)00824-3.

Tarshish, P.; Tobin, J. N.; Bernstein, J.; Edelmann, C. M., JR (1997): Prognostic significance of the early course of minimal change nephrotic syndrome: report of the International Study of Kidney Disease in Children. In *Journal of the American Society of Nephrology : JASN* 8 (5), pp. 769–776. DOI: 10.1681/ASN.V85769.

Thomas, Shailin; Caplan, Arthur (2019): The Orphan Drug Act Revisited. In *JAMA* 321 (9), pp. 833–834. DOI: 10.1001/jama.2019.0290.

Town, M.; Jean, G.; Cherqui, S.; Attard, M.; Forestier, L.; Whitmore, S. A. et al. (1998): A novel gene encoding an integral membrane protein is mutated in nephropathic cystinosis. In *Nature genetics* 18 (4), pp. 319–324. DOI: 10.1038/ng0498-319.

Trautmann, Agnes; Lipska-Ziętkiewicz, Beata S.; Schaefer, Franz (2018): Exploring the Clinical and Genetic Spectrum of Steroid Resistant Nephrotic Syndrome: The PodoNet Registry. In *Frontiers in pediatrics* 6, p. 200. DOI: 10.3389/fped.2018.00200.

Trautmann, Agnes; Schnaidt, Sven; Lipska-Ziętkiewicz, Beata S.; Bodria, Monica; Ozaltin, Fatih; Emma, Francesco et al. (2017): Long-Term Outcome of Steroid-Resistant Nephrotic Syndrome in Children. In *Journal of the American Society of Nephrology : JASN* 28 (10), pp. 3055–3065. DOI: 10.1681/ASN.2016101121.

Tryggvason, K. (1999): Unraveling the mechanisms of glomerular ultrafiltration: nephrin, a key component of the slit diaphragm. In *Journal of the American Society of Nephrology : JASN* 10 (11), pp. 2440–2445. DOI: 10.1681/ASN.V10112440.

Tryggvason, K.; Pettersson, E. (2003): Causes and consequences of proteinuria: the kidney filtration barrier and progressive renal failure. In *Journal of internal medicine* 254 (3), pp. 216–224. DOI: 10.1046/j.1365-2796.2003.01207.x.

Tryggvason, Karl; Patrakka, Jaakko; Wartiovaara, Jorma (2006): Hereditary proteinuria syndromes and mechanisms of proteinuria. In *The New England journal of medicine* 354 (13), pp. 1387–1401. DOI: 10.1056/NEJMra052131.

Valletta, Daniela; Czech, Barbara; Spruss, Thilo; Ikenberg, Kristian; Wild, Peter; Hartmann, Arndt et al. (2014): Regulation and function of the atypical cadherin FAT1 in hepatocellular carcinoma. In *Carcinogenesis* 35 (6), pp. 1407–1415. DOI: 10.1093/carcin/bgu054.

Venables, Julian P.; Strain, Lisa; Routledge, Danny; Bourn, David; Powell, Helen M.; Warwicker, Paul et al. (2006): Atypical haemolytic uraemic syndrome associated with a hybrid complement gene. In *PLoS medicine* 3 (10), e431. DOI: 10.1371/journal.pmed.0030431.

Venter, J. C.; Adams, M. D.; Myers, E. W.; Li, P. W.; Mural, R. J.; Sutton, G. G. et al. (2001): The sequence of the human genome. In *Science (New York, N.Y.)* 291 (5507), pp. 1304–1351. DOI: 10.1126/science.1058040.

Vivante, Asaf; Skorecki, Karl (2019): Introducing routine genetic testing for patients with CKD. In *Nature reviews. Nephrology* 15 (6), pp. 321–322. DOI: 10.1038/s41581-019-0140-9.

Vivarelli, Marina; Massella, Laura; Ruggiero, Barbara; Emma, Francesco (2017): Minimal Change Disease. In *Clinical journal of the American Society of Nephrology : CJASN* 12 (2), pp. 332–345. DOI: 10.2215/CJN.05000516.

Voets, Thomas; Nilius, Bernd; Hoefs, Susan; van der Kemp, Annemiete W C M; Droogmans, Guy; Bindels, Rene J. M.; Hoenderop, Joost G. J. (2004): TRPM6 forms the Mg2+ influx channel involved in intestinal and renal Mg2+ absorption. In *The Journal of biological chemistry* 279 (1), pp. 19–25. DOI: 10.1074/jbc.M311201200.

Wallace, M. A. (1998): Anatomy and physiology of the kidney. In *AORN journal* 68 (5), 800, 803-16, 819-20; quiz 821-4. DOI: 10.1016/s0001-2092(06)62377-6.

Wang, Shuai; Xie, Feng; Chu, Feng; Zhang, Zhengkui; Yang, Bing; Dai, Tong et al. (2017): Corrigendum: YAP antagonizes innate antiviral immunity and is targeted for lysosomal degradation through IKKε-mediated phosphorylation. In *Nature immunology* 18 (11), p. 1270. DOI: 10.1038/ni1117-1270d.

Wang, Yan-Ni; Ma, Shi-Xing; Chen, Yuan-Yuan; Chen, Lin; Liu, Bao-Li; Liu, Qing-Quan; Zhao, Ying-Yong (2019): Chronic kidney disease: Biomarker diagnosis to therapeutic targets. In *Clinica chimica acta; international journal of clinical chemistry* 499, pp. 54–63. DOI: 10.1016/j.cca.2019.08.030.

Warwicker, P.; Goodship, T. H.; Donne, R. L.; Pirson, Y.; Nicholls, A.; Ward, R. M. et al. (1998): Genetic studies into inherited and sporadic hemolytic uremic syndrome. In *Kidney international* 53 (4), pp. 836–844. DOI: 10.1111/j.1523-1755.1998.00824.x.

Watson, Michael S.; Epstein, Charles; Howell, R. Rodney; Jones, Marilyn C.; Korf, Bruce R.; McCabe, Edward R. B.; Simpson, Joe Leigh (2008): Developing a national collaborative study

system for rare genetic diseases. In *Genetics in medicine : official journal of the American College of Medical Genetics* 10 (5), pp. 325–329. DOI: 10.1097/GIM.0b013e31817b80fd.

WATSON, J. D.; CRICK, F. H. (1953): Molecular structure of nucleic acids; a structure for deoxyribose nucleic acid. In *Nature* 171 (4356), pp. 737–738. DOI: 10.1038/171737a0.

Weinstein, Arthur; Alexander, Roberta V.; Zack, Debra J. (2021): A Review of Complement Activation in SLE. In *Current rheumatology reports* 23 (3), p. 16. DOI: 10.1007/s11926-021-00984-1.

Whaley, K.; Ruddy, S. (1976): Modulation of the alternative complement pathways by beta 1 H globulin. In *The Journal of experimental medicine* 144 (5), pp. 1147–1163. DOI: 10.1084/jem.144.5.1147.

White, Shannon M.; Avantaggiati, Maria Laura; Nemazanyy, Ivan; Di Poto, Cristina; Yang, Yang; Pende, Mario et al. (2019): YAP/TAZ Inhibition Induces Metabolic and Signaling Rewiring Resulting in Targetable Vulnerabilities in NF2-Deficient Tumor Cells. In *Developmental cell* 49 (3), 425-443.e9. DOI: 10.1016/j.devcel.2019.04.014.

Williams, L. R.; Leggett, R. W. (1989): Reference values for resting blood flow to organs of man. In *Clinical physics and physiological measurement : an official journal of the Hospital Physicists' Association, Deutsche Gesellschaft fur Medizinische Physik and the European Federation of Organisations for Medical Physics* 10 (3), pp. 187–217. DOI: 10.1088/0143-0815/10/3/001.

Wong, William (2007): Idiopathic nephrotic syndrome in New Zealand children, demographic, clinical features, initial management and outcome after twelve-month follow-up: results of a three-year national surveillance study. In *Journal of paediatrics and child health* 43 (5), pp. 337–341. DOI: 10.1111/j.1440-1754.2007.01077.x.

Wu, Shian; Huang, Jianbin; Dong, Jixin; Pan, Duojia (2003): hippo encodes a Ste-20 family protein kinase that restricts cell proliferation and promotes apoptosis in conjunction with salvador and warts. In *Cell* 114 (4), pp. 445–456. DOI: 10.1016/s0092-8674(03)00549-x.

Wu, Zhengming; Guan, Kun-Liang (2021): Hippo Signaling in Embryogenesis and Development. In *Trends in biochemical sciences* 46 (1), pp. 51–63. DOI: 10.1016/j.tibs.2020.08.008.

Xing, Chang-Yang; Tarumi, Takashi; Liu, Jie; Zhang, Yinan; Turner, Marcel; Riley, Jonathan et al. (2017): Distribution of cardiac output to the brain across the adult lifespan. In *Journal of cerebral blood flow and metabolism : official journal of the International Society of Cerebral Blood Flow and Metabolism* 37 (8), pp. 2848–2856. DOI: 10.1177/0271678X16676826.

Xu, T.; Wang, W.; Zhang, S.; Stewart, R. A.; Yu, W. (1995): Identifying tumor suppressors in genetic mosaics: the Drosophila lats gene encodes a putative protein kinase. In *Development (Cambridge, England)* 121 (4), pp. 1053–1063. DOI: 10.1242/dev.121.4.1053.

Yamazaki, Hajime; Nozu, Kandai; Narita, Ichiei; Nagata, Michio; Nozu, Yoshimi; Fu, Xue Jun et al. (2009): Atypical phenotype of type I Bartter syndrome accompanied by focal segmental glomerulosclerosis. In *Pediatric nephrology (Berlin, Germany)* 24 (2), pp. 415–418. DOI: 10.1007/s00467-008-0999-3.

Yaoita, Eishin; Kurihara, Hidetake; Yoshida, Yutaka; Inoue, Tsutomu; Matsuki, Asako; Sakai, Tatsuo; Yamamoto, Tadashi (2005): Role of Fat1 in cell-cell contact formation of podocytes in puromycin aminonucleoside nephrosis and neonatal kidney. In *Kidney international* 68 (2), pp. 542–551. DOI: 10.1111/j.1523-1755.2005.00432.x.

Yousefi, Hassan; Delavar, Mahsa Rostamian; Piroozian, Fatemeh; Baghi, Masoud; Nguyen, Khoa; Cheng, Thomas et al. (2022): Hippo signaling pathway: A comprehensive gene expression profile analysis in breast cancer. In *Biomedicine & pharmacotherapy = Biomedecine & pharmacotherapie* 151, p. 113144. DOI: 10.1016/j.biopha.2022.113144.

Zhang, Chi; Li, Chuan-Lei; Xu, Ke-Xin; Zheng, Zhi-Huang; Cheng, Guo-Zhe; Wu, Hui-Juan; Liu, Jun (2022): The Hippo pathway and its correlation with acute kidney injury. In *Zoological research* 43 (5), pp. 897–910. DOI: 10.24272/j.issn.2095-8137.2022.110.

Zhang, Heng; Liu, Chen-Ying; Zha, Zheng-Yu; Zhao, Bin; Yao, Jun; Zhao, Shimin et al. (2009): TEAD transcription factors mediate the function of TAZ in cell growth and epithelial-mesenchymal transition. In *The Journal of biological chemistry* 284 (20), pp. 13355–13362. DOI: 10.1074/jbc.M900843200.

Zhao, Bin; Wei, Xiaomu; Li, Weiquan; Udan, Ryan S.; Yang, Qian; Kim, Joungmok et al. (2007): Inactivation of YAP oncoprotein by the Hippo pathway is involved in cell contact inhibition and tissue growth control. In *Genes & development* 21 (21), pp. 2747–2761. DOI: 10.1101/gad.1602907.

Zhao, Bin; Ye, Xin; Yu, Jindan; Li, Li; Li, Weiquan; Li, Siming et al. (2008): TEAD mediates YAP-dependent gene induction and growth control. In *Genes & development* 22 (14), pp. 1962–1971. DOI: 10.1101/gad.1664408.

Zhao, Qianying; Xiang, Qinqin; Tan, Yu; Xiao, Xiao; Xie, Hanbing; Wang, He et al. (2022): A novel CLCNKB variant in a Chinese family with classic Bartter syndrome and prenatal genetic diagnosis. In *Molecular genetics & genomic medicine*, e2027. DOI: 10.1002/mgg3.2027.

Zheng, Xinglong; Majerus, Elaine M.; Sadler, J. Evan (2002): ADAMTS13 and TTP. In *Current opinion in hematology* 9 (5), pp. 389–394. DOI: 10.1097/00062752-200209000-00001.

Zhong, Bozitao; Su, Xiaoming; Wen, Minhua; Zuo, Sichen; Hong, Liang; Lin, James (2021): ParaFold: Paralleling AlphaFold for Large-Scale Predictions. Available online at https://arxiv.org/pdf/2111.06340.

Zipfel, P. F.; Jokiranta, T. S.; Hellwage, J.; Koistinen, V.; Meri, S. (1999): The factor H protein family. In *Immunopharmacology* 42 (1-3), pp. 53–60. DOI: 10.1016/s0162-3109(99)00015-6.

Zuber, Julien; Fakhouri, Fadi; Roumenina, Lubka T.; Loirat, Chantal; Frémeaux-Bacchi, Véronique (2012): Use of eculizumab for atypical haemolytic uraemic syndrome and C3 glomerulopathies. In *Nature reviews. Nephrology* 8 (11), pp. 643–657. DOI: 10.1038/nrneph.2012.214.

Further publications

Long-term data on two sisters with C3GN due to an identical, homozygous CFH mutation and autoantibodies

Agnes Hackl, Florian Erger, Christine Skerka, Andrea Wenzel, **Nikolai Tschernoster**, Rasmus Ehren, Kathrin Burgmaier, Vera Riehmer, Christoph Licht, Michael Kirschfink, Lutz T Weber, Janine Altmueller, Peter F Zipfel, Sandra Habbig.

Published in Clin Nephrol. 2020 Oct;94(4):197-206. doi: 10.5414/CN110135

This case report further explains the discordant clinical course of the two siblings included in the second study: “Unraveling Structural Rearrangements of the CFH Gene Cluster in Atypical Hemolytic Uremic Syndrome Patients Using Molecular Combing and Long-Fragment Targeted Sequencing”

Alport syndrome and autosomal dominant tubulointerstitial kidney disease frequently underlie end-stage renal disease of unknown origin - a single-center analysis

Esther Leenen, Florian Erger, Janine Altmüller, Andrea Wenzel, Holger Thiele, Ana Harth, **Nikolai Tschernoster**, Shanti Lokhande, Achim Joerres, Jan-Ulrich Becker, Arif Ekici, Bruno Huettel, Bodo Beck, Alexander Weidemann

Published in Nephrol Dial Transplant. 2022 Sep 22;37(10):1895-1905. doi:10.1093/ndt/gfac163

Acknowledgements

First of all, I want to thank Prof. Dr. Peter Nürnberg, for the opportunity to write my thesis under his supervision at the Cologne Center for Genomics. With Prof. Dr. Klaus Zerres at the University Hospital of Aachen and you at the CCG in Cologne I am grateful to have worked under the supervision of two great experts of their fields. However, I accompanied both of them into their retirement.

Thanks to Prof. Dr. Paul Brinkkötter for taking on the task as second reviewer of this thesis.

Likewise, I want to thank Prof. Dr. Karin Schnetz for kindly agreeing to be the Chair of my Thesis defense committee.

I am very grateful to Dr. Bodo Beck and Dr. Janine Altmüller for their support over the years on a scientific level as well as on a personal level. I really enjoyed our time together since I started working with you back in April 2017 and will never forget the effort you two have put into these projects and your doctoral students.

I thank all members of the AG Beck and AG Altmüller, especially Florian Erger and Björn Reusch for the scientific discussions and their support, and the members of the CCG, namely Gerti Meyer, Nina Dalibor and Christian Becker who created the best working environment and enriched my personal life over all these years.

I thank my family for their support throughout many years of study.

Finally, and most importantly, I thank my wife Eva for her loving support, her patience and willingness to move to Cologne and back and wherever our life will bring us.

Supplemental Material

Supplementary Material Manuscript 1

Supplementary Table S1: 122 gene screening panel for monogenic causes of nephropathies associated to proteinuria.

Gene	Transcript	Ensembl transcript
ABCD4	NM_005050.3	ENST00000356924
ACTN4	NM_004924.4	ENST00000252699
ADAMTS13	NM_139025.4	ENST00000371929
ALG8	NM_024079.4	ENST00000299626
ALMS1	NM_015120.4	ENST00000613296
ANLN	NM_018685.4	ENST00000265748
APOA1	NM_000039.1	ENST00000236850
APOA2	NM_001643.1	ENST00000367990
APOC2	NM_000483.4	ENST00000252490
APOC3	NM_000040.1	ENST00000227667
APOL1	NM_003661.3	ENST00000397278
APOPT1	NM_032374.4	ENST00000409074
APP	NM_000484.3	ENST00000346798
ARHGAP24	NM_001025616.2	ENST00000395184
B2M	NM_004048.2	ENST00000558401
C3	NM_000064.3	ENST00000245907
CD2AP	NM_012120.2	ENST00000359314
CD46	NM_002389.4	ENST00000358170
CD151	NM_004357.4	ENST00000322008.8
CFB	NM_001710.5	ENST00000425368
CFH	NM_000186.3	ENST00000367429
CFHR1	NM_002113.2	ENST00000320493
CFHR2	NM_005666.2	ENST00000367415
CFHR3	NM_021023.5	ENST00000367425
CFHR4	NM_001201550.2	ENST00000367416
CFHR5	NM_030787.3	ENST00000256785
CFI	NM_000204.3	ENST00000394634
CLCN5	NM_000084.2	ENST00000376108
COL4A1	NM_001845.5	ENST00000375820
COL4A3	NM_000091.4	ENST00000396578
COL4A4	NM_000092.4	ENST00000396625
COL4A5	NM_000495.4	ENST00000361603
COQ2	NM_015697.7	ENST00000311469
COQ6	NM_182476.2	ENST00000334571
COQ8B	NM_024876.3	ENST00000324464
COX10	NM_001303.3	ENST00000261643
COX6B1	NM_001863.4	ENST00000246554
CRB2	NM_173689.6	ENST00000373631
CRKL	NM_005207.3	ENST00000354336.7
CST3	NM_000099.3	ENST00000376925
CUBN	NM_001081.3	ENST00000377833
DGKE	NM_003647.2	ENST00000284061
EHHADH	NM_001966.3	ENST00000231887
EMP2	NM_001424.4	ENST00000359543
ETFA	NM_000126.3	ENST00000557943
ETFB	NM_001985.2	ENST00000309244
ETFDH	NM_004453.3	ENST00000511912
FAH	NM_000137.2	ENST00000561421
FAN1	NM_014967.4	ENST00000362065
FASTKD2	NM_014929.3	ENST00000236980
FAT1	NM_005245.3	ENST00000441802
FGA	NM_021871.2	ENST00000403106
FH	NM_000143.3	ENST00000366560
FN1	NM_212482.1	ENST00000354785
FRAS1	NM_025074.6	ENST00000512123
FREM1	NM_144966.5	ENST00000422223
FREM2	NM_207361.5	ENST00000280481
G6PC	NM_000151.3	ENST00000253801
GALT	NM_000155.3	ENST00000378842
GCDH	NM_000159.3	ENST00000222214
GDNF	NM_000514.3	ENST00000326524.6
GLA	NM_000169.2	ENST00000218516
GRIP1	NM_021150.3	ENST00000398016
GSN	NM_000177.4	ENST00000373818
HADHA	NM_000182.4	ENST00000380649
HADHB	NM_000183.2	ENST00000317799
INF2	NM_022489.3	ENST00000392634
ITGA3	NM_002204.2	ENST00000320031
KANK1	NM_015158.3	ENST00000382297
KANK2	NM_001136191.2	ENST00000586659
KANK3	NM_198471	ENST00000330915
KANK4	NM_181712.4	ENST00000371153
LAGE3	NM_006014.4	ENST00000357360.4
LAMA5	NM_005560.4	ENST00000252999
LAMB2	NM_002292.3	ENST00000418109
LCAT	NM_000229.1	ENST00000264005
LMBRD1	NM_018368.3	ENST00000370577
LMX1B	NM_002316.3	ENST00000526117
LRP2	NM_004525.2	ENST00000263816
LYZ	NM_000239.2	ENST00000261267
MAFB	NM_005461.4	ENST00000373313
MEFV	NM_000243.2	ENST00000219596
MMAA	NM_172250.2	ENST00000281317
MMAB	NM_052845.3	ENST00000545712
MMACHC	NM_015506.2	ENST00000401061
MMADHC	NM_015702	ENST00000303319
MUT	NM_000255.3	ENST00000274813
MYH9	NM_002473.5	ENST00000216181
MYO1E	NM_004998.3	ENST00000288235
NLRP3	NM_004895.4	ENST00000336119.7
NPHS1	NM_004646.3	ENST00000378910
NPHS2	NM_014625.2	ENST00000367615
NUP107	NM_020401.2	ENST00000229179
NUP133	NM_018230	ENST00000261396.3
NUP160	NM_015231	ENST00000378460.2
NUP205	NM_015135	ENST00000285968
NUP85	NM_024844	ENST00000245544.4
NUP93	NM_014669.4	ENST00000308159.9
NXF5	NM_032946.2	ENST00000473265.2
OCRL	NM_000276.3	ENST00000371113
OSGEP	NM_017807.3	ENST00000206542.8
PAX2	NM_003987.3	ENST00000428433
PDSS2	NM_020381.3	ENST00000369037
PLCE1	NM_016341.3	ENST00000260766
PMM2	NM_000303.2	ENST00000268261
PRNP	NM_000311.3	ENST00000379440
PTPRO	NM_030667.2	ENST00000281171
SCARB2	NM_005506.3	ENST00000264896
SEC61A1	NM_013336.3	ENST00000243253.7
SGPL1	NM_003901.3	ENST00000373202
SLC34A1	NM_003052.4	ENST00000324417
SMARCAL1	NM_014140.3	ENST00000357276
SOX18	NM_018419.2	ENST00000340356
TACO1	NM_016360.3	ENST00000258975
THBD	NM_000361.2	ENST00000377103
TP53RK	NM_033550.3	ENST00000372114.3
TPRKB	NM_001330390.1	ENST00000318190.7
TRPC6	NM_004621.5	ENST00000344327
TTR	NM_000371.3	ENST00000237014
WDR73	NM_032856.3	ENST00000434634
WT1	NM_024426.4	ENST00000332351
XPO5	NM_020750.2	ENST00000265351

Supplementary Table S2: List of probe-based assays.

Probe based assay	gene	company
Hs.PT.58.45621572	HPRT	IDT
Hs00172187_m1	POLR2A	Applied Biosystems
Hs00169587_m1	GADD45B	Applied Biosystems
Hs99999905_m1	GAPDH	Applied Biosystems
Hs00274384_m1	IQCB1	Applied Biosystems
Hs01026927_g1	CTGF	Applied Biosystems
Hs00998500_g1	CYR61	Applied Biosystems
Hs00950669_m1	AREG	Applied Biosystems
Hs00923599_m1	ANKRD1	Applied Biosystems
Hs00985639_m1	IL6	Applied Biosystems
Hs00159357_m1	MUC1	Applied Biosystems
Hs00560416_m1	SAV1	Applied Biosystems
Hs01125523_m1	LATS1	Applied Biosystems
Hs00966302_m1	NF2	Applied Biosystems
Hs00153380_m1	CCND2	Applied Biosystems
Hs00324396_m1	LATS2	Applied Biosystems
Hs00964416_m1	MOB1A	Applied Biosystems
Hs01397675_m1	MOB1B	Applied Biosystems
Hs00178979_m1	STK4 (MST2)	Applied Biosystems
Hs00169491_m1	STK3 (MST1)	Applied Biosystems
Hs00902712_g1	YAP1	Applied Biosystems
Hs00918044_g1	CDC42	Applied Biosystems

Supplementary figure S1

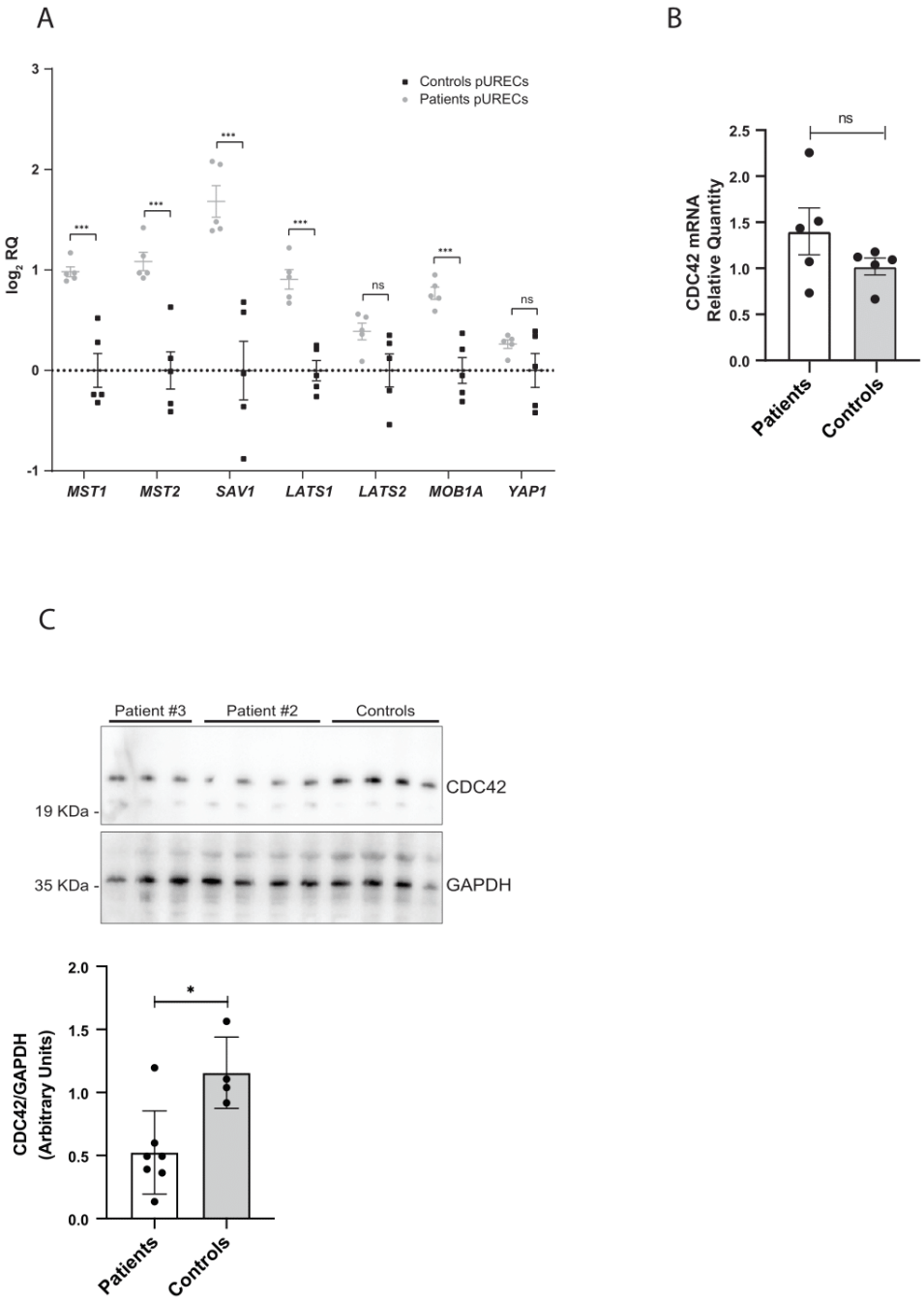

Supplementary Figure S1:

*qPCR analysis of RNA extracted from pURECS derived from patients #2 and #3 indicated an upregulation of the Hippo central components at mRNA level as compared to healthy controls (A). qPCR analysis revealed no statistically significant differences in CDC42 mRNA amounts (B). Immunoblot analysis of protein extracts of pURECs revealed a reduction in CDC42 levels in patients (#2 and #3) compared to controls as shown in the western blot and in the densitometric analysis (C). Bars are depicting SEM, asterisks indicate statistical significance as follows: *p<0.05, **p<0.01, ***p<0,005, ****p<0,001, ns=not significant).*

Supplementary Material Manuscript 2

*Suppl. Table S1: Patient cohort. eur: European, tur: Turkish, n/a: data not available. *Detailed clinical course of the two sisters of family F10 carrying the homozygous CFH variant c.671_673del (p.Lys224del) are described in more detail by Hackl et al.[35]*

Family ID	Sex	Age at study	Ethnicity	Clinical diagnosis	DEAP- HUS	Results
F1	f	34	eur	aHUS (biopsy: TMA)	no	WT / WT
F2	m	4	eur	C3G	no	WT / WT
F3	m	31	eur	aHUS (biopsy: TMA)	no	*CFH/CFHR1* hybrid gene / WT
F4	f	48	eur	aHUS	no	*CFHR3/CFHR1* del / WT
F5	f	7	eur	aHUS (biopsy: TMA)	no	*CFHR3/CFHR1* del / WT
F6	m	37	eur	aHUS (biopsy: TMA)	no	WT / WT
F7	f	22	eur	C3G	no	*CFHR3/CFHR1* del / WT
F8	f	30	eur	aHUS (biopsy: TMA)	no	WT / WT
F9	m	59	eur	C3G	no	WT / WT
F10.1*	f	22	tur	C3G	no	WT / WT (structural)
F10.2*	f	17	tur	C3G	no	WT / WT (structural)
F11	f	8	eur	aHUS	yes	*CFHR3/CFHR1* del / *CFHR3/CFHR1* del
F12	m	11	eur	C3G	n/a	WT / WT
F13	m	5	eur	aHUS	yes	*CFHR3/CFHR1* del / *CFHR3/CFHR1* del
F14	m	24	eur	aHUS (biopsy: TMA)	no	*CFHR3/CFHR1* del / WT

F15	m	(<18)	eur	aHUS	no	*CFH/CFHR1* hybrid gene / WT
F16	m	16	eur	aHUS (biopsy: TMA)	no	WT / WT
F17	f	43	eur	aHUS (biopsy: TMA)	no	WT / WT
F18	f	40	eur	aHUS (biopsy: FSGS)	no	*CFHR4/CFHR1* del / *CFHR3/CFHR1* del
F19	m	n/a	eur	aHUS	no	*CFHR3/CFHR1* del / WT
F20	m	65	eur	aHUS	no	*CFH/CFHR3* hybrid gene / WT

*Suppl. Table S2: Review of the literature regarding eculizumab treatment in patients with SVs in the CFH gene cluster. The term "n/a" was used as representative of "not mentioned / information not available". *Breville et al. "Eculizumab was considered but not retained due to stabilization of laboratory parameters and a joint decision between the medical staff and the patient after presenting the risks, benefits, and economic burden. Eculizumab was retained as a second line treatment option in case of nonresponse or premature relapse".[50] †Togarsimalemath et al. "[Eculizumab] was not available in the family's country".[51] ‡Tortajada et al. Patients were treated with angiotensin converting enzyme inhibitor therapy. Eculizumab was mentioned as potential beneficial therapy but was not mentioned as treatment for the patients in this study.[53] §Gale et al. Eculizumab is mentioned as potential beneficial treatment but it was not mentioned that eculizumab was given to the patients in this study.[54]*

Structural variant	**Disease**	**Eculizumab therapy**	**outcome**	**Reference**
***CFH/CFHR1* hybrid gene**	aHUS,	yes	beneficial	[44, 32]
***CFH/CFHR3* hybrid gene**	aHUS	yes	beneficial	[9]
***CFHR3/CFHR1* deletion**	aHUS, DEAP-HUS	yes	beneficial	[46]
***CFHR3/CFHR1* deletion**	SLE, TMA	yes	beneficial	[47, 48]
***CFHR4/CFHR1* deletion**	aHUS, DEAP-HUS	n/a	n/a	[49, 22]
***CFHR4/CFHR1* deletion**	IgG4-RD	no*	n/a	[50]
***CFHR3/CFHR1* hybrid gene**	C3G	n/a	n/a	[14]

***CFHR1/CFH* hybrid gene**	aHUS	yes	beneficial	[7]
***CFHR1/CFHR5* hybrid gene**	C3G	no[†]	n/a	[51]
***CFHR2/CFHR5* hybrid gene**	C3G-DDD	yes	no effect	[15]
***CFHR5/CFHR2* hybrid gene**	C3G	n/a	n/a	[52]
Intra *CFHR1* duplication	C3G	no[‡]	n/a	[53]
Intra *CFHR5* duplication	C3G	no[§]	n/a	[54]
Intra *CFHR5* duplication	C3G	n/a	n/a	[55]
Intra *CFHR3* deletion	C3G	n/a	n/a	[13]
***CFHR3/CFHR4* hybrid gene**	C3G	n/a	n/a	[13]
***CFH* deletion**	IC-MPGN	n/a	n/a	[13]
***CFHR4/CFHR1* duplication**	C3G, IC-MPGN	n/a	n/a	[13]

Suppl. Table S3: Cost estimate by the authors. Calculation of costs is based on the premise that the laboratory already has all of the necessary instruments and analysis software.

Method	**Purpose**	**Cost estimate per sample**
NGS/WES based gene panel	1st line routine, SNV and CNV analysis	~ $300 depending on target size and sequencing device
MLPA *CFH* gene cluster	2nd line CNV detection Nota bene: Exon coverage is incomplete with the commercially available MLPA kit (P236, MRC Holland, Amsterdam, Netherlands)	~ $60 including costs for sex matched MLPA control sample. Gene rearrangements without copy number changes will not be identified by MLPA
Molecular combing of *CFH* gene cluster	2nd line SV detection in unsolved cases or those cases where more precise information of haplotypes is needed and	~ $50 including HMW DNA extraction, non-recurring investment in fluorescent probe design needs to be done in addition

	NGS/MLPA analyses is insufficient to reconstruct both alleles	
Target enrichment (Samplix) and long-read sequencing (ONT or PacBio)	validation of conspicuous SV findings	~ $220 enrichment and ~ $220 sequencing costs (depends on the pooling strategies, a long read WGS would be ~ $1700)
PCR and Sanger sequencing	any validation or segregation within families of SNV or SV (breakpoints)	less than $15

control	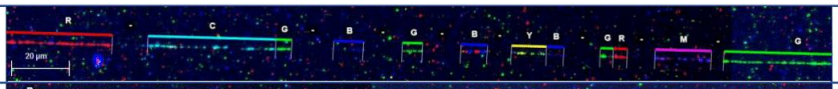	WT Allele
F1 20982	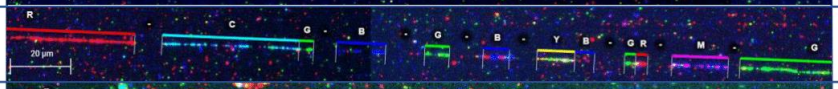	WT Allele
F2 0727	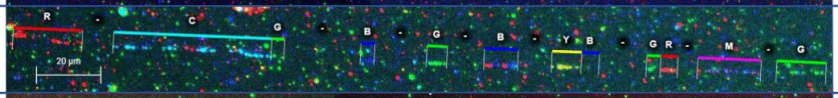	WT Allele
F3 15622	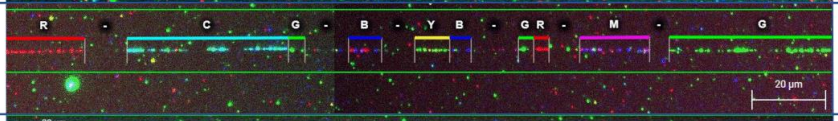	*CFH/CFHR1* hybrid gene
F3 15622	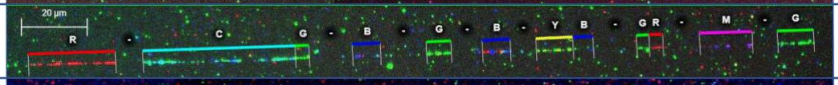	WT Allele
F4 19446	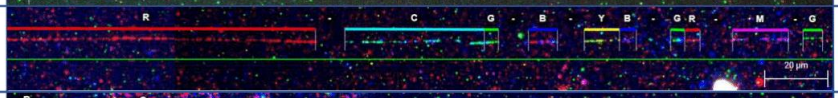	*CFHR3/CFHR1* del
F4 19446	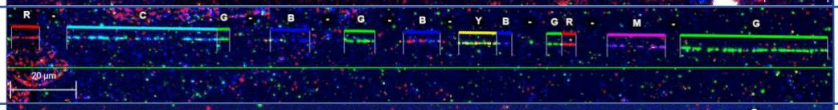	WT Allele
F5 20334	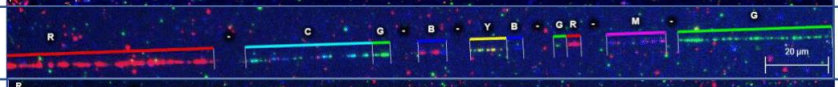	*CFHR3/CFHR1* del
F5 20334	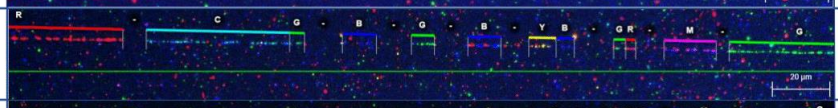	WT Allele
F6 20437	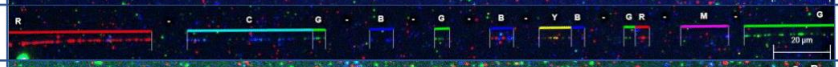	WT Allele
F7 20458	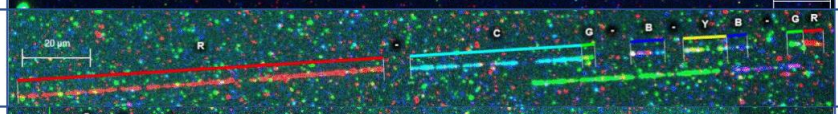	*CFHR3/CFHR1* Del*
F7 20458	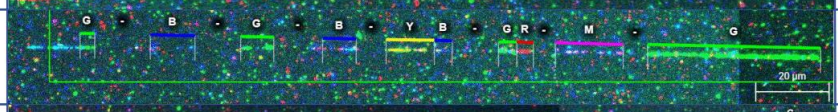	WT Allele*
F8 21044	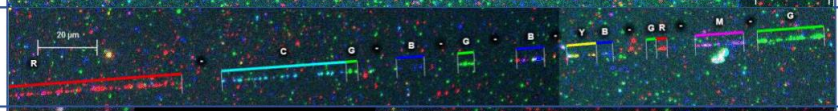	WT Allele
F9 2606	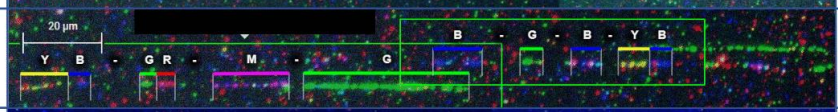	WT Allele†
F10 5407142	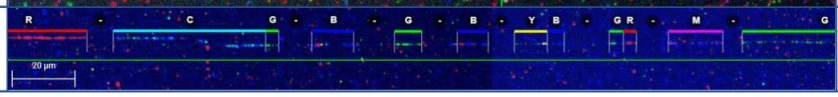	WT Allele

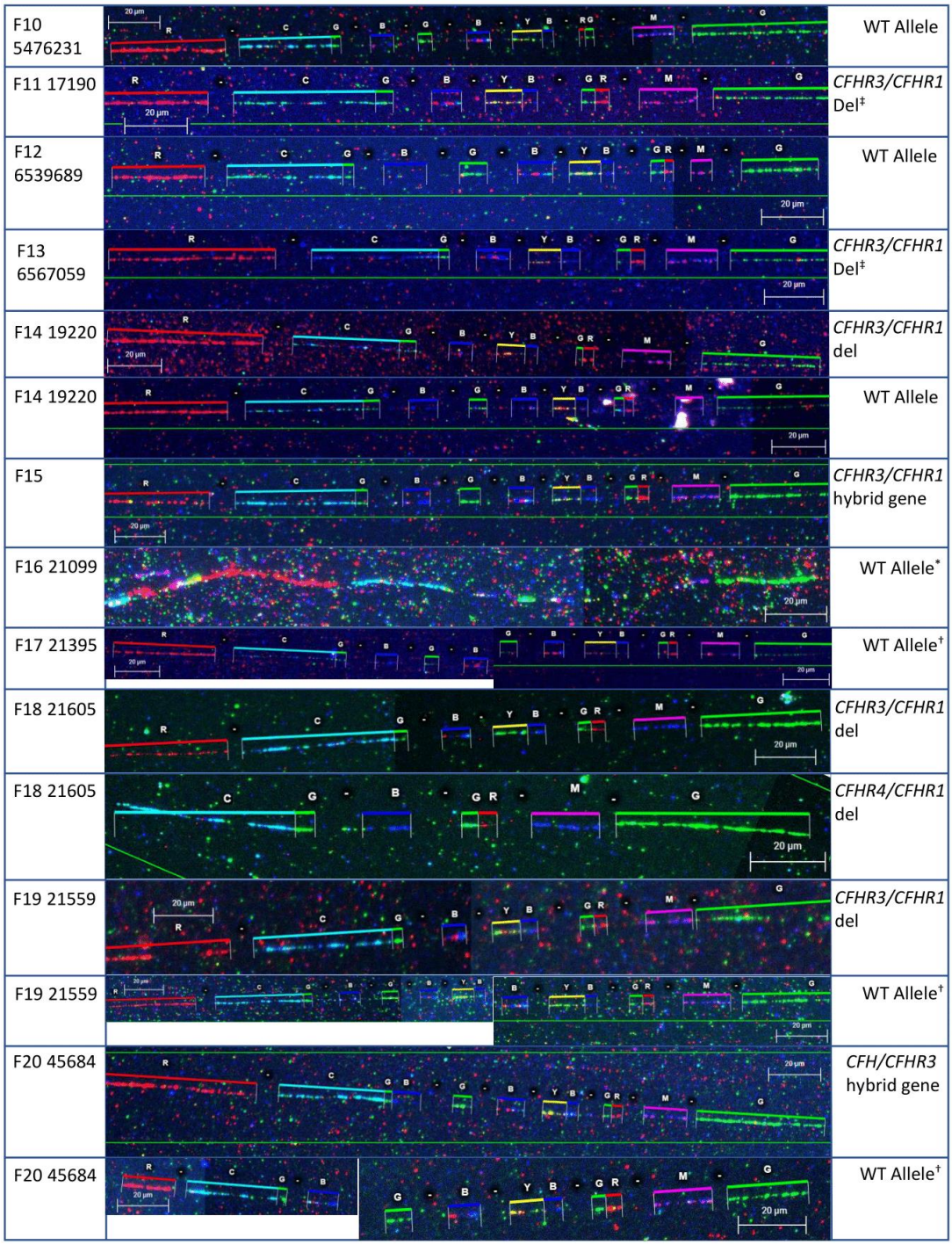

*Suppl. Figure S1: FiberVision fluorescent in situ complement factor H (CFH) gene cluster hybridization. Molecular combing signals of the 20 families (21 patients). One signal is shown when there is only one haplotype. Each haplotype is shown if the structural variants are heterozygous. The value of 1 pixel = 0.164 µm. *No complete signal available, nearly complete signal shown. †No complete signal available, two halves of the signals shown. ‡Homozygous CFHR3/CFHR1 deletion. Scale bar = 20 µm. Original magnification, ×40. Del, deletion; WT, wild type.*

Supplementary Material Manuscript 3

Suppl. Table 1: Molecular genetic analyses performed on each patient. a Long-range PCR was performed but no PCR fragment could be generated. b degraded DNA, low DNA quality.

Patient	Exome	Linked-read	Samplix Xdrop	Long-range PCR	Long-read WGS (PacBio)
P1.1	Yes			Yes (not sequenced)	
P1.2	Yes	Yes	Yes	Yes	
P1.3	Yes			Yes	
P2				Yes	
P3				Yes	
P4				Yes	Yes
P5				Yes	
P6				No[a]	Yes
P7			Yes	Yes	
P8				Yes	
P9			Yes	Yes	
P10				No[a]	Yes
P11			Yes	No[a]	
P12				Yes	
P13				Yes	
P14				Yes	
P15.1				Yes	
P15.2				Yes	
P16[b]				No[a]	

P17				Yes	
P18				No[a]	
P19				Yes	
P20				Yes	
P21				Yes	
P22				No[a]	
P23				Yes	
P24				Yes	
P25				No[a]	
P26[b]				No[a]	
P27				Yes	
P28				Yes	
P29				Yes	
P30				Yes	

Suppl. Table 2: Breakpoint-region coordinates found in this study. Breakpoint region coordinates of the eight breakpoint alleles (A-H) including the sequence transposition haplotypes of 2.2 and 3 kb length in the CLCNKA 3' UTR. Coordinates refer to the GRCh37/hg19 human reference. [a] breakpoint allele in a heterozygous state.

	Breakpoint Coordinates (GRCh37/hg19) found in this study							
Patient	**Chr1:16.353.282 -16.353.336 to Chr1:16.375.088 -16.375.142**	**Chr1:16.357.450 -16.357.595 to Chr1:16.379.176 -16.379.321**	**Chr1:16.360.410 -16.360.478 to Chr1:16.383.668 -16.383.736 Transposition haplotype 5' breakpoint region**	**Chr1:16.362.210 -16.362.445 to Chr1:16.385.815 -16.385.874 Transposition haplotype 3' breakpoint region 2.2 kb**	**Chr1:16.363.41 3 to chr1:16.386.67 7 Transposition haplotype 3' breakpoint region 3 kb**	**Chr1:16.363.748 -16.363.772 to Chr1:16.387.006 -16.387.030**	**Chr1:16.363.772 -16.363.803 to Chr1:16.387.030 -16.387.061**	**Chr1:16.366.734 -16.366.847 to Chr1:16.389.242 -16.389.355**
P1.1			X	X			X	
P1.2			X	X			X	
P1.3			X	X			X	
P10			X	X				X
P9[a] Allele1			X					
P9[a] Allele2			X		X	X		
P18[a] Allele 1			X					
P18[a] Allele 2			X		X	X		
P5			X		X	X		
P18[a]			X		X	X		
P23			X		X	X		
P3			X		X		X	
P13			X		X		X	
P12			X		X		X	
P2			X		X		X	
P21			X		X		X	
P24			X		X		X	
P27			X		X		X	
P28			X		X		X	
P29			X		X		X	
P7			X					
P8			X					
P17			X					
P20			X					
P30			X					
P11	X				X		X	
P6		X						
P4				X				
P15.1				X				
P15.2				X				

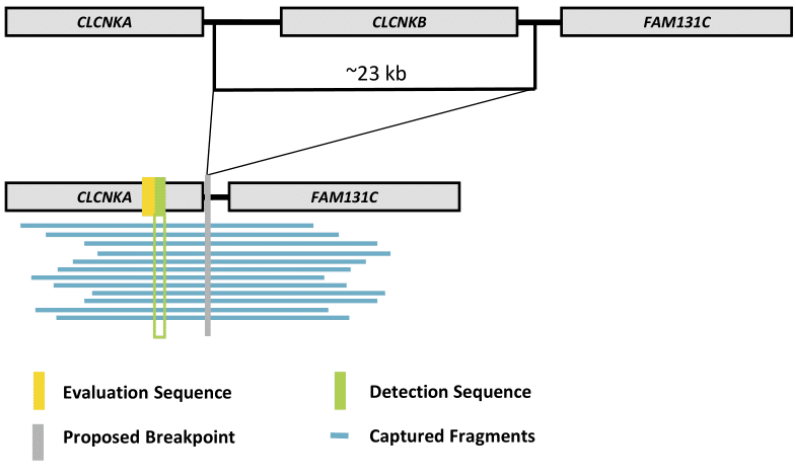

Suppl. Figure S1: Schematic view of the Samplix Xdrop custom sequence capture design.

Detection and evaluation sequence designed in CLCNKA to capture up to 50 kb of HMW genomic DNA fragments covering CLCNKA and CLCNKB. Proposed breakpoints in the region between CLCNKA and CLCNKB.

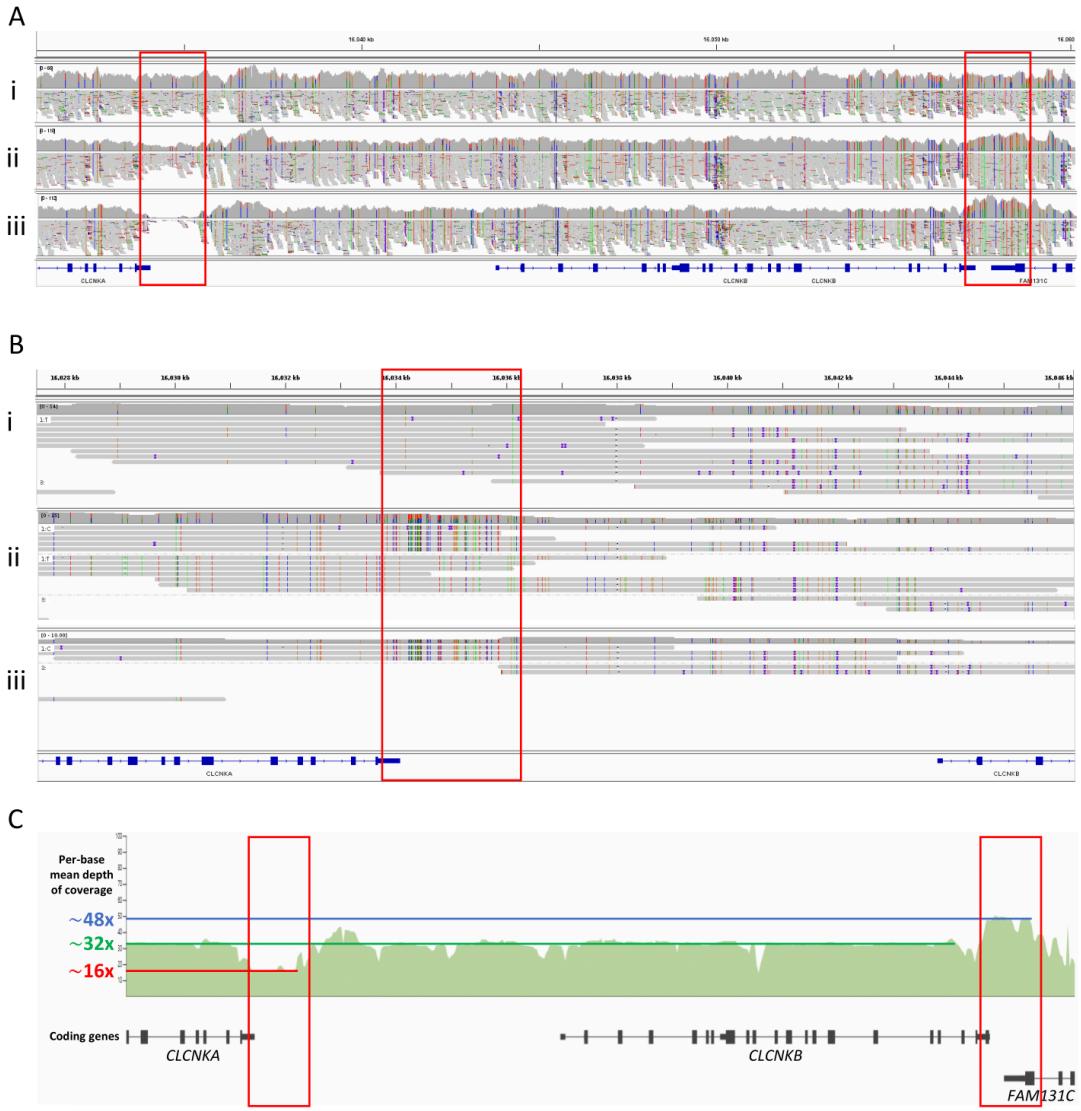

Suppl. Figure S2: Workup of the CLCNKA 3' UTR sequence transposition haplotype found in this study.

CLCNKA 3' UTR sequence transposition haplotype in short- and long-read whole genome in-house CLCNKB deletion control datasets. Whole genome data of the reference (i) and the heterozygous (ii) and homozygous (iii) variant haplotype, respectively. Sequences are visualized in IGV. Genes are indicated in blue; Exons are indicated as vertical bars; Gene orientation is indicated by arrows. Genomic coordinates refer to the hg38 human reference. A In the short-read alignment, the duplicated 2.2-3 kb 3' UTR of CLCNKB are aligned in the CLCNKB 3' UTR (right red square), leading to a coverage gain in the variant haplotype carriers. The loss of the 3' UTR of CLCNKA is indicated by the reduced coverage (left red square). B In the long-read alignment, the inserted CLCNKB 3' UTR fragment (red square) is indicated by the differentiating nucleotides that distinguish the CLCNKA 3' UTR and the CLCNKB 3' UTR. C Coverage plot of the CLCNKA/CLCNKB gene locus adapted from gnomAD SV (v. 2.1). Reduced coverage depth in the CLCNKA 3' UTR (left red square) and elevated coverage in the CLCNKB 3' UTR (right red square) are visible in the normal population data. This data indicates a 2.2-3 kb loss of CLCNKA 3' UTR sequence and a duplication of the CLCNKB 3' UTR sequence in approximately 50 % of control alleles, corresponding to the expected representation of the transposition haplotype in short-read NGS data.

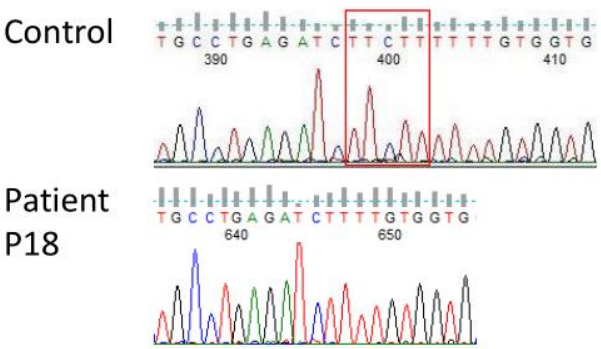

Suppl. Figure S3: 5 bp deletion confirmed by Sanger Sequencing in patient P18.

Sanger Sequencing of CLCNKB exon 9 in P18 (lower panel) and a control (upper panel). The 5 bp deletion appears homozygous because of the CLCNKB deletion allele F in trans.

Deletion allele A

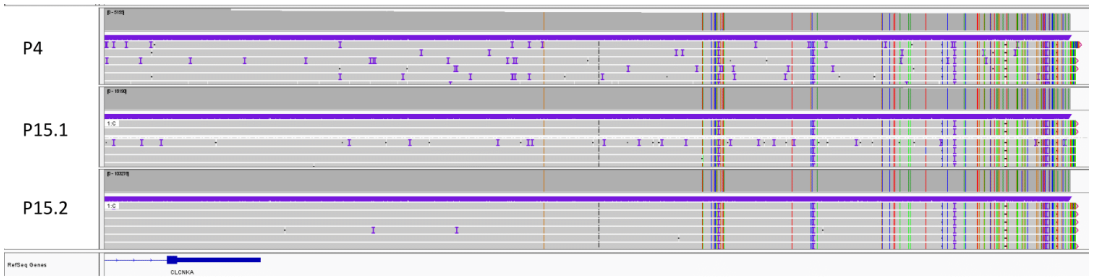

Deletion allele B

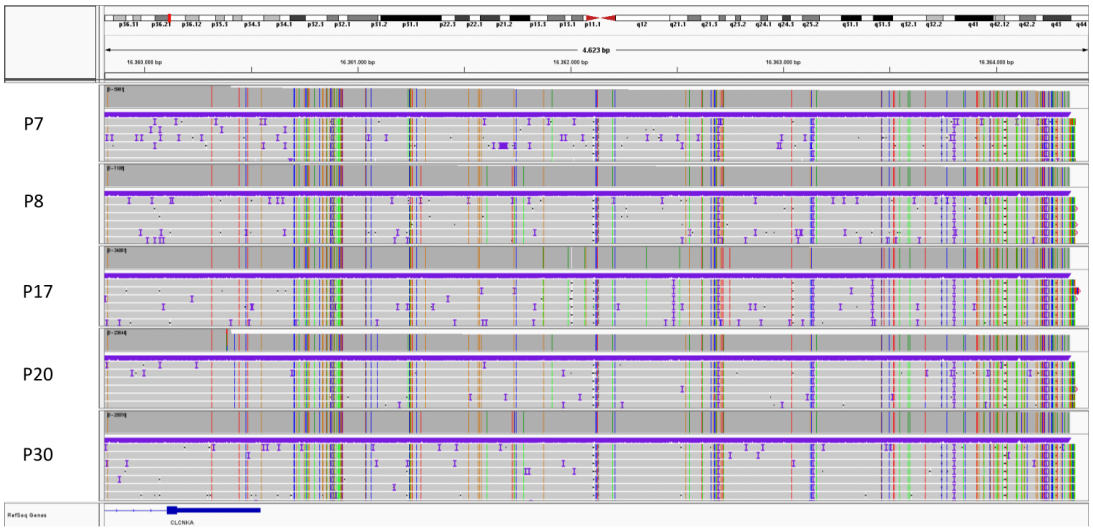

Deletion allele C

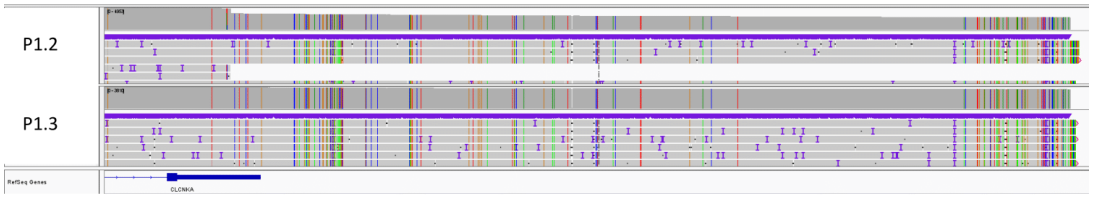

Deletion allele D

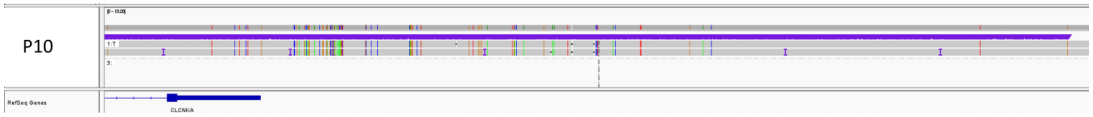

Deletion allele E

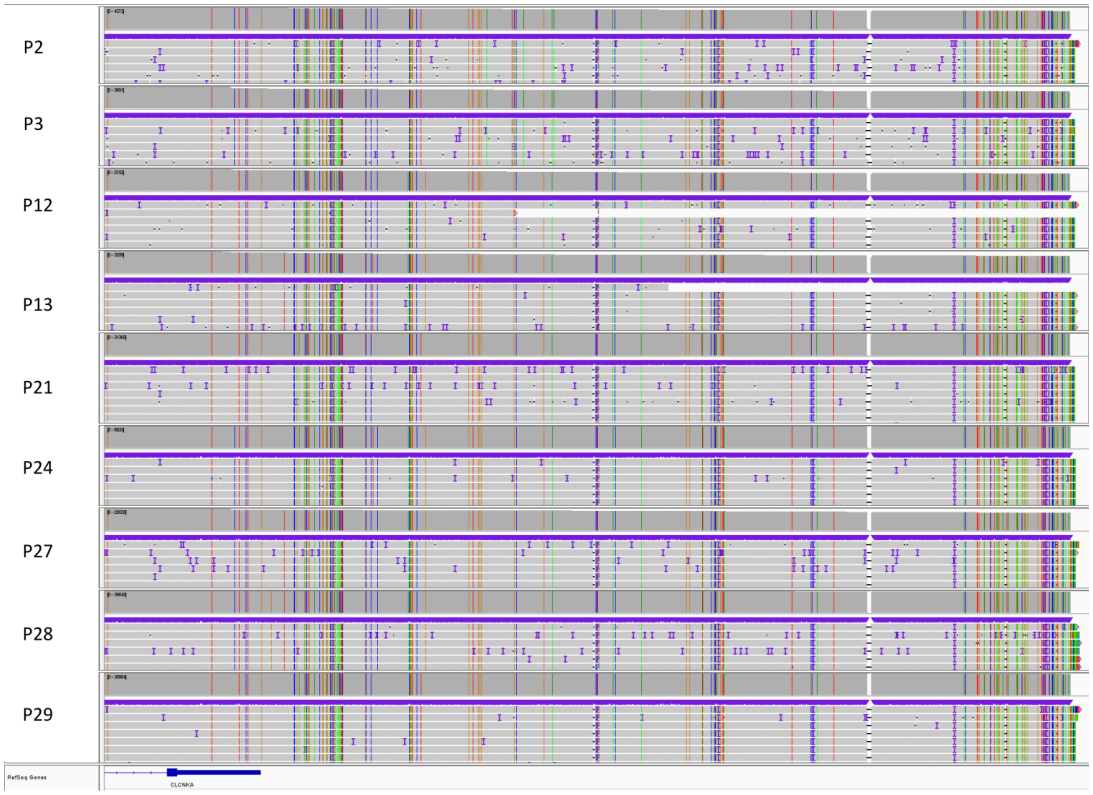

Deletion allele F

Deletion allele B + F

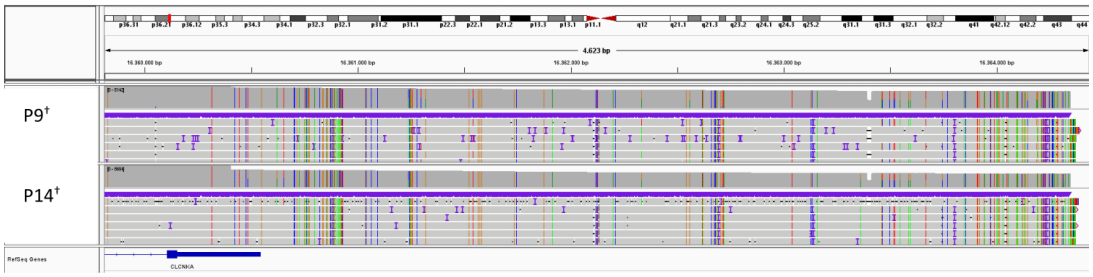

Deletion allele G

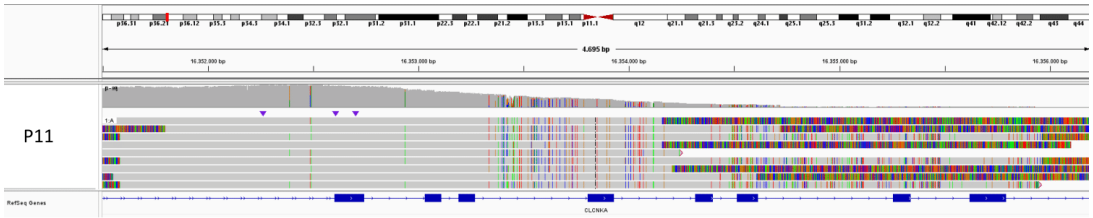

Deletion allele H

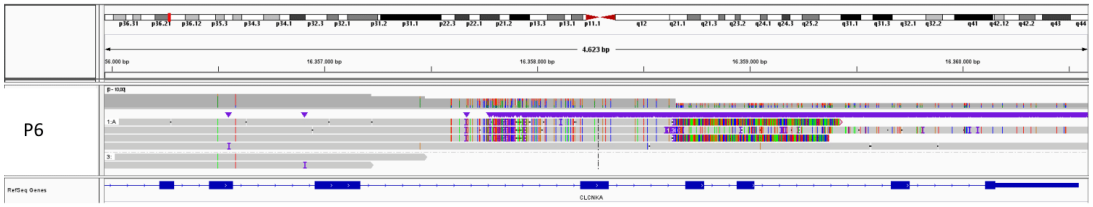

Suppl. Figure S4: Long-read Sequencing data.

Long-read Sequencing data of eight different deletion alleles identified in 28 patients from this study visualized in IGV.

Nikolai Tschernoster

21.06.1992 / Aachen

Universitätsstraße 20
50937, Köln
0221-478-96804
nikolai.tschernoster@uk-koeln.de

Bildung

06/2018 – (07/2023)	**Promotion**, Cologne Center for Genomics (CCG), Köln - Thema: "Genomic profiling in rare kidney disease"
11/2017 – 05/2018	**Masterarbeit**, Cologne Center for Genomics (CCG), Köln - Analysis of structural variations in paediatric patients with rare kidney disease (aHUS)
10/2015 – 05/2018	**Masterstudium**, Biologie, RWTH Aachen, Aachen - Molekulare Zellbiologie / Mikrobiologie und Genetik
04/2015 – 08/2015	**Bachelorarbeit**, Genetik, Uniklinik RWTH Aachen
10/2012 – 09/2015	**Bachelorstudium** Biologie, Universität zu Köln, Köln
Juni 2012	**Allgemeine Hochschulreife** (Abitur), Aachen
2002 - 2012	Anne-Frank-Gymnasium, Aachen

Publikationsliste

03/23 Am J Hum Genet.	Epigenetic regulation of plastin 3 expression by the macrosatellite DXZ4 and the transcriptional regulator CHD4. Strathmann EA, Hölker I, **Tschernoster N**, Hosseinibarkooie S, Come J, Martinat C, Altmüller J, Wirth B.
09/22 Neph. Dial Transpl.	Alport syndrome and autosomal dominant tubulointerstitial kidney disease frequently underlie end-stage renal disease of unknown origin-a single-center analysis. Leenen E, Erger F, Altmüller J, Wenzel A, Thiele H, Harth A, **Tschernoster N**, Lokhande S, Joerres A, Becker JU, Ekici A, Huettel B, Beck B, Weidemann A.
06/22 J Mol Diagn.	Unraveling Structural Rearrangements of the CFH Gene Cluster in Atypical Hemolytic Uremic Syndrome Patients Using Molecular Combing and Long-Fragment Targeted Sequencing. **Tschernoster N**, Erger F, Walsh PR, McNicholas B, Fistrek M, Habbig S, Schumacher AL, Folz-Donahue K, Kukat C, Toliat MR, Becker C, Thiele H, Kavanagh D, Nürnberg P, Beck BB, Altmüller J.
06/21 Lancet	Post-COVID syndrome in non-hospitalised patients with COVID-19: a longitudinal prospective cohort study. Augustin M, Schommers P, Stecher M, Dewald F, Gieselmann L, Gruell H, Horn C, Vanshylla K, Cristanziano VD, Osebold L, Roventa M, Riaz T, **Tschernoster N**, Altmueller J, Rose L, Salomon S, Priesner V, Luers JC, Albus C, Rosenkranz S, Gathof B, Fätkenheuer G, Hallek M, Klein F, Suárez I, Lehmann C.
02/21 Sci Rep.	MTBP phosphorylation controls DNA replication origin firing. Ferreira P, Höfer V, Kronshage N, Marko A, Reusswig KU, Tetik B, Dießel C, Köhler K, **Tschernoster N**, Altmüller J, Schulze N, Pfander B, Boos D.

Seite 2

01/21 Kidney Int Rep.	Expanding the Spectrum of FAT1 Nephropathies by Novel Mutations That Affect Hippo Signaling. Fabretti F, **Tschernoster N**, Erger F, Hedergott A, Buescher AK, Dafinger C, Reusch B, Köntges VK, Kohl S, Bartram MP, Weber LT, Thiele H, Altmueller J, Schermer B, Beck BB, Habbig S.
10/20 Clin Nephrol.	Long-term data on two sisters with C3GN due to an identical, homozygous CFH mutation and autoantibodies. Hackl A, Erger F, Skerka C, Wenzel A, **Tschernoster N**, Ehren R, Burgmaier K, Riehmer V, Licht C, Kirschfink M, Weber LT, Altmueller J, Zipfel PF, Habbig S.
10/19 Nat Commun.	Unstable TTTTA/TTTCA expansions in MARCH6 are associated with Familial Adult Myoclonic Epilepsy type 3. Florian RT, Kraft F, Leitão E, Kaya S, Klebe S, Magnin E, van Rootselaar AF, Buratti J, Kühnel T, Schröder C, Giesselmann S, **Tschernoster N**, Altmueller J, Lamiral A, Keren B, […] FAME consortium; LeGuern E, Klein KM, Labauge P, Bennett MF, Bahlo M, Gecz J, Corbett MA, Tijssen MAJ, van den Maagdenberg AMJM, Depienne C.

Präsentationen

28.-30. März 2019	50. Jahrestagung der Nephrologie (GPN)**, Poster Vortrag**, Köln
6.-7. Februar 2019	CMMC Annual Retreat, **Poster Präsentation**, Nümbrecht
13. Juni 2018	Genomic Vision Workshop, **Gastredner**, CCG, Köln
21.-22. Februar 2018	CMMC Annual Retreat, **Poster Präsentation**, Köln
6.-7. Oktober 2017	Gen-Diagnostik (AGD) Meeting, **Poster Präsentation**, Potsdam

Arbeitstätigkeiten

06/2018 – aktuell	Wissenschaftl. Mitarbeiter, Cologne Center for Genomics, Köln
06/2020 – 08/2020	Wissenschaftl. Aushilfe, Atlas Biolabs, Köln
11/2018 – 12/2019	Nebentätigkeit, Fahrzeuglogistik Drivement GmbH, Köln
10/2017 – 05/2018	Wissenschaftl. Hilfskraft B.Sc., Cologne Center for Genomics, Köln
10/2016 – 02/2017	Fahrdienst, BMW Kohl Automobile, Aachen
2015 – 09/2016	Studentische Hilfskraft, Humangenetik, Uniklinik RWTH-Aachen
März – April 2015	Berufspraktikum, Humangenetik, Uniklinik RWTH-Aachen
Februar – März 2015	Laborpraktikum, Humangenetik, Uniklinik RWTH-Aachen
Juni 2009	Schülerpraktikum, Organische Chemie, RWTH-Aachen

Köln, 28.04.2023, 

Ort, Datum, Unterschrift

Eidestattliche Erklärung

Hiermit versichere ich an Eides statt, dass ich die vorliegende Dissertation selbstständig und ohne die Benutzung anderer als der angegebenen Hilfsmittel und Literatur angefertigt habe. Alle Stellen, die wörtlich oder sinngemäß aus veröffentlichten und nicht veröffentlichten Werken dem Wortlaut oder dem Sinn nach entnommen wurden, sind als solche kenntlich gemacht. Ich versichere an Eides statt, dass diese Dissertation noch keiner anderen Fakultät oder Universität zur Prüfung vorgelegen hat; dass sie - abgesehen von unten angegebenen Teilpublikationen und eingebundenen Artikeln und Manuskripten - noch nicht veröffentlicht worden ist sowie, dass ich eine Veröffentlichung der Dissertation vor Abschluss der Promotion nicht ohne Genehmigung des Promotionsausschusses vornehmen werde. Die Bestimmungen dieser Ordnung sind mir bekannt. Darüber hinaus erkläre ich hiermit, dass ich die Ordnung zur Sicherung guter wissenschaftlicher Praxis und zum Umgang mit wissenschaftlichem Fehlverhalten der Universität zu Köln gelesen und sie bei der Durchführung der Dissertation zugrundeliegenden Arbeiten und der schriftlich verfassten Dissertation beachtet habe und verpflichte mich hiermit, die dort genannten Vorgaben bei allen wissenschaftlichen Tätigkeiten zu beachten und umzusetzen. Ich versichere, dass die eingereichte elektronische Fassung der eingereichten Druckfassung vollständig entspricht

Köln , 28.04.2023 , N. Tschanter

Ort, Datum, Unterschrift